NASA/TM–2016-218972

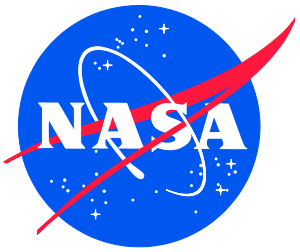

The Behavior of a Stitched Composite Large-Scale Multi-Bay Pressure Box

Dawn C. Jegley, Marshall Rouse, Adam Przekop, and Andrew E. Lovejoy
Langley Research Center, Hampton, Virginia

April 2016

NASA STI Program . . . in Profile

Since its founding, NASA has been dedicated to the advancement of aeronautics and space science. The NASA scientific and technical information (STI) program plays a key part in helping NASA maintain this important role.

The NASA STI program operates under the auspices of the Agency Chief Information Officer. It collects, organizes, provides for archiving, and disseminates NASA's STI. The NASA STI program provides access to the NTRS Registered and its public interface, the NASA Technical Reports Server, thus providing one of the largest collections of aeronautical and space science STI in the world. Results are published in both non-NASA channels and by NASA in the NASA STI Report Series, which includes the following report types:

- TECHNICAL PUBLICATION. Reports of completed research or a major significant phase of research that present the results of NASA Programs and include extensive data or theoretical analysis. Includes compilations of significant scientific and technical data and information deemed to be of continuing reference value. NASA counter-part of peer-reviewed formal professional papers but has less stringent limitations on manuscript length and extent of graphic presentations.

- TECHNICAL MEMORANDUM. Scientific and technical findings that are preliminary or of specialized interest, e.g., quick release reports, working papers, and bibliographies that contain minimal annotation. Does not contain extensive analysis.

- CONTRACTOR REPORT. Scientific and technical findings by NASA-sponsored contractors and grantees.

- CONFERENCE PUBLICATION. Collected papers from scientific and technical conferences, symposia, seminars, or other meetings sponsored or co-sponsored by NASA.

- SPECIAL PUBLICATION. Scientific, technical, or historical information from NASA programs, projects, and missions, often concerned with subjects having substantial public interest.

- TECHNICAL TRANSLATION. English-language translations of foreign scientific and technical material pertinent to NASA's mission.

Specialized services also include organizing and publishing research results, distributing specialized research announcements and feeds, providing information desk and personal search support, and enabling data exchange services.

For more information about the NASA STI program, see the following:

- Access the NASA STI program home page at *http://www.sti.nasa.gov*

- E-mail your question to help@sti.nasa.gov

- Phone the NASA STI Information Desk at 757-864-9658

- Write to:
  NASA STI Information Desk
  Mail Stop 148
  NASA Langley Research Center
  Hampton, VA 23681-2199

NASA/TM–2016-218972

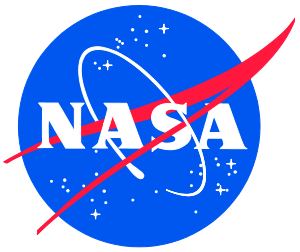

The Behavior of a Stitched Composite Large-Scale Multi-Bay Pressure Box

Dawn C. Jegley, Marshall Rouse, Adam Przekop, and Andrew E. Lovejoy
Langley Research Center, Hampton, Virginia

National Aeronautics and
Space Administration

Langley Research Center
Hampton, Virginia 23681-2199

April 2016

Available from:

NASA Center for AeroSpace Information
7115 Standard Drive
Hanover, MD 21076-1320
443-757-5802

Abstract

NASA has created the Environmentally Responsible Aviation (ERA) Project to develop technologies to reduce impact of aviation on the environment. A critical aspect of this pursuit is the development of a lighter, more robust airframe to enable the introduction of unconventional aircraft configurations. NASA and The Boeing Company have worked together to develop a structural concept that is lightweight and an advancement beyond state-of-the-art composite structures. The Pultruded Rod Stitched Efficient Unitized Structure (PRSEUS) is an integrally stiffened panel design where elements are stitched together and designed to maintain residual load-carrying capabilities under a variety of damage scenarios. With the PRSEUS concept, through-the-thickness stitches are applied through dry fabric prior to resin infusion, and replace fasteners throughout each integral panel. Through-the-thickness reinforcement at discontinuities, such as along flange edges, has been shown to suppress delamination and turn cracks, which expands the design space and leads to lighter designs. The pultruded rod provides stiffening away from the more vulnerable skin surface and improves bending stiffness. A series of building block tests were evaluated to explore the fundamental assumptions related to the capability and advantages of PRSEUS panels. The final step in the building block series of tests is an 80%-scale pressure box representing a portion of the center section of a Hybrid Wing Body (HWB) transport aircraft. The testing of this test article under maneuver and internal pressure loading conditions is the subject of this paper. The experimental evaluation of this article, along with the other building block tests and the accompanying analyses, has demonstrated the viability of a PRSEUS center body for the HWB vehicle. Additionally, much of the development effort is also applicable to traditional tube-and-wing aircraft, advanced aircraft configurations, and other structures where weight and through-the-thickness strength are design considerations.

I. Introduction

NASA has created the Environmentally Responsible Aviation (ERA) Project to explore and document the feasibility, benefits and technical risk of advanced vehicle configurations and enabling technologies to reduce impact of aviation on the environment. A critical aspect of this pursuit is the development of a lighter, more robust airframe to enable the introduction of unconventional aircraft configurations that have higher lift-to-drag ratios, reduced drag, and lower community noise. The Hybrid Wing Body (HWB) configuration is a significant improvement in aerodynamic performance compared to the traditional tube-and-wing aircraft. However, the HWB configuration poses challenges in the design of a non-circular pressure cabin that is lightweight and economical to produce. Developing a structural concept that supports the HWB cabin design is the primary technical challenge to the implementation of a large lifting-body design like the HWB.[1]

To address this technical challenge, researchers at NASA and The Boeing Company (Boeing) have worked together to develop a new structural concept called the Pultruded Rod Stitched Efficient Unitized Structure (PRSEUS).[2-5] PRSEUS is an integral structural concept that evolved from stitching technology development started in the NASA-Boeing Advanced Composites Technology (ACT) Program in the 1990s.[6] The goal of the ACT

wing program was to develop stitching technology to reduce structural weight and fabrication cost of a conventional wing on a large commercial transport aircraft. Through-the-thickness stitching was demonstrated to arrest damage and prevent delamination.

Under the NASA Subsonic Fixed Wing and ERA projects, the PRSEUS concept has been applied to a HWB centerbody. For this structure, flat panels must support large bending loads in both in-plane directions, along with the pressure load associated with internal cabin pressure. The use of a traditional composite material system would require fasteners to suppress delaminations and to join structural elements, ultimately leading to fastener pull-through as a critical failure mode or heavy pad-ups in the fastener regions. In contrast, through-the-thickness stitches, applied through dry fabric prior to resin infusion, replace these fasteners throughout each integral panel. This approach eliminates fasteners and their associated holes, which significantly simplifies the assembly process, reduces part count, and removes a primary source of crack initiation throughout the life of the aircraft. Through-the-thickness reinforcement using stitches at discontinuities, such as along flange edges, has been shown to suppress delamination and turn cracks, which increases the design space and leads to lighter designs.[2] Additionally, the infusion and cure processes for PRSEUS panels require high temperatures, but only vacuum pressure, which eliminates the need for an autoclave. This manufacturing approach leads to substantial cost savings and eliminates the out-time limitations associated with traditional prepreg. NASA and Boeing have worked to develop PRSEUS technologies that could be implemented on a transport-size airplane design in the future.

In ERA Project and previous programs, the PRSEUS concept was evaluated analytically and experimentally using a building-block approach.[7-14] As the final step in a building-block process, a 30-foot-long multi-bay pressure box has been constructed which contains 11 PRSEUS panels. This pressure box test article has been subjected to a series of loadings. The testing of this large-scale test article is the subject of this paper.

II. HWB Structural Concept

While the HWB provides many aerodynamic advantages, the HWB presents challenges to the structural design of the center fuselage section due to the non-circular shape of the HWB, as shown in the aircraft image in Figure 1. Although significantly lighter than conventional aluminum structures, even the most highly efficient composite primary structures used on today's state-of-the-art aircraft would not be adequate to overcome the weight and cost penalties introduced by the highly contoured airframe of the HWB. A particularly difficult region to address is the pressure cabin where design is driven by out-of-plane loading considerations. In this region, a traditional layered material system would require thousands of mechanical attachments to suppress delaminations and to join structural elements, ultimately leading to fastener pull-through as a critical failure mode in the thin-gauge skins. Another disadvantage of a conventional composite for this application is the high manufacturing costs associated with the highly contoured airframe. The essential characteristics of a more capable HWB structural solution are ones that operate effectively in out-of-plane loading scenarios, while simultaneously meeting the demanding producibility requirements inherent in building a highly contoured airframe.

In addition to the secondary bending stresses experienced during pressurization, another key difference between the HWB shell and the traditional cylindrical fuselage is the unique bi-axial loading pattern that occurs during maneuver loading conditions, as shown in Figure 1. For the HWB, the load magnitudes are nearly equal in each in-plane direction (Nx and Ny), which is in contrast to the loading that is typically found in conventional tube-and-wing fuselage arrangements, where the cantilevered fuselage is more highly loaded in the Nx direction, along the stringer, than in the Ny direction, along the frame. This single difference has a profound effect on the structural concept selection because it dictates that the optimum panel geometry should have continuous load paths in both directions (Nx and Ny), in addition to efficiently transmitting internal pressure loads (Nz) for the near-flat panel geometry, as shown in Figure 1. Additionally, for a conventional skin-stringer-frame built-up panel, the frame shear clip is typically discontinuous to allow the stringer to pass through the frame. If such an arrangement were used for the HWB, the frame would be less effective in bending and axial loading than a continuous frame that is attached directly to the skin, ultimately resulting in a heavier panel.

To overcome these challenges, an improved fuselage panel should be designed as a bi-directionally stiffened panel, where the wing bending loads are carried by the frame members and the fuselage bending loads are carried by the stringers. The panel design should also include continuous load paths in both directions, stringer and frame laminates that are highly tailored, thin skins designed to operate well into the post-buckled design regime, and with crack-arresting features designed to minimize damage propagation. These features are necessary to overcome the inherent weight penalties of the non-circular pressure cabin.

III. PRSEUS Concept

The PRSEUS design-and-fabrication approach incorporates damage arrestment, improved load paths, and weight reducing-design features, which results in a highly efficient structural concept. It is a conscious progression away from conventional laminated and bonded methods of assembly, and has evolved to become a one-piece co-cured panel design with seamless transitions and damage-arrest interfaces. The highly integrated nature of the PRSEUS stiffened panel design is enabled by the use of through-the-thickness stitching, which ultimately leads to unprecedented levels of fiber tailoring and structural optimization potential.

The PRSEUS panel concept is a combination of dry carbon warp-knit fabric, pultruded rods, foam core, and stitching threads. The fabric consists of AS4 carbon fiber layers with a (44/44/12) fiber architecture, where the values are percentages of (0/±45/90) degree plies. Each stack has a nominal cured thickness of 0.052 inches. Multiple stacks of the warp-knit material can be used to build up the desired part stiffness, strength, and configuration. These materials are brought together in a unique manner to create a stiffened panel geometry that utilizes resin infusion and out-of-autoclave curing to reduce recurring fabrication costs and allow the construction of very large panels. The resulting panels are one-piece unitized assemblies with a highly integrated, stiffened-panel design enabled by the use of through-the-thickness stitching, which ultimately leads to

unprecedented levels of fiber tailoring and load-path continuity between the individual structural elements.

Structural continuity is maintained by eliminating mechanical attachments, gaps, and mouse holes to provide uninterrupted load paths between the skin, stringer, and frame elements, as shown in Figure 2. The stringer contains a pre-cured high-stiffness pultruded rod, made of Toray unidirectional T800 fibers with a 3900-2B resin above the thin web, with the flanges stitched to the skin. Stacks of fabric are used for all webs, flanges, tear straps, and the skin. Foam-filled frames are perpendicular to the stringers and also have flanges which are stitched to the skin. Load-path continuity at the stringer-frame intersection is maintained in both directions by passing the rod-stringer through a small keyhole in the frame web. The 0-degree fiber dominated pultruded rod increases local strength and stability of the stringer section while simultaneously shifting the neutral axis away from the skin to further enhance the overall panel-bending capability. Frames are placed directly on the inner moldline (IML) skin surface, and are designed to take advantage of carbon fiber tailoring by placing bending and shear-conducive lay-ups where they are most effective. By shifting the neutral axis away from the skin, this design creates efficient load paths in both directions that are beneficial to the stability and bending resistance of the panel. Vectran threads are used to stitch the stiffeners to the skin and at other discontinuities. Since all the interfaces are stitched together to provide through-the-thickness strength, a high degree of fiber tailoring is possible even with layered composite material systems, which are known to be brittle and prone to delamination. Extra thickness in the skin and flanges is not needed to resist out-of-plane motion.

The stitching is also used to suppress out-of-plane failure modes. Suppressing these failure modes enables a higher degree of tailoring than would be possible using conventional laminated materials. Stitching arrests cracks and controls damage propagation within a layered material system. By strategically placing stitch rows along the key structural interfaces, traditional resin-dominated failure modes can be suppressed, so that the optimum strength of the panel can be more nearly realized. Using through-the-thickness stitching to locally reinforce the out-of-plane-direction interfaces not only makes integral construction possible, but stitching also enables a new type of damage arrest and fail-safe redundancy into the structure that was previously reserved for ductile materials and not normally associated with brittle composite systems.[15-17]

The resulting bi-directionally stiffened panel design is ideal for the HWB pressure cabin because the design is highly efficient in all three loading directions, and the stitching on the panel reacts pull-off loading and increases panel survivability. These features are also applicable to barrel-fuselage sections with thin skins and for wing structures to improve structural efficiency and reduce weight. This approach would allow thin fuselage skins to safely buckle. The PRSEUS concept also allows the stringer to pass through fuselage frames and wing rib and spar caps.

IV. PRSEUS Manufacturing

Developing the manufacturing process to build large unitized stitched panels was necessary to apply this technology to large commercial transport aircraft. This unitization is enabled by the use of dry material forms, single-sided stitching, and the unique self-supporting preform design that is used to eliminate internal moldline cure tooling. Using these technologies, complicated stitched preforms can be fabricated without exacting tolerances, and then accurately net molded in a single oven-cure operation using high precision outer moldline (OML) tooling. Since all of the materials in the stitched assembly are dry, there are no out-time limitations as with prepreg systems, which can restrict the size of an assembly because the assembly must be cured within a limited processing envelope. Additionally, the infusion and cure processes for PRSEUS panels require high temperatures, but only vacuum pressure, which eliminates the need for an autoclave and the limitations based on the size of the autoclave.

Hexcel HexFlow VRM 34 resin infusion is accomplished using a soft-tooled fabrication scheme where the bagging film conforms to the IML surface of the preform geometry and seals against a rigid OML tool. The success of this approach has been demonstrated on PRSEUS panels up to 30 feet long, as shown in Figure 3. This panel contains rod-stiffened stringers, foam-filled frames, and integral caps. Integral caps are similar to the foam-filled frames in that the stringers pass through the integral caps at keyholes, but the integral caps are solid laminates that only occur at locations where one panel joins to another. All elements are stitched together with no need for fasteners or fittings within the panel. Additional manufacturing details are presented in References 18-19.

Completed panels can be mechanically joined using the integral cap features to further reduce the number of separate details and eliminate fasteners through the exterior surface of the panel. As such, the fasteners are loaded in shear, and any pull-off load is reacted directly into the adjacent panel through the stitched integral cap layers.

V. PRSEUS Development

A series of building block tests were conducted to explore the fundamental assumptions related to the capability and advantages of PRSEUS panels. Since the application primarily being considered is the HWB center body, only thinner and lightly loaded structures are considered in this project. The building block tests addressed tension,[5,14] compression,[5,7,9,10] and pressure loading conditions[5,12,13] of the HWB pressure cabin as illustrated in Figure 4. The emphasis of the development work has been to assess the loading capability, damage arrestment features, repairability, post-buckling behavior, and response of flat panels to out-of-plane pressure loading. Each building block test was accompanied by analysis for prediction and post-test comparisons. All test articles were fabricated at the Boeing stitching center in Huntington Beach, CA. The design, analysis, and testing activities were divided between NASA and Boeing. This series of tests, with their corresponding analyses, have demonstrated that PRSEUS panels are capable of meeting the unique tension, compression, and pressure loading conditions of a HWB pressure cabin.

VI. Multi-Bay Pressure Box Test Article

The knowledge gained from the earlier steps of the building block development program was used to develop a large-scale multi-bay box test article. This multi-bay pressure box test article was the last step in the building block process for the HWB center fuselage section. This test article was an 80% scale component representing a section of the most heavily loaded portion of the HWB center section. This size was selected to be large enough to be representative of full scale structure while still allowing largest panels to fit in the available oven for cure and allowing the assembled structure to fit in the test chamber. The multi-bay pressure box panel arrangement consists of 11 PRSEUS panels that form the exterior shell and floor members, along with four interior sandwich rib panels that were used to divide the box width into thirds, as shown in Figure 5. The design and fabrication of this test article is described in References 18-21.

This test article was used to demonstrate structural performance and manufacturing scale-up. The manufacturing process demonstrated the inherent differences in fabricating the eight-foot-long building block panels and the 30-foot-long multi-bay pressure box panels. The refinement of manufacturing techniques and processes has demonstrated the capability of PRSEUS technology to be broadly applied to primary structures on transport aircraft. A photograph of a 30-foot-long panel prior to assembly into the double deck closed box multi-bay pressure box test article is shown in Figure 3. The components of the multi-bay pressure box are shown in Figure 6.

The first of these PRSEUS panels to be fabricated was the crown panel. This panel was the first 30-foot-long PRSEUS panel that had ever been fabricated. As such, the manufacturing process was affected by scaled-up induced imperfections. The only imperfection requiring repair was caused by motion of the caul plates during resin infusion and cure. The plates on the OML shifted in such a way as to create dents in the OML surface of the panel. Since the panel skin is 0.052 inches thick in some places, these dents raised concerns about the load-carrying capability of the crown panel in compression. To ensure that the crown panel would not fail prematurely due to the dents, bonded patches were added to the crown as described in Reference 21. These bonded patches were only placed over the dents so the external bonded patches caused an unsmooth surface on the crown OML; the crown is therefore not symmetric lengthwise or widthwise.

The multi-bay pressure box was assembled at the Boeing C-17 assembly site in Long Beach, CA. The cured panels were loaded into an assembly fixture where they were mechanically joined together using the integral cap features that locate the panels. These integral cap features along the panel edges reduce the number of metallic fittings required in panel-to-panel joints and eliminate many of the fasteners through the exterior surface of the panels. A photograph of the completed multi-bay pressure box is shown in Figure 7.

End fittings were added at the corners of the pressure-tight cell to impart bending loads that simulate the loads of the wing carry-through structure that would be induced during a flight maneuver. Load-introduction hardware elements, identified as adaptor boxes in Figure 5, and seen as the green elements on the sides in Figure 7, were added to the test article to mate with the platens in the test facility, and ensure that the load was imparted to the test article in such a way as to avoid failure at these outer rib locations. After installation on the test article, these adaptor boxes were milled flat, so as to have the

upper and lower boxes be coplanar on each side. Additionally, they were milled such that the planes would be parallel to each other to ensure seamless mating to the platens in the test facility. A detailed description of this procedure is given in Reference 21. Prior to delivery to NASA, the interior and exterior of the test article were painted white to improve the visibility of cracks and delaminations that could form during testing. A graphic of the test article in the Combined Loads Test System (COLTS) Facility[24] at NASA Langley Research Center is shown in Figure 8.

Linear and nonlinear finite element analyses were performed to validate the design of the multi-bay pressure box and predict the behavior of the multi-bay pressure box under five critical loading conditions.[22,23] These loading conditions were:

1) Internal pressure load only, where the maximum load was 18.4 psi
2) Load simulating a 2.5-g up-bending condition which subjects the crown panel to compressive loads
3) Negative 1-g down-bending condition which subjects the crown panel to tensile loads
4) Combination of pressure and down-bending
5) Combination of pressure and up-bending.

VII. Test Arrangements

The multi-bay pressure box was subjected to a series of loadings in COLTS. Testing was conducted with the structure in the pristine condition, with intentional minor damage and with intentional severe damage. The results of the pristine testing and the testing of the multi-bay pressure box with minor damage are the subject of the current paper.

Installation in Facility

Prior to installation of the multi-bay pressure box in the test chamber, the COLTS platens were placed 30 feet apart. A series of checkout tests using a steel I-beam as a dummy test article were conducted to verify that the control system would move the platens as intended.[25,26] Then the test article was lowered between the platens at COLTS and positioned in a "cradle" which was bolted to the platens to assure correct positioning, as shown in Figure 9. With the test article resting in the cradle, but still connected to the overhead crane, bolts were used to connect the load-adaptor boxes to the platens. A photograph of the test article between the platens in the COLTS Facility is shown in Figure 10.

Instrumentation

Several types of instrumentation were used to monitor and record data during each test. There were 262 linear and 36 rosette strain gauges, 15 linear variable displacement transducers (LVDTs), four pressure transducers, four fiber optic wires, four video digital image correlation systems, 26 acoustic emission sensors, and nine video cameras used to record the behavior of the test article and the COLTS system.

Data from the strain gauges, transducers, and load cells were recorded at a rate of 10 scans per second. The LVDTs were located on the platens, forward bulkheads, and one

side keel, as shown in Figure 11a. Strain gauges were located on all panels and on most load-introduction elements. Typical strain gauge locations for the stringers, frames and skin are shown in Figure 12. Strain gauge locations on the metal fittings are shown in Figure 13. Strain gauge locations associated with intentionally applied damage sites are shown in Figure 14. Two or four strain gauges were added after the application of impact damage to enable the tracking of damage emanating from the impact site. For the interior impacts to the top of the stringer and the top of the frame, these additional gauges were parallel to the stiffener and one inch on either side of the impact. Four gauges were added to the skin in back-to-back pairs for the internal and external mid-bay impact sites where the gauges were placed one inch away from the impact site. For the external impact sites, which were at flanges, strain gauges were added in back-to-back pairs approximately 0.5 inches away from the impact sites.

Plots of critical strain gauges and LVDTs were monitored during each test to track the structural behavior in real time to compare to predictions and evaluate the operation of the loading system. Selected full-field displacements and strains were also monitored. A speckle pattern, consisting of black paint dots on a white-paint background, was applied to a portion of the aft bulkhead, the crown, and the center keel, as shown in Figure 11b. Two still-image cameras were positioned to view each speckled region to simultaneously photograph the pattern every five seconds during each test. These images were compared to determine the displacements in the x-, y-, and z-directions and the in-plane strains. These systems provided real-time, full-field imaging of displacements and strains.[27] Limited data from the fiber optic and acoustic emission systems were available for real-time structural response evaluation since the data from these sources required extensive processing. Data from these systems will be used in post-test test-analysis correlation and are not documented herein.

Video cameras were placed inside each of the six bays of the test article to record cracks and deformations in the bulkheads, crown and keel. Additional video cameras were placed outside the test article to obtain a global view of the structure. These video images were monitored during each test.

Load Application

Mechanical loads were applied to the test article to simulate critical flight conditions and internal pressure loads were applied to represent cabin pressure. The mechanical loads were applied to the test article through four actuators, located at the four corners of the test article, which were used to rotate the platens relative to each other. Pressure was pumped into the test article to simulate cabin pressure. During testing, mechanical loads were applied alone, pressure was applied alone, and combinations of internal pressure and mechanical loads were applied. In each case, loading was quasi-static and slow enough to ensure that the actuators stayed synchronized with each other and with the pressure load. When mechanical loading is applied in COLTS, both platens rotate around their center of gravity, but only the “loading” platen translates. This behavior means that the platen displacements caused by the rotation of the “stationary” platen are not the same as the displacements caused by the rotation and translation of the loading platen. Each actuator applies a load and displacement, but since each actuator is connected to both

platens, the relative motion is controlled, even though the individual motion of the platens is not.

Although the applied actuator loads were nominally identical in magnitude, the lower actuators operated in the opposite direction compared to the upper actuators; therefore, when the load in the upper actuators was positive, the load in the lower actuators was negative. This connection was accomplished by slaving all actuators to a single actuator and controlling the load in that actuator. The test article was subjected to design ultimate load (DUL) level in all load conditions. The test article was subjected to DUL in the pristine condition and with intentional damage.

Actuator load as a function of time is shown in Figure 15 for the pristine DUL up-bending load case to demonstrate the accuracy of the control system in controlling the applied actuator loads. Load magnitudes for the four active actuators stayed in excellent agreement with each other throughout the test. This level of synchronization of the actuators was typical of the loading all design limit load (DLL) and DUL tests. The applied actuator and pressure loads at DUL for each condition are shown in Table 1.

Table 1 Applied Load for DUL Tests

	Mechanical load (kips)	**Pressure (psi)**
Pristine		
Down-bending	95.4	0
Down-bending plus pressure	95.6	13.8
Up-bending	240.3	0
Up-bending plus pressure	240.4	13.8
Pressure only	0	18.4
With Impact Damage		
Down-bending	95.6	0
Down-bending plus pressure	95.6	13.8
Pressure only	0	18.4
Up-bending	240.5	0
Up-bending plus pressure	240.7	13.8
Up-bending plus pressure	263	13.8
Up-bending	263	0

Internal pressure was introduced into the test article through a valve in an upper bulkhead panel access door. Holes in the floor ensured that the pressure remained constant in the upper and lower sections of the test article. Four pressure transducers measured the pressure around the interior of the box to evaluate the uniformity of the pressure loading.

First, DLL and DUL loadings were conducted for the pristine structure. These tests are listed in Table 1 in the order in which they were conducted. In all loadings to DUL or less, when pressure loading was applied simultaneously with the mechanical load, the pressure load and actuator load were programmed to ramp together from zero to maximum loading. When mechanical loading greater than DUL was applied, pressure ramped with the mechanical load, but was programmed to not exceed the DUL condition

for pressure. In each test, loads were ramped from zero to the maximum load with short pauses to compare test data to predictions. When the maximum load was reached, the load was held briefly and then the structure was unloaded. The load rate was faster for unloading than for loading, and pressure and mechanical loads did not always stay in sync for unloading.

Impact Applications

After the completion of the pristine structure tests, barely visible impact damage (BVID) was inflicted to the forward upper bulkhead and center keel panels. Three impacts to the interior of the structure, on the stiffened side of the upper bulkhead, and three impacts to the exterior of the structure, on the unstiffened side of center keel, were inflicted. Damage to the interior was inflicted using a spring-loaded impactor, as shown in Figure 16a, at locations at the top of a stringer at the top of a frame, and at a mid-bay location between stiffeners, as indicated in Figure 17a. Interior impacts were intended to represent a range of locations and the type of damage possible due to service events such as tool drops. Damage to the exterior was inflicted using a gravity-fed apparatus, as shown in Figure 16b, to locations at the flange edge of a stringer, at the flange edge of a frame and at a skin mid-bay location between the stiffeners as shown in Figure 17b. Exterior impacts were inflicted to an area of the structure that would buckle during loading to evaluate whether typical exterior impacts would degrade the performance in buckled structure. In each case, a weight with a one-inch-diameter hemispherical tup was used for the impact.

BVID for the interior sites corresponds to 20 ft-lb for the top of the stiffeners, which causes little damage but is the maximum energy required for internal impacts for commercial aircraft, and 15 ft-lb for the skin mid-bay location, where visible damage is clearly evident. BVID for the exterior sites corresponds to energy levels of 60 ft-lb, 50 ft-lb, and 15 ft-lb for the frame flange, the stringer flange and the mid-bay locations, respectively. Impact energies for each impact and a photograph of the panels prior to assembly into the test article are shown in Figures 17a and 17b with the impact sites indicated by a circle, square, and triangle on the photograph, representing the frame, mid-bay, and stringer impact locations, respectively. A sketch of the location for the exterior impacts relative to the stiffener flange is show in Figure 18.

One of the exterior impacts was inflicted slightly away from the planned impact site. This impact was into the thin-skin region instead of at the adjacent flange. Therefore, the damage was more severe than intended. The damage was clearly visible from the exterior and interior and, in fact, a through-hole was created. A photograph of the damage from the exterior of the test article is shown in Figure 19. Evaluation of the damage at this location indicated that this damage would not reduce the ability of the structure to sustain mechanical load, but could reduce the ability of the structure to support internal pressure loads. Therefore, a non-structural patch was taped over the hole on the inside stiffened side of the center keel. Ultrasonic scans were conducted immediately before and immediately after the impacts, so that the extent of damage caused by the impacts could be quantified. These scans indicated that delamination occurred at the keel skin and flange impact sites, but was arrested at the closest stitch line to the impact site. Scans of the bulkhead stiffener impacts found no damage. Scans of

the skin interior impact showed delamination from the impact site to the closest stitch line to the impact site, which was at the adjacent flange edges. Ultrasonic results will be presented in future publications.

Loading Greater than DUL

After the application of BVID, the DLL and DUL loadings were repeated, with the final BVID test to a load greater than DUL in the up-bending and up-bending plus pressure case. The loads were applied using the same methodology as in the earlier tests. A detailed description of the test sequence for the test to loading greater than DUL is shown in Figure 20. In this test, first, the load was ramped to DUL in the up-bending plus pressure condition, represented by the red line in the figure. Then, the pressure was held constant while the mechanical load was increased by 10%. Then, the mechanical load was decreased to DUL. The purple line in the figure represents the pressure-hold sections of the loading. Then, the mechanical load was held constant while the pressure load was removed, leaving the test article at DUL in the up-bending condition without pressure. This portion of the load sequence is represented by the blue line. Then, the mechanical load was increased to 10% greater than DUL, and held briefly. This portion of the load sequence is represented by the green line. Finally, the mechanical load was removed.

VIII. Results and Discussion

The results presented herein focus on the DUL tests since the tests to lesser loads generally did not demonstrate any significant behavioral difference from the DUL tests. Results for the final failure test are not presented herein since that test included severe damage and was not part of the original test plan. Results are shown first for the pristine structure and then, selected results are shown for the tests of the damaged structure.

Displacement transducer results are shown, followed by full-field displacement results at DUL and at selected load levels. Then, strain gauge results are shown, followed by full-field strain results at DUL and at selected load levels. The locations to place the strain gauges were primarily based on the linear finite element method (FEM) analysis.[22] However, additional strain gauges were added based on the results of the nonlinear FEM analysis.[23] Each strain gauge location was selected based on predictions from a specific load case. The strain gauge results presented herein include the results for each gauge for the load case which was used to select that location. Only the down-bending, up-bending and pressure-only load cases were critical in determining strain gauge locations. Since there are more critical locations based on the pressure-only load case and on the up-bending load case, more strain gauges were required to evaluate the behavior of the test article in those conditions.

Strain gauge results are presented for the test article in the pristine condition with loading to DUL in the down-bending load case first, followed by strains for the up-bending load case and, finally, for the pressure-only load case. Results are then shown for a few locations under combined loads to DUL. Then, results are presented for strain gauges at the impact sites. Since the impact damage had local effects on strain in some cases, but no effect on global behavior, for the BVID tests with loading to DUL, only

strains in the impact areas are presented. Finally, selected results are shown for the test in which load was increased greater than DUL. Strain gauge results are grouped into plots based on the location and orientation of the gauges. In most cases, an inset image is included in the figure identifying the location of the gauge where boxes, which corresponds to gauge locations, are shown on a sketch of the panel. These boxes represent either a single gauge or a back-to-back pair. When colored boxes (e.g., red, blue) are used in the inset image, the colors of the curves in the plot correspond to the strain gauge location shown on the inset. When grey boxes are used, typically one panel sketch is used to represent multiple symmetric locations on the test article and a legend is used to identify which panel or other specific location on the test article the gauge is located.

There were some initial concerns that some of the metal fittings could experience strains that would be large enough to induce plasticity. Plasticity in the metal fittings could cause some redistribution of loading into the test article. To monitor the possible redistribution, strain gauges were added to some fittings. These strains are shown in subsequent sections for the load cases where there was initially concern.

Displacements

Measured displacements at the platens are shown in Figures 21 through 25 for the five load cases with loading to DUL. The displacement scales for the up-bending and up-bending plus pressure are the same, as are the displacement scales for the down-bending and down-bending plus pressure. When mechanical load is present, the controlled actuator load is used for plotting; pressure is therefore only shown in the pressure-only load case.

Displacements of the stationary platen are represented by solid curves, and displacements of the loading platen are represented by dashed curves in all platen displacement plots. Displacements near the top of the platens are shown in red and orange, for the aft and forward platens, respectively. Displacements near the bottom of the platens are shown in blue and light blue, for the aft and forward platens, respectively. Even though there were four LVDTs on each platen, it was discovered after testing that one of those LVDTs was bumped between two of the early tests, so results for only seven platen locations are shown. Displacements for the down-bending and down-bending plus pressure load cases are presented first, followed by the up-bending and up-bending plus pressure load cases, and, finally, for the pressure-only load case.

The discontinuities in slope in the plots represent slippage in the COLTS platen support system and not damage to the test article. The slippage primarily affects the stationary platen. This type of discontinuity is seen in all load cases where mechanical load was applied. Since they are an artifact of COLTS and not the test article, they are not discussed in this paper beyond the observation that the slip in the COLTS platen mechanism occurred near the forward side of the test article at the stationary platen, which is where the largest discontinuities are seen.

Ideally, measured displacements on the platens would occur in pairs, e.g., the aft and forward LVDTs near the top of the stationary platen would be the same. Since loads were controlled in these tests, not displacements, displacements are not exactly the same

even when loads agreed well. However, displacements tracked each other reasonably well throughout the testing.

Since the mechanical loading was the primary influence on the platen motion, the displacement magnitudes and patterns are the same for the down-bending and down-bending plus pressure load cases, with a maximum displacement of approximately -0.2 inches near the crown of the test article and 0.3 inches near the keel of the test article, where positive displacements represent movement of the platens together and negative displacements represent moving the platens apart. Similarly, the displacement magnitudes and patterns are the same for the up-bending and up-bending plus pressure load cases, with a maximum displacement of approximately 0.4 inches near the crown of the test article and -0.3 inches near the keel of the test article. The platen motion for the pressure only case is less than 0.05 inches in magnitude, since the platens were pushed apart as the test article expanded with no additional loading.

Measured displacements from LVDTs at six forward bulkhead locations and one side keel location, shown in Figure 11, are shown in Figures 26 through 30 for the five load cases for loading to DUL. Displacements near the stationary platen are represented by solid curves. Displacements near the center of the test article are represented by long dashed curves. Displacements near the loading platen are represented by short dashed curves. Displacements of the upper bulkhead are shown in red. Displacements of the lower bulkhead are shown in blue, and displacement of the side keel is shown in light blue. Since the LVDTs were positioned to measure the out-of-plane motion of each panel, the largest displacements occur in the largest panel bay, i.e., the center section of the upper bulkhead. Since most of the out-of-plane motion is caused by internal pressure, the displacement in the up-bending and down-bending load cases is less than 0.15 inches in magnitude, while the displacement in the up-bending and down-bending plus pressure load cases is up to approximately 0.6 inches when the maximum pressure was 13.8 psi. The pressure-only load case, where the maximum pressure is 18.4 psi, results in a maximum deformation of approximately 0.8 inches.

Full-field out-of-plane displacements for a portion of the crown, aft bulkhead, and keel are shown in Figures 31 through 39 at DUL for the five load cases. Displacements are shown for the down-bending and down-bending plus pressure cases in Figures 31 through 33, for the up-bending and up-bending plus pressure load cases in Figures 34 through 36, and for the pressure-only load case in Figures 37 through 39. In each case, the crown is shown, followed by the bulkhead and, finally, the keel. In all full-field displacement figures, positive displacements are outward from the plane of the panel. The white regions in each plot are areas where data could not be acquired due to features on the surface of the panels such as fittings, fasteners, strain gauges, and wires.

These full-field images indicate that when mechanical load is applied, the skin of the panel in compression (crown for up-bending and keel for down-bending) buckles between the stiffeners. However, the results for the combined load cases show that the pressure loading has more influence on the crown and keel panels than the mechanical load. When pressure is applied, all panels bow outward. In the combined load cases, the deformation pattern is a combination of pressure pillowing and buckling. Consistent with the LVDT results, the largest displacement is in the pressure-only load case in the bulkhead panel. Behaviors that the point measurements cannot capture include the small buckles between the stiffeners in the bulkhead panel in the up-bending load case. These

buckles occur near the bulkhead-to-crown attachments and are caused by the shear loading in the bulkheads induced by the bending of the test article. While buckles in the crown and keel acquire an in-out pattern early in the test and retain that pattern, the buckle mode shape in the bulkheads change with loading. Deformation patterns for the bulkhead at additional load levels are shown in Figures 40a and 40b. This change includes changes in the number of half-waves in the buckled region. Regardless of the cause or magnitude, these buckles occurred in DLL and DUL tests and did not appear to cause damage to the test article and did not compromise the ability of the test article to support DUL.

Strains

Down-bending load case

The down-bending load case applies tension to the crown panel, compression to the keel panels and floor, and shear load into the bulkheads. Strain gauges on the floor and on the center keel were located to capture behavior in the down-bending load case. These strains are shown in Figures 41 and 42, respectively. These strain gauges are on the skin in back-to-back pairs parallel to the frames to capture local skin buckling behavior. In these figures, the strain gauges on the unstiffened side of the panel are represented by solid curves, and the strain gauges on the stiffened side of the panel are represented by dashed curves. The colored boxes on the inset image of each panel show the location of a back-to-back pair. These results indicate that the keel panel buckles between the stiffeners at a load of approximately 40 kips and that the floor panel buckles between the stiffeners at a load of approximately 50 kips. Nevertheless, the magnitude of the strains in the buckled regions never exceeded 0.002 in./in.

The strains chosen to monitor the behavior in the down-bending load case never exceed the design allowable values, and did not indicate any failures in the regions where down-bending significantly contributed to the design.

Up-bending load case

The up-bending load case applies a combination of compression and bending into the crown, shear load into the bulkheads, and tension loads into the keels. Strain gauges on the crown, center keel, side keels, and upper bulkheads were located to capture behavior in the up-bending load case. These strains are shown in Figures 43 through 51.

Strain gauge results for the crown panel skin between the stiffeners in back-to-back pairs parallel to the frames are shown in Figures 43 and 44. In these figures, the strain gauges on the unstiffened side of the panel are represented by solid curves and the strain gauges on the stiffened side of the panel are represented by dashed curves. The colored boxes on the inset image of each panel show the location of a back-to-back pair. These results indicate that the crown panel skin begins to deform out-of-plane immediately after loading begins in most bays. Nevertheless, the magnitude of the strains in the buckled regions never exceeds 0.004 in./in. Initial imperfections in the panel geometry and the patches to the outer surface influence the deformation shape. As discussed previously, the mode shapes do not change through the course of loading.

Strain gauge results for the crown panel skin on the stiffened (interior) side near the outer frame flanges and halfway between the stringers are shown in Figure 45. These strain gauges were rosettes measuring strain parallel to the frame, perpendicular to the frame and at a 45-degree angle to the frame. The solid curves represent the gauge toward the forward side of the test article, and the dashed curves represent the gauge toward the aft side of the test article. These measurements show that the largest magnitude of these strains is parallel to the frame and does not exceed 0.006 in./in. This strain exceeds the design allowable strain of -0.0048 in./in. for damaged structure, but not the unnotched (pristine) allowable of -0.008 in./in. Since the skin in the crown is expected to buckle locally without causing damage to the structure, and any damage at this location would be unable to spread into the stiffeners because it would be arrested at stitch lines, no damage was anticipated despite the high strain. No visible damage was evident.

Strain gauge results for the crown panel frames are shown in Figures 46 and 47. Strain gauges were placed on the center frame web approximately 0.3-inches away from the keyhole and parallel to the frame. The results for these strain gauges are shown in Figure 46 at the locations indicated by the colored boxes shown in the inset image of the crown panel. The solid curve represents the strain at the center stringer, the short dashes represent the strain at the stringers toward the stationary platen, and the long dashed curves represent the strain toward the loading platen. The keyhole strains did not exceed a magnitude of 0.004 in./in.

Strain gauges were placed on the crown frames on the web approximately one inch from the top of the frame and oriented parallel to the frame. The results for these gauges are shown in Figure 47 at the locations indicated by the colored boxes in the inset image of the crown panel. The solid curve represents the strain on the forward face of the frame, and the dashed curves represent the strains at the stringers on the aft face of the frame. The strains do not exceed a magnitude of 0.004 in./in.

Strain gauges were placed on the center keel frame webs approximately 0.3-inches away from the keyhole and parallel to the frame. The results for these strain gauges are shown in Figure 48 at the locations indicated by the colored boxes in the inset image of the keel panel. The keyhole strains do not exceed a magnitude of 0.002 in./in.

Strain gauges were placed at the top of the side keel center frame oriented parallel to the frame. The results for these gauges are shown in Figure 49 at the locations indicated by the colored boxes in the inset image of the side keel panel. The solid curve represents the strains on the left side keel (toward the stationary platen) and the dashed curves represent the strains on the right side keel (toward the loading platen). The colors on the inset image correspond to the curves on the plot. The blue curve represents strains at the connection to the inner rib, where the strain is positive, but less than 0.004 in./in.

Strain gauges were placed on the skin of the upper bulkhead panel on the unstiffened (exterior) side near the connection to the crown panel in three quadrants of the test article (the fourth similar location was in the region where full-field data were acquired). Results for these strain gauges are shown in Figures 50 and 51. These strain gauges were rosettes measuring strain parallel to the frame, perpendicular to the frame, and at a 45-degree angle to the frame. The colors of the curves on the plot correspond to the strain gauges shown in the inset image of the crown panel and the solid curves represent the gauge toward the aft side of the test article. The long and short dashed curves represent the gauges toward the forward side of the test article closer to the loading platen and the

stationary platen, respectively. These measurements show that the largest magnitude of these strains is parallel to the frame and does not exceed 0.004 in./in. The strain in the direction parallel to the stringer indicates that the skin between the stiffeners buckled at this location at a load of approximately 155 kips.

The strains used to monitor the behavior in the up-bending load case never exceed the design allowable values, and did not indicate any failures in the regions where up-bending significantly contributed to the design.

Pressure-only load case

The pressure-only load case applies internal pressure to the entire test article, which pushes all panels outward except the floor and inner ribs. Strain gauges on the crown, center and side keels, upper and lower bulkheads, and inner and outer ribs were located to capture behavior in the pressure-only load case. These strains are shown in Figures 52 through 78.

One of the key features of PRSEUS is the way in which panels are connected together. The crown, keels and upper bulkheads contain integral T-caps, where an up-standing stiffener is constructed near the edge of the panel so that its adjacent panel can be connected with a minimum number of fittings and fasteners. A T-cap in an upper bulkhead panel is shown in Figure 3. This construction approach is valuable for unitized structure, but introduces loading into the T-cap in a way that is not typical of composite assemblies. Therefore, strain gauges were added to the critical T-cap locations. The results for these strain gauges for the crown forward and aft T-caps are shown in Figure 52. Strain gauges were located perpendicular to the crown skin next to selected stringer webs and parallel to the crown skin at the edge of the T-cap, as shown in the insets in the figure. Strain gauge locations are shown in Figure 52, as indicated by the colored boxes in the inset image. The solid and long dashed curves represent strain gauges perpendicular to the crown on the forward and aft T-caps, respectively. The short dash and dotted curves represent strain gauges parallel to the crown on the forward and aft T-caps, respectively. The strains in the T-cap near the stringer webs remain less than 0.002 in./in. in magnitude. The strains at the T-cap edge are extremely small. Crown T-cap strain gauge results remain linear, and show no discontinuities that could indicate damage in the test article.

Strain gauge results for the crown panel stringers are shown in Figures 53 and 54. Strain gauges were placed on the top of the stringer parallel to the rod and adjacent to the keyhole. The results for these gauges are shown in Figure 53 at the locations indicated by the colored boxes in the inset sketch of the crown panel. Strain gauges are located at the center stringer and the first three stringers outboard of the center stringer, toward the loading and stationary platens. The flange of the second stringer away from the center stringer in each direction is attached to an external fitting. The photograph in Figure 53 shows the stringer-frame intersection, and includes a fastener for an external fitting. The other stringer-frame intersection locations look the same as this location, except that no fastener is present. The solid curve represents the strain at the center stringer and the long dashes represent the strain at the first stringer outboard from the center stringer. In the plot, the dashes in the curves get shorter as the location is farther away from the center stringer. The strains on the top of the stringer do not exceed 0.004 in./in. In

general, the closer to the center, the higher the strain; however, the strains where an external fitting is present are significantly less than the strains where there is no external fitting.

Strain gauge rosettes were placed on the webs of the stringers near the center of the crown panel near their intersection with the forward and aft frames. The results for these strain rosettes are shown in Figure 54. The rosettes are oriented such that measurements are taken perpendicular to the rod and at $\pm$45 degrees to the rod. These locations are indicated by the gray boxes on the crown panel sketch in the figure. The colors of the curves in the plot indicate the direction of the measurement and the frame. Solid curves represent strains on the center stringer and dashed curves represent strains on the first and second stringer outboard from the center stringer in the direction of the stationary platen and the direction of the loading platen. The strains in the web do not exceed 0.003 in./in. in magnitude. The strains in the stringers at the external fittings are substantially less than the strains in the other stringers.

Strain gauge results for the crown panel frames are shown in Figures 55, 56, and 57 at the locations indicated by the colored boxes in the inset sketches of the crown panel in each figure. Results for strain gauges on the frame webs approximately 0.3 inches away from the keyhole and parallel to the frame top are shown in Figures 55 and 56. Strains at the center frame are shown in Figure 55, and strains on the forward and aft frames are shown in Figure 56. Strains near the keyhole are represented by solid curves and strains on the top of the frame are represented by dashed curves. The strains near the keyhole are extremely small, and the strains at the top of the frame do not exceed a magnitude of 0.002 in./in. Strains on the external surface at the location of the center frame and parallel to the frame are shown in Figure 57 at the center of the panel and two outboard locations. At DUL, these strains are less than 0.001 in./in.

The results for strain gauges on the center keel are shown in Figure 58 for the forward and aft T-caps, Figure 59 for the top of the stringer at the forward and aft frames, Figure 60 for the stringer webs, and Figure 61 for the top of the center frame. Strain gauges were located perpendicular to the center keel skin next to selected stringer webs as shown in the sketch in Figure 58. Strain gauge locations are shown in the figure as indicated by the colored boxes in the inset sketch. The solid and dashed curves represent strain gauges on the forward and aft T-caps, respectively. The magnitude of the strains in the T-caps near the stringer webs remains less than 0.002 in./in. Center keel T-cap strain gauge results remain linear, and show no discontinuities that could indicate damage to the test article.

Strain gauge results for the center keel panel stringers are shown in Figures 59 and 60. Results for strain gauges placed on the top of the stringer parallel to the rod and adjacent to the keyhole are shown in Figure 59 at the locations indicated by the colored boxes in the inset sketch of the keel panel. Strain gauges at the top of stringers were located at the center stringer, and the first three stringers outboard from the center stringer toward the loading and stationary platens. The flange of the second stringer away from the center stringer in each direction was attached to an external fitting. The solid curve represents the strain at the center stringer, the long dashes represent the strain at the first stringer outboard from the center stringer, with the dashes getting shorter the farther away from the center stringer. The strains at the top of the stringer do not exceed 0.004 in./in. In general, the locations closer to the center have higher strains. However,

the strains where an external fitting is present are significantly less than the strains where there is no external fitting. The strain in the center stringer near the aft frame records a linear strain but at a greater magnitude than the center stringer near the forward strain. Additionally, the strain gauge at the aft frame records a discontinuity in the slope of the strain data at approximately 16 psi and at approximately 18 psi. This area was examined after the test, but no damage was seen.

Strain gauge rosettes were placed on the webs of the stringers near the center of the center keel panel near their intersection with the forward and aft frames. The rosettes are oriented such that measurements were taken perpendicular to the rod and at $\pm$45 degrees to the rod. The results for these strain gauges are shown in Figure 60 at the locations indicated by the gray boxes on the crown panel sketch in the figure. The colors of the curves in the plot indicate the direction of the measurement and the frame. Solid curves represent strains on the center stringer, whereas dashed curves represent strains on the first and second stringer outboard from the center stringer in the direction of the stationary platen and the direction of the loading platen. The strains in the web do not exceed 0.003 in./in. in magnitude. The strains in the stringers at the external fittings are substantially less than the strains in the other stringers.

Strain gauge results for the center frame of the center keel panel are shown in Figure 61 at the location indicated by the red box in the inset sketch of the center keel panel in the figure. Strains were measured at the top of the frame and on the external surface parallel to the frame. These strains do not exceed a magnitude of 0.0025 in./in.

Strain gauge results for the side keel panels are shown in Figures 62 through 66. Strains in the panel skin between the stiffeners in back-to-back pairs parallel to the frames are shown in Figure 62 at the locations shown on the inset sketches of the side keel panel in the figure. The strain gauges on the unstiffened side of the panel are represented by solid curves and the strain gauges on the stiffened side of the panel are represented by dashed curves. The colored boxes on the inset image of each panel show the location of a back-to-back pair. Results for both side keel panels are shown. These results indicate that the skin begins to deform out-of-plane immediately after loading begins in a nonlinear manner. Nevertheless, the magnitude of the strains between the stiffeners never exceeds 0.0025 in./in.

The results for strain gauges on the side keels forward and aft T-caps are shown in Figures 63. Strain gauges were located perpendicular to the side keel skin next to the second stringer from the inboard edge near the stringer webs, as shown using the gray box in the sketch in Figure 63. Four gauges were located at symmetric locations on the left and right side keels, forward and aft. The blue curves represent strain on the side keel near the stationary platen and the red curves represent strain on the side near the loading platen. The solid and dashed curves represent strain gauges on the forward and aft T-caps, respectively. The forward and aft strains were so similar that the solid and dashed curves on the plot are almost indistinguishable from one another. The magnitude of the strains in the T-caps remains less than 0.002 in./in. in magnitude. Side keel T-cap strain gauge results remain linear, and show no discontinuities that could indicate damage to the structure.

Strain gauge results for the stringers of the side keel panels are shown in Figure 64. Strain gauges were placed on the top of the stringer in the locations marked with the gray boxes in the inset sketch of a center keel in the figure. Strain gauges were located on top

of the stringers 4, 8, and 12 stringers outboard from the inner rib toward the loading and stationary platens, and at the forward and aft frames. The solid curves represent the strains at the fourth stringer from the inner rib. The long dashes represent the strains at the eighth stringer outboard from the center rib, and the short dashes represent the strains at the twelfth stringer outboard from the center rib, near the interior strut fitting. Blue and light blue curves represent the strains near the forward frame toward the stationary and loading platens, respectively. Red and orange curves represent the strains near the aft frame toward the stationary and loading platens, respectively. The strains at the top of the stringer do not exceed 0.004 in./in. In general, the locations closer to the center have higher strains.

Strain gauge results for the center frame of the side keel panels are shown in Figure 65 at the location indicated by the gray box in the inset sketch of a side keel panel in the figure. Strains were measured at the top of the frame and on the external surface parallel to the frame. Blue and red curves represent the strains in the keel near the stationary and loading platens, respectively. Strains on the unstiffened (exterior) surface are represented by solid curves, and strains on the frames are represented by dashed curves. These strains do not exceed a magnitude of 0.0025 in./in.

Strain gauge results for the center frame webs of the side keel panels are shown in Figure 66 at the locations indicated by the gray boxes in the inset sketch of a side keel panel in the figure. Strains in the frame web facing the aft bulkhead are shown in dashed curves and strains in the frame web facing the forward bulkhead are shown in solid curves. Strain gauges on the inboard location are near the top of the frame, while strains on the outboard location are near the bottom of the frame web. Blue and light blue curves represent the strains in the outboard strain gauge, while red and orange represent strains closer to the center keel. These strains remain linear throughout loading and do not exceed a magnitude of 0.004 in./in.

Strain gauge results for the upper bulkhead panels are shown in Figures 67 through 71. Results for the panel skin between the stiffeners in back-to-back pairs parallel to the frames are shown in Figure 67 at the locations shown, as indicated by the gray boxes on the inset sketch of an upper bulkhead panel in the figure. The strain gauges on the unstiffened (exterior) side of the panel are represented by solid curves and the strain gauges on the stiffened side of the panel are represented by dashed curves. A different color is used for each pair, for example the strain gauges in the center of the aft upper bulkhead panel above the access door are represented by blue curves. These results indicate that the skin begins to deform out-of-plane in a nonlinear manner immediately after loading begins. Nevertheless, the magnitude of the strains between the stiffeners never exceeds 0.0025 in./in.

Strain gauge results at the top of three stringers in the upper bulkhead panels are shown in Figure 68. Strain gauges were placed on the top of the stringer, parallel to the rod and near the keyhole. The results for these gauges are shown in Figure 68 at the location indicated by the gray boxes in the inset sketch, where only half of one bulkhead panel is shown since the other locations are symmetric. The fourth strain gauge at these symmetric locations is not shown since the gauge stopped functioning early in the test sequence. The strains at the top of the stringer do not exceed 0.006 in./in.

Results for strain gauges on the frames near the keyholes and parallel to the frames on the upper bulkheads are shown in Figures 69 and 70. Results for the frames adjacent to

the access doors are shown in Figure 69, and strains at the frame outboard from the inner rib are shown in Figure 70. Strain gauges were placed near the floor, near the crown, and just above the access door. The locations for the strain gauges near the center of the panel are indicated by the colored boxes in the inset sketch of an upper bulkhead panel in Figure 69. Strains on the aft bulkhead panel are represented by solid curves and strains on the forward bulkhead panel are represented by dashed curves. The locations of the strain gauges outboard of the inner rib near the floor and near the crown are represented by the gray boxes on the inset sketch in Figure 70, where these boxes represent symmetric locations toward each platen and on each bulkhead. These keyhole strains do not exceed a magnitude of 0.001 in./in. In most locations, these strain gauge results remain linear and show no discontinuities that would indicate a failure. However, the strain gauges on the frames near the access doors on the aft bulkhead near the floor, on the forward bulkhead near the crown, and on the outboard aft bulkhead near the crown show some anomalies, but no visible damage could be found at these locations.

Strain gauge results for frames of the upper bulkhead panels are shown in Figure 71 at the locations indicated by the gray boxes in the inset sketch of an upper bulkhead panel in the figure. Strains were measured at the top of the frame and on the external surface parallel to the frame. Strains on the unstiffened (exterior) surface are represented by solid curves and strains on the frames are represented by dashed curves. These strains do not exceed a magnitude of 0.005 in./in.

Strain gauge results for the lower bulkhead panels are shown in Figures 72 through 75. Results for the panel skin between the stiffeners in back-to-back pairs parallel to the frames are shown in Figure 72 at the locations shown with gray lines on the inset sketch of a lower bulkhead panel, where only half of one bulkhead panel is shown since the other locations are symmetric. The strains on the unstiffened (exterior) side of the panel are represented by solid curves and the strains on the stiffened side of the panel are represented by dashed curves. A different color is used for each pair. These results indicate that the skin begins to deform out-of-plane in a nonlinear manner immediately after loading begins. Nevertheless, the magnitude of the strains between the stiffeners never exceeds 0.003 in./in.

Strain gauge results for four stringers in the lower bulkhead panels are shown in Figure 73. Strain gauges were placed on the top of the stringer, parallel to the rod. The results for these strain gauges are shown in Figure 73 at the location indicated by the gray box in the inset sketch, where only half of one bulkhead panel is shown since the other locations are symmetric. The strains in the top of the stringer do not exceed 0.004 in./in.

Results for strain gauges on the frames on the lower bulkheads at the frames adjacent to the access doors are shown in Figures 74 and 75. Strain gauges were placed near the keel, adjacent to the floor, and just below the access door. Strains near the keyholes, parallel to the frames, are shown in Figure 74 at the locations indicated by the gray box in the inset sketch, where only half of one bulkhead panel is shown since the other locations are symmetric. Strains on the aft bulkhead panel are represented by solid curves and strains on the forward bulkhead panel are represented by dashed curves. These keyhole strains do not exceed a magnitude of 0.002 in./in. These strain gauge results remain linear through most of the loading range, and show no discontinuities that would indicate a failure.

Strain gauge results for frames of the lower bulkhead panels are shown in Figure 75 at the location indicated by the gray box in the inset sketch of a lower bulkhead panel in the figure. Strains were measured at the top of the frame parallel to the frame. Strains on the aft bulkhead are represented by solid curves and strains on the forward bulkhead are represented by dashed curves. These strains do not exceed a magnitude of 0.005 in./in.

Strain gauge results in the upper and lower inner ribs are shown in Figures 76 and 77, respectively. Linear strain gauges were located on the inner ribs at the corners of the cutouts. Strain gauge rosettes were placed along one edge just above the bottom and just below the top near the long edge of the cutout, with the rosette oriented with one gauge parallel with the opening and the others at $\pm$45-degree angles to the cutout edge. The colors of the curves in the plots in Figures 76 and 77 correspond to the rosettes sketched on the photographs at the strain gauge locations shown. Strains just above the bottom of the cutout and parallel to the long edge of the cutout are shown. These strains do not exceed a magnitude of 0.0025 in./in.

Strains in the outer ribs are shown in Figure 78. Strains in the skin, in the center frame, and at the top of a stringer are shown. The colored boxes on the inset sketch of the outer rib panel in the figure show the location of the gauges. Strains in the outer rib at the stationary platen are represented by solid curves and strains in the outer rib at the loading platen are represented by dashed curves. These strains do not exceed a magnitude of 0.004 in./in.

Combined bending and pressure load cases

When combining pressure with mechanical load, the strain can increase or decrease, depending on the location in the structure. Internal pressure can reduce the amount of inward deformation in the thin skin under compressive mechanical loading, but it pushes the stiffeners and joints outward. However, except for three locations, the strains shown in Figures 41 through 78 for the pristine structure are less than 0.004 in./in. in magnitude. So, except for those locations, the strains are significantly less than the allowable strain values of 0.0059 in./in. in tension and -0.0048 in./in. in compression for notched or damaged structure, and therefore not critical. The strains shown in Figure 68 and 71 for the upper bulkhead in the pressure-only load case are greater in magnitude than 0.004 in./in, so these strains warrant examination in the combined mechanical loading with pressure- load conditions. Additionally, the strain in one leg of the rosette strain gauge on the crown shown in Figure 45 for the up-bending load case should be examined.

The strains on the top of the stringers that are shown in Figure 68 and at the frame locations shown in Figure 71 for the up-bending condition are repeated in Figures 79 and 80, respectively. The strains for the same locations are shown for the up-bending plus pressure condition in Figures 79 and 80. The same color scheme is used in these figures as in the earlier figures, but the new data are shown in additional dashed curves. Note that in the combined load case, the maximum pressure is 13.8 psi rather than the 18.4 psi in the pressure-only load case. There is no discernable difference for these strains between the two load cases. Therefore, it is clear that the pressure load influences these strains more than the mechanical loading. The strains on the top of the stringer rod do not exceed 0.006 in./in., and the strains at the top of the frame and on the external surface in parallel to the frame do not exceed a magnitude of 0.005 in./in.

The strains shown in the skin in the outboard area shown in Figure 45 for the up-bending condition are shown in Figure 81 along with the strains for the up-bending plus pressure condition. The same color scheme is used in Figure 81 as in Figure 45, with the new data shown as additional dashed curves. The strains in the combined-load case are slightly greater than the strains in the up-bending load case. Therefore, it is clear that the mechanical load influences these strains more than the pressure loading. As for the up-bending load case, this strain exceeds the design allowable strain of -0.0048 in./in. for damaged structure. No visible damage was evident.

Impact sites

After the pristine tests were completed, the test article was subjected to six barely visible impacts. Strain gauges were added in the vicinity of each impact site and then the structure was again loaded to DUL in all five loading conditions. The strain at each impact site is shown in Figures 82 through 89. For each load case, strains are shown for the three interior impacts (to the forward upper bulkhead) followed by the strains at the three exterior impacts (to the center keel). The locations of the impacts are shown in the inset photograph with the yellow symbols representing the locations of the three types of impacts, as previously described with the impact methodology description. Two or four strain gauges were added near each impact site after the application of impact damage to enable the tracking of damage emanating from the impact site. The results are presented first for the down-bending load case, followed by the down-bending plus pressure load case, then the up-bending load case, and, finally, the pressure-only load case. The up-bending plus pressure load case to DUL was combined with the test to loading greater than DUL, so those results are presented together. Results are presented for each load case: first for the interior impacts and then for the exterior impacts.

In each strain plot for the interior impacts, solid curves represent strains in the top of the stiffener, and dashed curves represent strains in the skin. Red and pink solid curves represent strains on the top of the frame, and blue and light blue solid curves represent strains on the top of the stringer. Red and pink dashed curves represent strains on the skin on the interior of the test article, while blue and light blue dashed curves represent strains on the skin on the exterior of the test article.

In each strain plot for the exterior impacts, solid curves represent strains at the frame flange impact, long dashed curves represent strains in the stringer flange impact, and the short dashed curves represent strains near the mid-bay skin impact. Red and pink curves represent strains on the exterior of the test article, and blue and light blue represent strains on the interior of the test article.

Most strains in the vicinity of the impacts remain linear throughout the loadings. The three exceptions are: 1) the center keel skin gauges at the mid-bay impact in the down-bending and down-bending with pressure loading conditions, 2) in the center keel stringer flange gauges in the down-bending and down-bending with pressure loading conditions, and 3) in the skin near the mid-bay impact in the up-bending and up-bending plus pressure conditions. These regions are in the buckling areas and there is no indication that the impacts had a significant influence on the behavior at these locations. In all load cases, the strains never exceed the allowable values of 0.0059 in./in. in tension and -0.0048 in./in. in compression for damaged structure. Strains at the impact sites for the

down-bending, down-bending plus pressure, and up-bending and pressure-only load cases do not exceed the damaged allowable values and no damage growth is evident.

The last loading of the test article with BVID where it was required to support DUL was to a load of 10% greater than DUL in the up-bending and up-bending plus pressure load cases. The loading sequence is described in Figure 20, which shows the initial loading to DUL in the up-bending plus pressure condition, followed by an increase in mechanical load but no increase in pressure. Then, mechanical loading was reduced back to DUL and pressure was reduced to zero. Finally, the mechanical load was then increased to 10% greater than DUL. The strains at the impact sites for this test are shown in Figures 90 and 91 for the interior and exterior impact sites, respectively. Strains at the interior sites remain at less than 0.004 in./in. in magnitude.

The effect of the combination of loads can clearly be seen, since at the interior impact sites the strain does not increase as mechanical load increases whether pressure is present or not, implying that pressure is the driving factor in the upper bulkhead at these locations. Most notably, the top of the frame is subjected to a significant compression load; when pressure stops increasing, strain stops increasing. Alternately, a different response is seen for the exterior impact sites. The largest strains are at the stringer flange impact sites where the exterior strain gauges recorded an increase in strain through DUL even though pressure was held constant between 238 kips and 265 kips. The difference in behavior is based more on the difference in loading in the two locations than the presence of impact damage.

Another behavior to consider is the strains in the crown skin at mid-bay locations, as shown in Figure 92, using the same color scheme and curve type as described for Figure 43. These results show that there is a change in buckle pattern early in the loading sequence, evidenced by the reversal in direction of the mid-bay back-to-back strain gauge results for the four mid-bay strain gauges closest to the center of the panel. After this reversal, strains increase in magnitude smoothly until the maximum mechanical load is reached, then decrease in magnitude as mechanical load is removed. Then, they change direction as pressure is removed. i.e., the tension surface goes into compression and the compression surface goes into tension. Finally, the strains increase again in magnitude, but at significantly less magnitude as the mechanical load is increased when no pressure is present. In order to clarify the behavior, consider the results using one back-to-back pair. The dark blue dashed and solid curves are an example of interior and exterior mid-bay strains. Each strain reverses direction at approximately 20 kips. Then, the strain magnitude increases smoothly until the maximum mechanical load is achieved, even though the pressure loading was not increased after 138 kips. At the maximum mechanical load, the strain decreases in magnitude on almost the same path as it went up. However, when the pressure load is removed, the strains reverse direction while the mechanical load is held, indicating that the buckle in that bay has changed from outward (the exterior strain is in tension) to inward (the exterior strain is in compression). This change in deformation pattern is evident in the full-field measurements shown in Figure 93, where the deformation at 110% DUL is shown with internal pressure and without internal pressure. All deformation half-waves are outward when internal pressure is present while, for the most part, the half-waves alternate in direction when pressure is not present.

Finally, the only other high strains are shown in Figures 94 and 95, where strain in the crown is shown in the center frame web, and at the skin strain rosettes, respectively. The linear nature of the frame web behavior for strains on the front face and the back face indicates that the frame does not buckle. Strains on the webs of the center frame of the crown panel exhibit relatively high strains, as shown in Figure 94. These strains remain linear throughout each phase of testing and do not indicate any buckling or rolling of the frames.

The mid-bay skin gauges whose results are shown for the up-bending load case are shown in Figure 95 for the loading greater than DUL. Strains are greater than the design allowable, but no damage is evident. The maximum strain in the rosette is large but does not show any indication of failures in this area. No visible damage growth was observed at any of the impact sites following the DUL or over DUL tests. Additionally, ultrasonic scans performed in between loadings found no growth in damage compared to the damage found immediately following the impacts.

Fittings

Metal fittings were used to assemble the test article and to attach it to the test fixture. Some of these fittings were monitored. As with the composite parts of the test article, strain gauge locations were selected based on predictions from a specific load case. The fitting strain gauge results presented herein are the results for each fitting strain gauge for the load case which was used to select that location. Only the up-bending and pressure-only load cases were critical in determining strain gauge locations on the fittings. Since the test article is largely symmetric widthwise and lengthwise, there are four instances of each fitting that could be of concern. Therefore, the four gauges for the symmetric location are grouped together in the fitting strain plots. One example of the general area of each fitting is shown in Figure 13, where the labels are be referenced in the descriptions of the fitting behavior. Strains for metal fittings are shown in Figures 96 through 105, in which the aft side of the test article at the stationary platen is represented by the blue curve, the aft side of the test article at the loading platen is represented by the red curve, the forward side of the test article at the stationary platen is represented by the light blue curve, and the forward side of the test article at the loading platen is represented by the orange curve.

Two fitting types were potentially critical for the up-bending case; both were external fittings in the load introduction areas. Strains in the fittings at the crown-bulkhead connection at the corner where load is introduced into the test article, labeled A in Figure 13, are shown in Figure 96. Strains in the fittings at the floor-bulkhead connection at the corner where load is introduced into the test article, labeled B in Figure 13, are shown in Figure 97. In the upper load introduction fittings, the strain gauge was placed at the edge of the flange of the fitting. In the lower load-introduction fittings, one strain gauge was placed at the edge of the flange of the fitting and one strain gauge was placed immediately adjacent to that strain gauge to determine if there was a significant strain gradient in that region. None of these gauges in the upper fittings recorded strains with magnitude greater than 0.001 in./in. However, the gauges in the lower fittings recorded strains up to approximately 0.006 in./in. Nevertheless, the strains were not large enough to indicate any failures or plastic behavior.

Two external fitting types were potentially critical for the pressure-only load case. These fittings were at the taper in the fitting on the unstiffened surface of the center keel, labeled C in Figure 13, and on the unstiffened surface of the crown labeled D in Figure 13, as shown in Figures 98 and 99, respectively. These fittings were the fittings closest to the center of the panels. Strains remained linear and did not exceed a magnitude of 0.004 in./in.

Six internal fittings types were potentially critical for the pressure-only load case. These fittings were at the connection between the floor and the lower bulkhead. (labeled E in Figure 13), the connection between the side keel and the lower bulkhead (labeled F and G), and at the internal struts (labeled H, I, and J).

The strain in the fitting connecting the floor stringer to the aft lower bulkhead is shown in Figure 100. The strain gauge was on the edge of the fitting. While the measured strains remained linear through most of the load range and were low enough to indicate that no damage occurred to the fitting itself, the discontinuities in slope in all four fittings indicate that there was one or more failures or shifts in position of the structure somewhere near these fittings. These shifts took place between 14 psi and 18 psi. No visible damage could be seen in this region in the interior or exterior of the structure after the test was completed.

The strain in the elements connecting the bulkhead and side keel is shown in Figure 101 and between the inner rib and the side keel near the bulkhead are shown in Figure 102. All these strains were nearly linear and less than 0.006 in./in.

The strain in the strut fittings and the struts that connect the outer ribs to the upper bulkheads are shown in Figures 103, 104, and 105. While the strains in the adapters connected to the struts are not linear, they remain less than 0.001 in./in. The strains in the struts themselves remain linear and remain less than 0.002 in./in. These strain values are low enough that no damage occurred in these fittings.

IX. Concluding Remarks

For more than 20 years, NASA and Boeing have been developing technology to improve damage tolerance and reduce the weight of composite structures for commercial transport aircraft applications through the use of through-the-thickness stitching. Most recently, under the NASA ERA Project, a partnership between NASA and Boeing has advanced this technology in an attempt to encourage and enable advanced aircraft configurations such as the HWB design.

Stitching through the thickness has been shown to suppress delaminations, arrest damage, and reduce or eliminate the need for fasteners in the acreage of composite panels. Removing the need for fasteners eliminates the need to drill holes, the need to add doublers to account for stress concentrations around holes, and the need to inspect fastener holes through the life of the aircraft.

In the current stitched structural concept, PRSEUS, the addition of a pultruded rod to the stringer in one direction and a tall foam-filled frame perpendicular to the stringer improves the bending stiffness in both directions compared to traditional construction, which is critical to the HWB configuration. PRSEUS also provides efficient load paths by integrating all panel elements into one unit prior to cure, which eliminates the need for shear clips and other added elements that add weight to the structure. The PRSEUS panel

architecture is a significant step beyond state-of-the-art conventional layered composite systems.

A building-block test program starting with coupons and ending with a 30-foot-long large-scale pressure box test has been successfully executed to demonstrate the viability of a PRSEUS center body for the HWB transport aircraft. This building block test program included testing and analysis of numerous PRSEUS test articles, so that designs could be refined and the risk of premature failure could be reduced as more complex parts were introduced to demonstrate the PRSEUS capabilities.

This final step in the building-block process is the 80%-scale multi-bay pressure box tested in the COLTS Facility at NASA Langley Research Center. The multi-bay pressure box has been fabricated from PRSEUS panels and has undergone testing under combined load conditions representative of critical flight conditions. This test article has been subjected to up-bending and down-bending flight-maneuver load conditions and internal pressurization in a ground-test program that demonstrates that the technology is capable of meeting the structural weight goals established for the HWB airframe. The test article was loaded to DUL in all critical conditions in the pristine conditions and then again after imparting BVID to the interior and exterior of the test article. The test article demonstrated post-buckling behavior as anticipated, and no damage growth from the impact sites was detected in a preliminary evaluation. All DUL testing has been completed and test results demonstrate the viability of the PRSEUS concept for HWB center section-type structure. While this development program was aimed at demonstrating PRSEUS viability for the HWB center body, the benefits demonstrated could also be applied to traditional tube-and-wing aircraft configurations, other advanced configurations, spacecraft, and other structures where weight and through-the-thickness strength are design considerations.

References

1. Liebeck, R., "Design of Blended Wing Body Subsonic Transport," *Journal of Aircraft*, Vol. 41, No. 1, January-February, 2004, pp. 10-25.
2. Velicki A., and Thrash P.J., "Advanced Structural Concept Development Using Stitched Composites," 49th AIAA/ASME/ASCE/AHS/ASC Structures, Structural Dynamics, and Materials Conference, Paper Number AIAA-2008-2329, June 2008, Schaumburg, IL.
3. Jegley, D. C., Velicki, A., and Hansen, D. A., "Structural Efficiency of Stitched Rod-Stiffened Composite Panels with Stiffener Crippling," Proceedings of the 49th AIAA/ASME/ASCE/AHS/ASC Structures, Structural Dynamics and Materials Conference, AIAA-2008-2170, 2008, Schaumburg, IL.
4. Velicki, A., "Damage Arresting Composites for Shaped Vehicles, Phase I Final Report," NASA CR-2009-215932, September 2009, NASA Langley Research Center, Hampton, VA.
5. Velicki, A., Yovanof, N. P., Baraja, J., Linton, K., Li, V., Hawley, A., Thrash, P., DeCoux, S., and Pickell, R., "Damage Arresting Composites for Shaped Vehicles – Phase II Final Report," NASA CR-2011-216880, January 2011, NASA Langley Research Center, Hampton, VA.

6. Karal, M., "AST Composite Wing Program - Executive Summary," NASA CR 2001-210650, March 2001, NASA Langley Research Center, Hampton, VA.
7. Yovanof, N., and Jegley, D., "Compressive Behavior of Frame-Stiffened Composite Panels," 52nd AIAA Structures Dynamics and Materials Conference, Paper Number AIAA-2011-1913, April 2011, Denver, CO.
8. Gould, K., Lovejoy, A., Neal, A., Linton, K., Bergan, A., and Bakuckas Jr, J., "Nonlinear Analysis and Post-Test Correlation for a Curved PRSEUS Panel," 54th AIAA Structures, Structural Dynamics, and Materials Conference, Paper Number AIAA-2013-1736, April 2013, Boston, MA.
9. Jegley, D., "Structural Efficiency and Behavior of Pristine and Notched Stitched Structure," presented at SAMPE Fall Technical Conference, October 2011, Fort Worth, TX.
10. Jegley, D., "Behavior of Frame-Stiffened Composite Panels with Damage," 54th AIAA Structures, Structural Dynamics, and Materials Conference, Paper Number AIAA-2013-1738, April 2013, Boston, MA.
11. Allen, A., and Przekop, A., "Vibroacoustic Characterization of a New Hybrid Wing-Body Fuselage Concept," INTER-NOISE 2012 Conference, August 19–22, 2012, New York City, NY.
12. Lovejoy, A., Rouse, M., Linton, K., and Li, V., "Pressure Testing of a Minimum Gauge PRSEUS Panel," 52nd AIAA Structures Dynamics and Materials Conference, Paper Number AIAA-2011-1813, April 2011, Denver, CO.
13. Yovanof, N., Baraja, J, Lovejoy, A., Gould, K., "Design, Analysis, and Testing of a PRSEUS Pressure Cube to Investigate Assembly Joints," 2012 Aircraft Airworthiness & Sustainment Conference, Paper Number TP5431, April 2012, Baltimore, MD.
14. Przekop, A., "Repair Concepts as Design Constraints of a Stiffened Composite PRSEUS Panel," Proceedings of the 53rd AIAA/ASME/ASCE/AHS/ASC Structures, Structural Dynamics and Materials Conference, AIAA-2012-1444, May 2012, Honolulu, HI.
15. Velicki, A., "Damage Arrest Design Approach with Composite Materials," presented at the Aging Aircraft Conference, Kansas City Convention Center, May 4-7, 2009, Kansas City, KS.
16. Velicki, A. and Thrash, P., "Damage Arrest Design Approach Using Stitched Composites," 2nd Aircraft Structural Design Conference, October 26–28, 2010, London, England.
17. Velicki, A. and Thrash, P., "Damage Arrest Design Approach Using Stitched Composites," *The Aeronautical Journal*, Vol. 115. pp. 789-795.
18. Linton, K., Velicki, A., Hoffman, K., Thrash, P., Pickell, R., and Turley, R., "PRSEUS Panel Fabrication Final Report," NASA-CR-2014-218149, January 2014, NASA Langley Research Center, Hampton, VA.
19. Thrash, P., "Manufacturing of a Stitched Resin Infused Fuselage Test Article," presented at SAMPE Fall Technical Conference, October 2014, Dallas, TX.
20. Velicki, A., Linton, K., and Hoffman, K., "Fabrication of Lower Section and Upper Forward Bulkhead Panels of the Multi-bay Box and Panel Preparation," Final Report, Contract NNL10AA05B, Task Order NNL13AB38, March 2015, NASA Langley Research Center, Hampton, VA.

21. Velicki, A., Hoffman, K., Linton, K., Baraja, J., Wu, H., Thrash, P., "Hybrid Wing Body Multi-Bay Test Article Analysis and Assembly," Final Report, Contract NNL10AA05B, Task Order NNL11AA68T, July 2015, NASA Langley Research Center, Hampton, VA.
22. Wu, H. T., Shaw, P., and Przekop, A., "Analysis of a Hybrid Wing Body Center Section Test Article," 54th AIAA Structures, Structural Dynamics, and Materials Conference, Paper Number AIAA-2013-1734, April 2013, Boston, MA.
23. Przekop, A., Wu, H. T., and Shaw, P., "Nonlinear Finite Element Analysis of a Composite Non-Cylindrical Pressurized Aircraft Fuselage Structure," 55th AIAA Structures, Structural Dynamics, and Materials Conference, Paper Number AIAA-2014-1064, January 13-17, 2014, National Harbor, MD.
24. Ambur, D. R., Rouse, M., Starnes, J. H., and Shuart, M. J., "Facilities for Combined Loads Testing of Aircraft Structures to Satisfy Structural Technology Development Requirements," presented at the 5th Annual Advanced Composites Technology Conference, August 22-26, 1994, Seattle, WA.
25. Rouse, M., "Methodologies for Combined Loads Tests Using a Multi-Actuator Test Machine," presented at the Society for Experimental Mechanics meeting, June 2013, Chicago, IL.
26. Rouse, M. and Jegley, D., "Preparation for Testing a Multi-Bay Box Subjected to Combined Loads," presented at the Society for Experimental Mechanics meeting, June 2015, Costa Mesa, CA.
27. McGowan, D., Ambur, D., and McNeil, S., "Full-field Structural Response of Composite Structures: Analysis and Experiment," presented at the 44th AIAA/ASME/ASCE/AHS Structures, Dynamics and Materials Conference, AIAA 2003-1623, April 2003, Norfolk, VA.

Acknowledgements

The authors wish to acknowledge the team from Boeing who built the test article and worked with LaRC supporting all the testing activities. We particularly want to acknowledge the work of Mr. Alex Velicki, Mr. Kim Linton, Dr. Tom Wu, Mr. Krishna Hoffman, Mr. Patrick Thrash, Mr. Jaime Baraja, Mr. Robert Pickell and Mr. Andy Harbor. Their participation in the creation of the test article, planning and implementation was critical to the success of the test program.

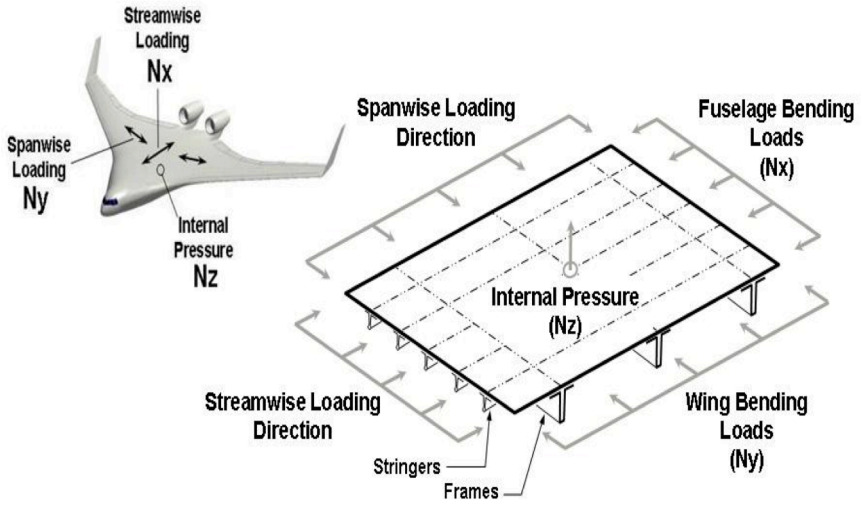

Figure 1. Combined loading on the HWB pressure cabin.

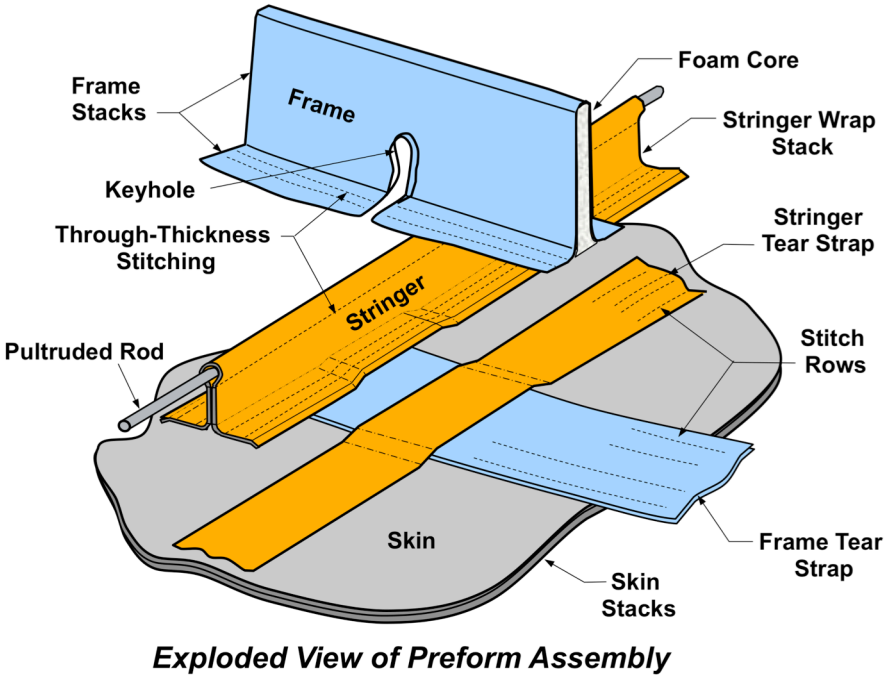

Figure 2. Exploded view of the PRSEUS concept.

Figure 3. PRSEUS panel being prepared for assembly.

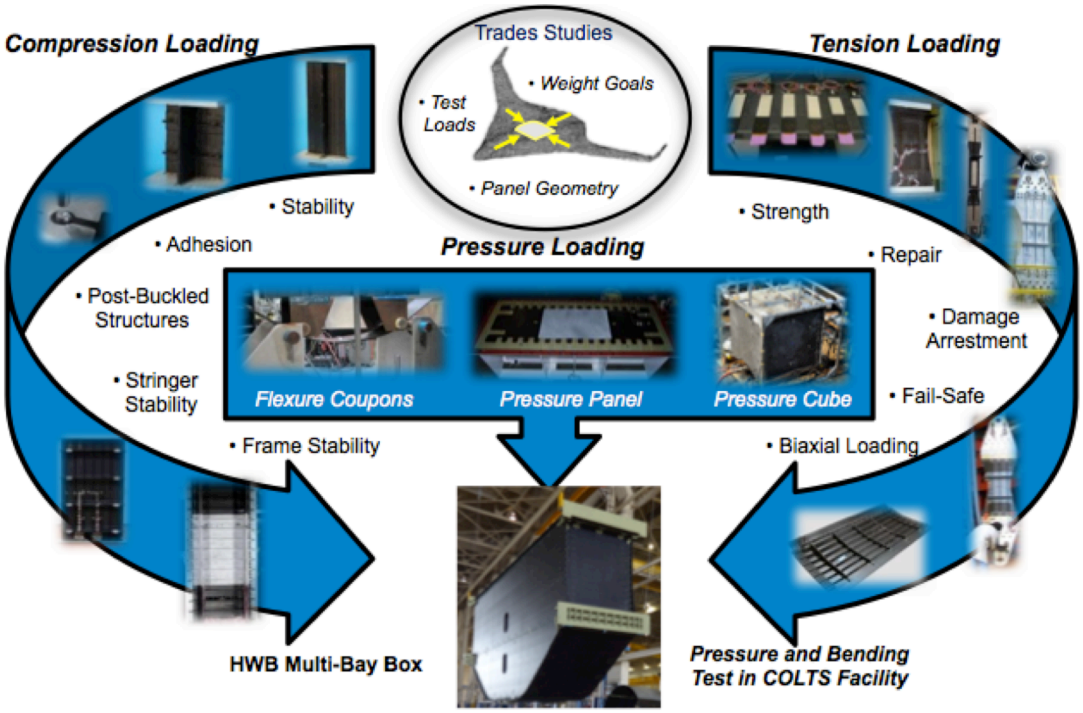

Figure 4. Development path leading to the HWB large-scale test article.

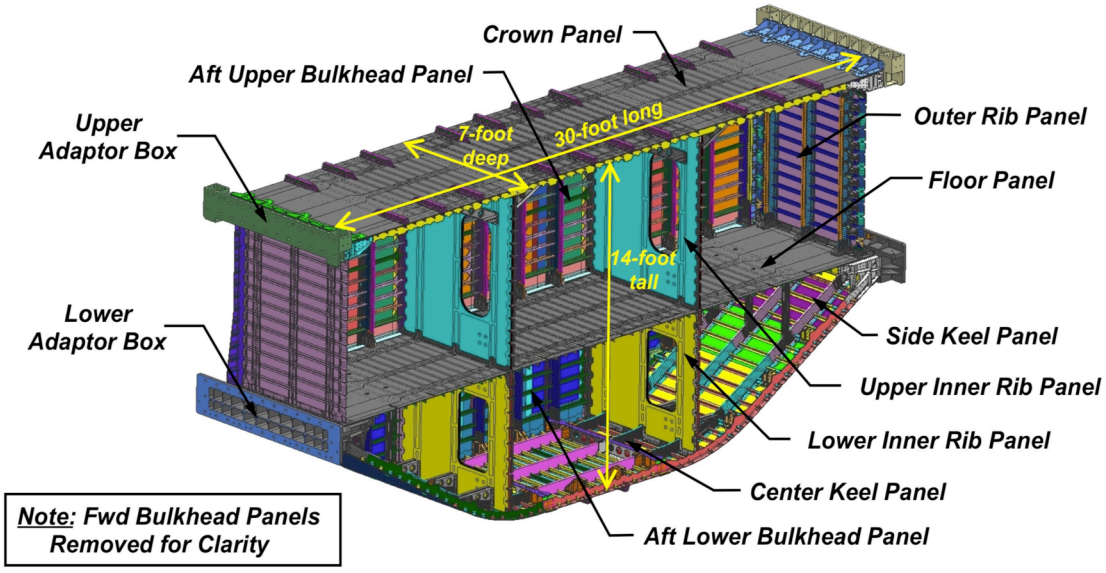

Figure 5. Multi-bay pressure box components.

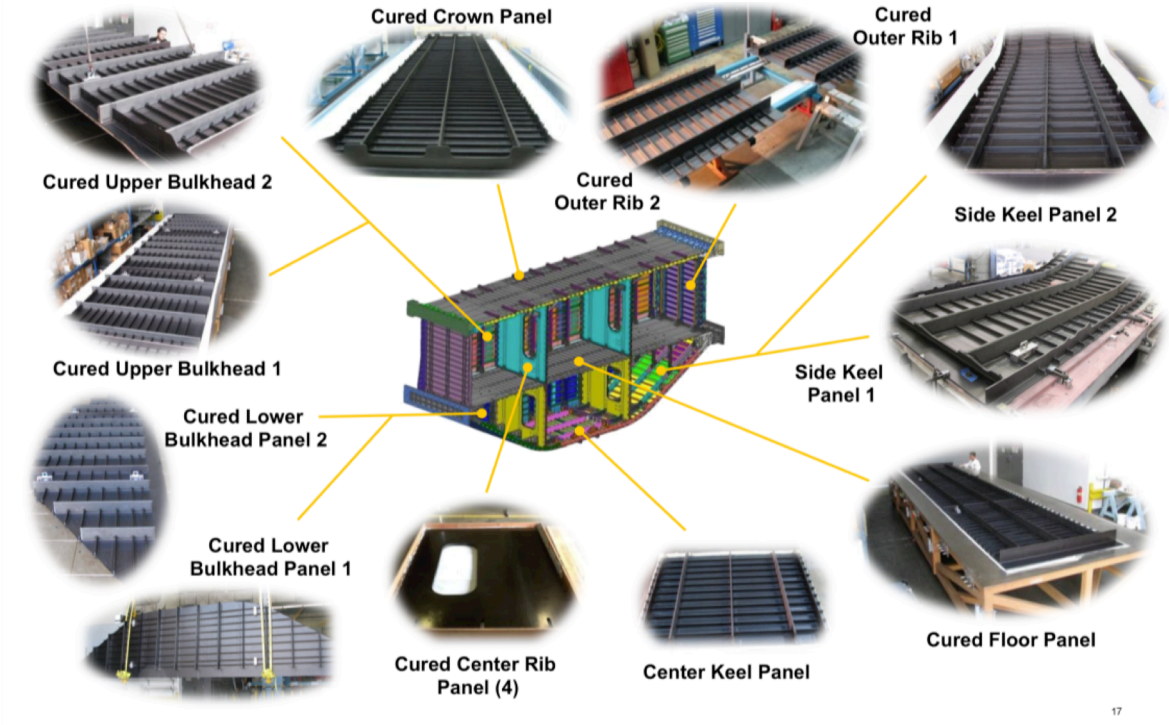

Figure 6. Composite panels in the multi-bay pressure box.

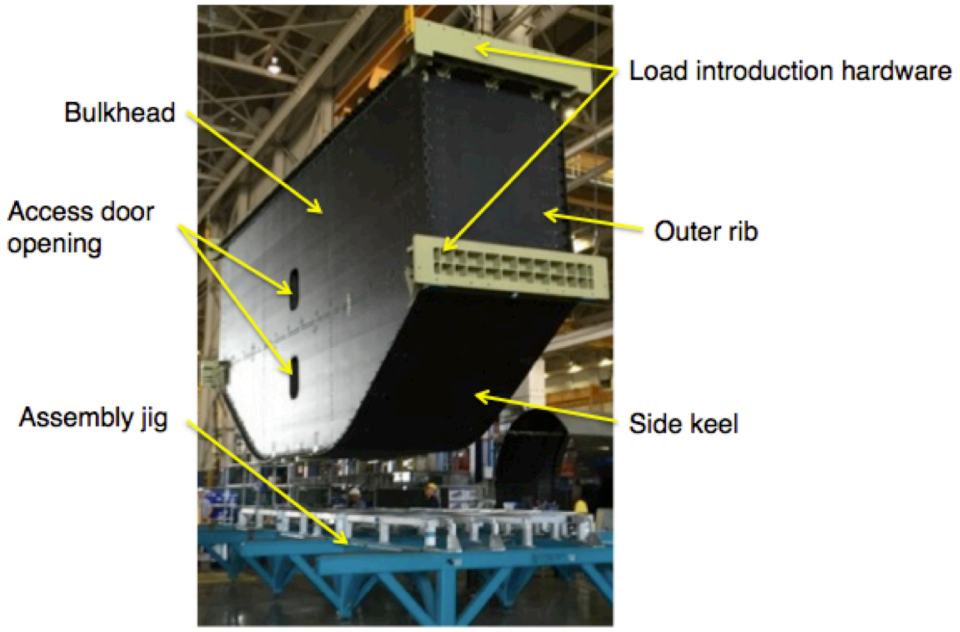

Figure 7. Fully assembled multi-bay pressure box.

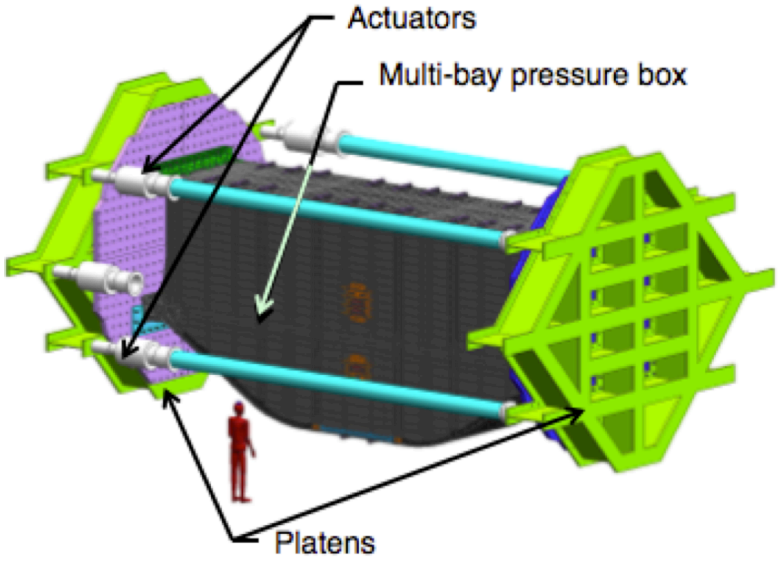

Figure 8. Test article between the platens in COLTS.

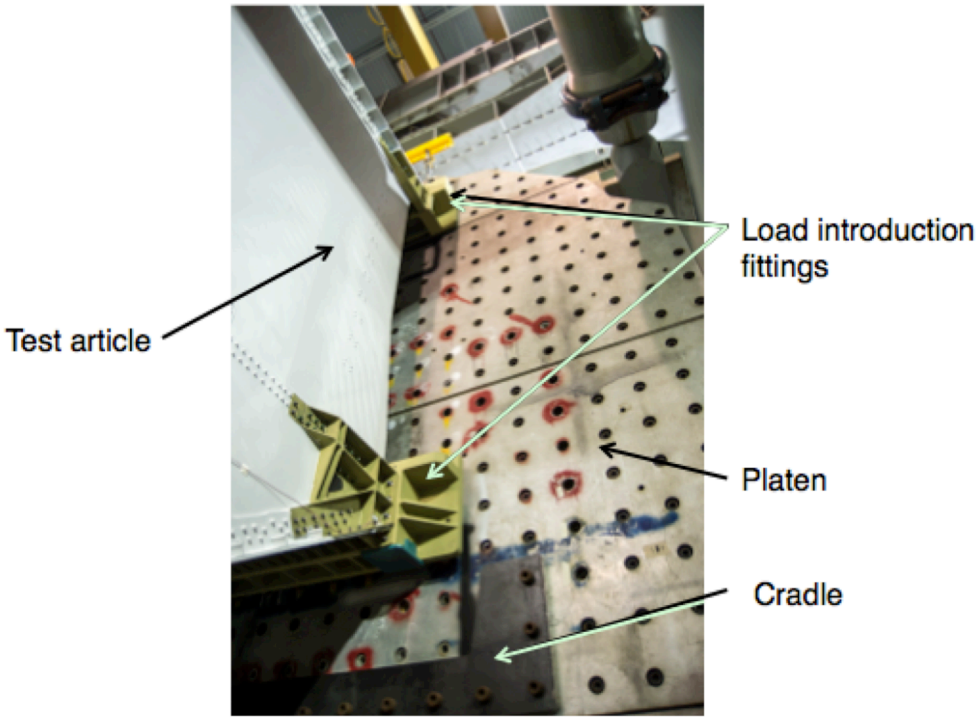

Figure 9. Test article being lowered into position against a platen.

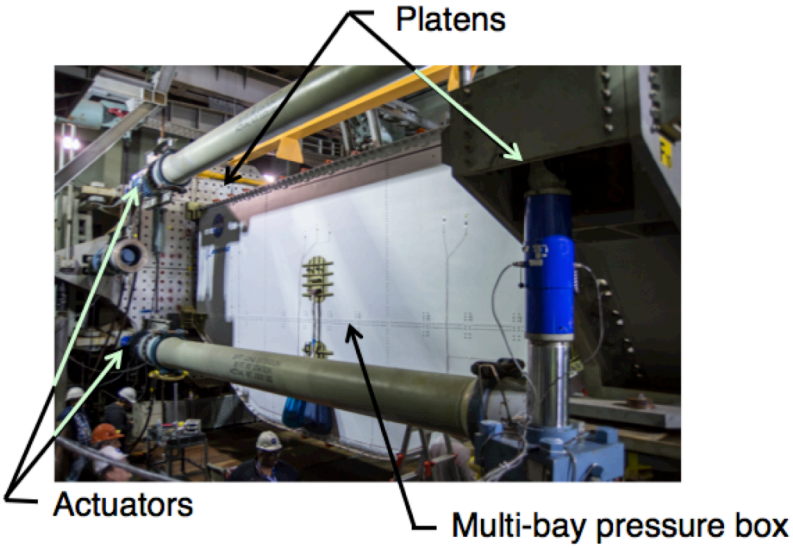

Figure 10. Multi-bay pressure box in the test chamber.

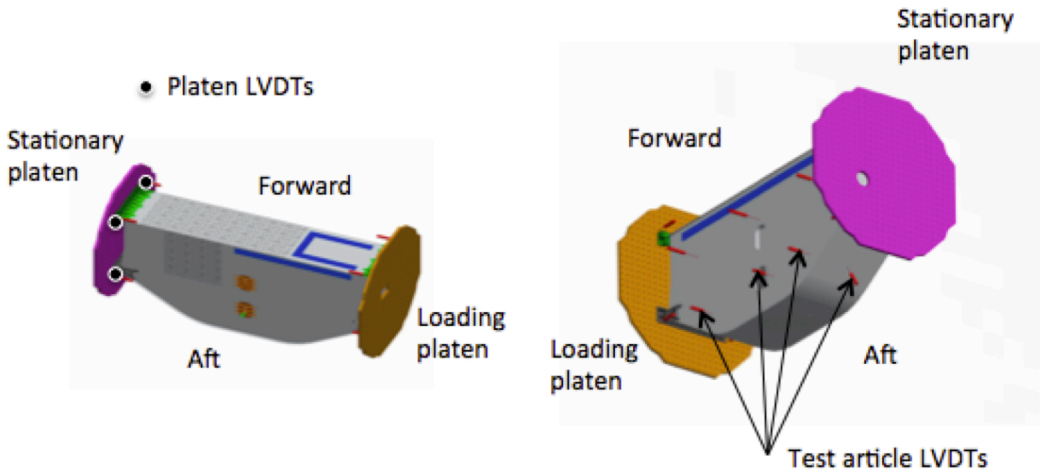

a) LVDT locations

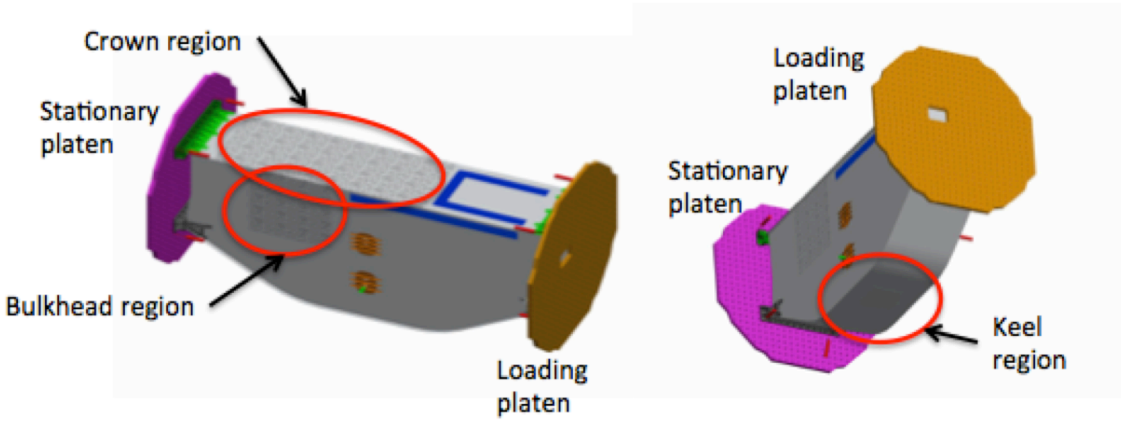

b) Digital video correlation regions

Figure 11. Displacement measurement locations.

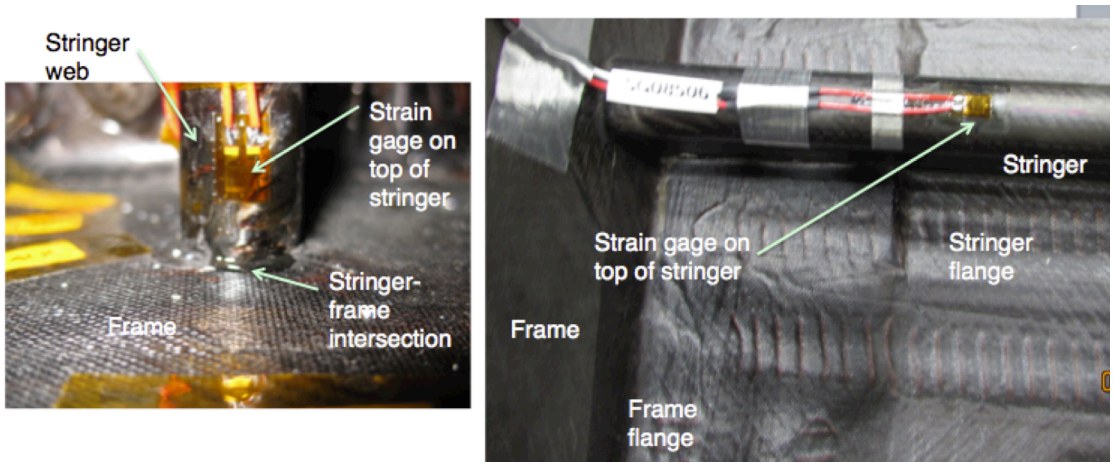

a) Top of stringers

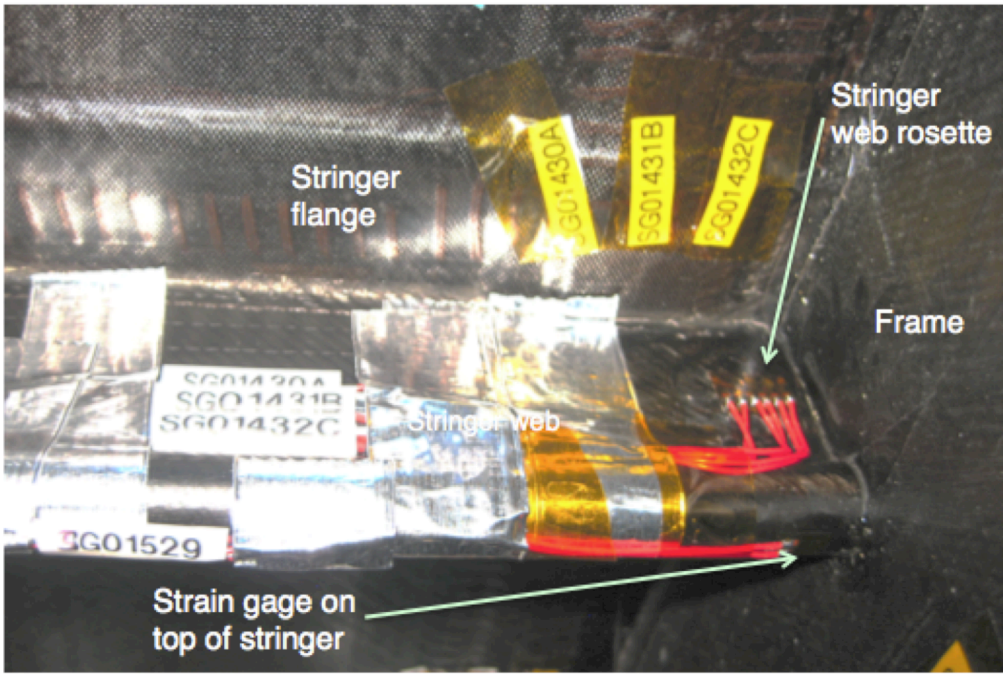

b) Stringers

Figure 12. Typical strain gauge locations.

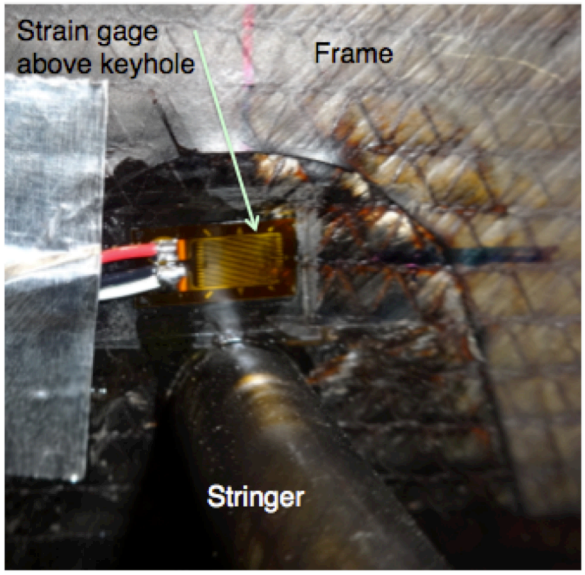

c) Keyhole

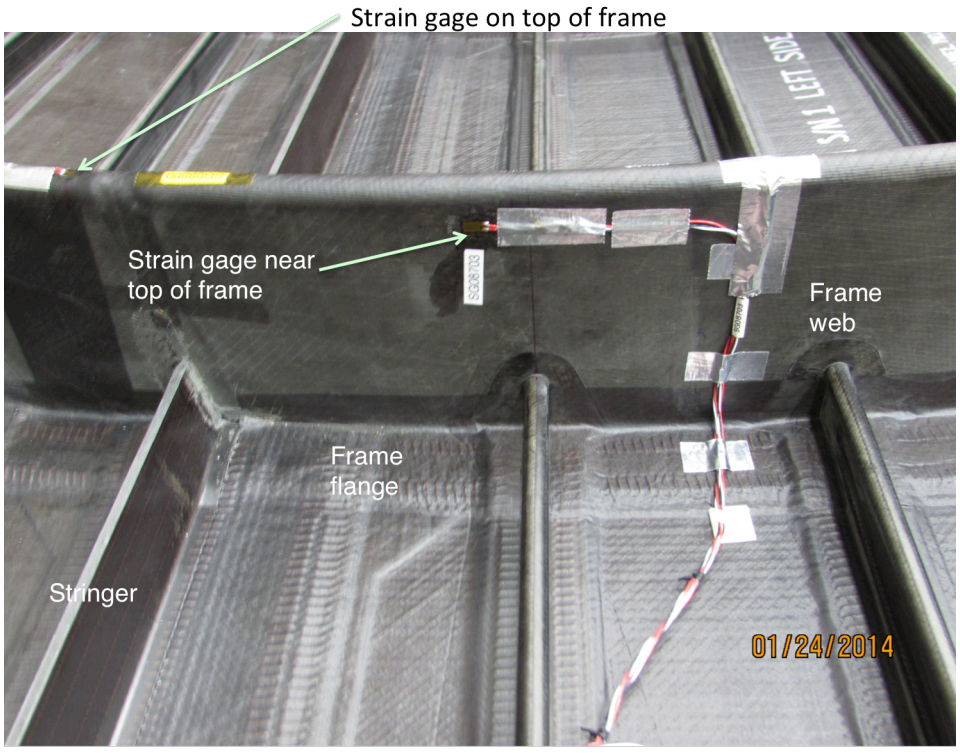

d) Frame

Figure 12. Typical strain gauge locations (continued).

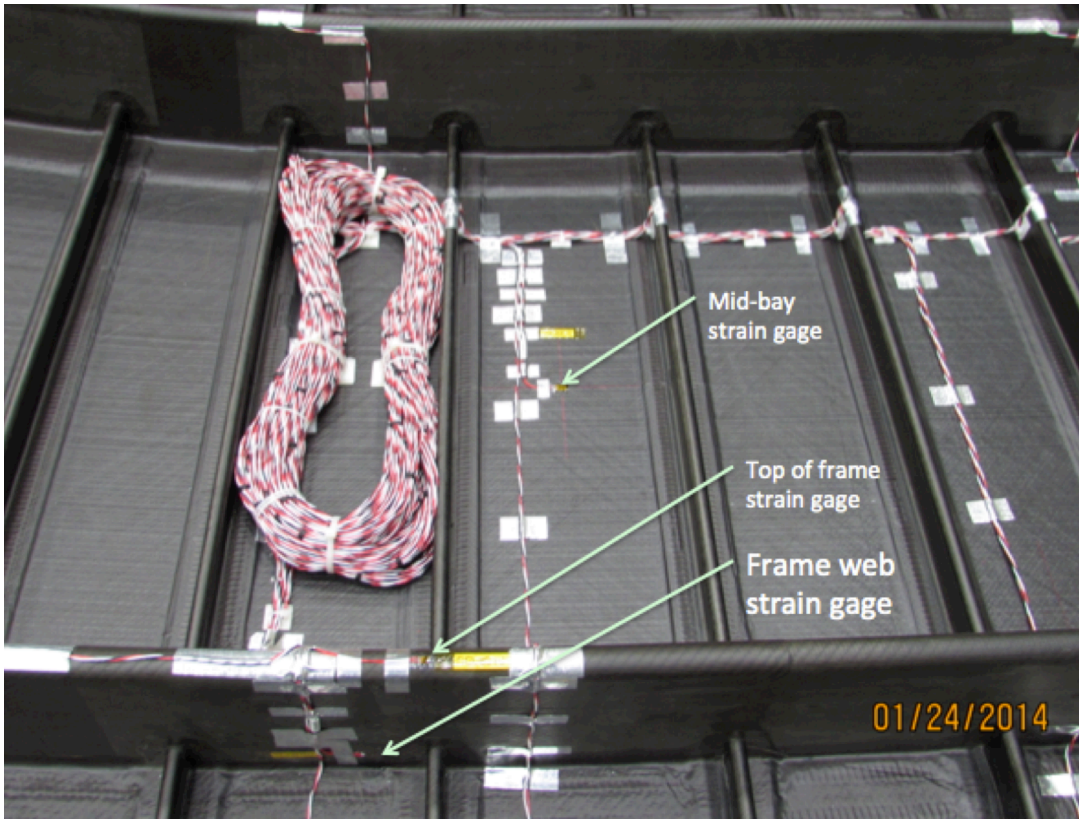

e) Mid-bay skin

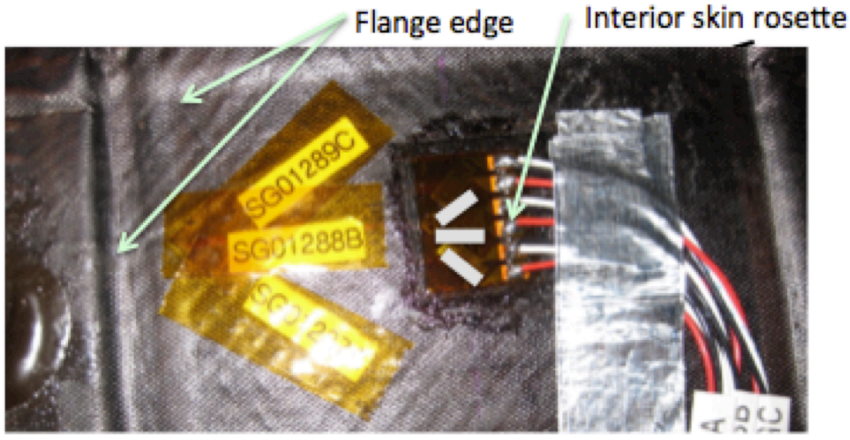

f) Skin rosette

Figure 12. Typical strain gauge locations (concluded).

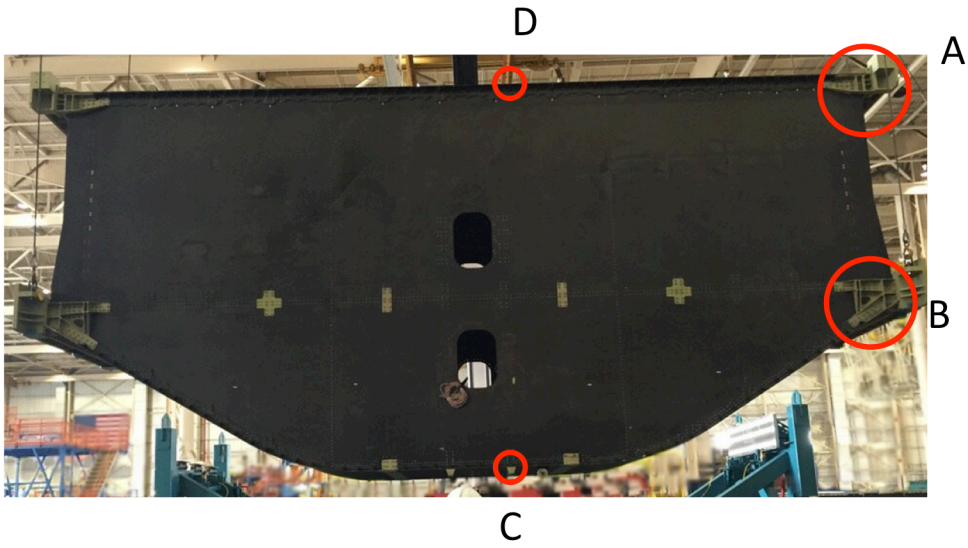

a) Exterior

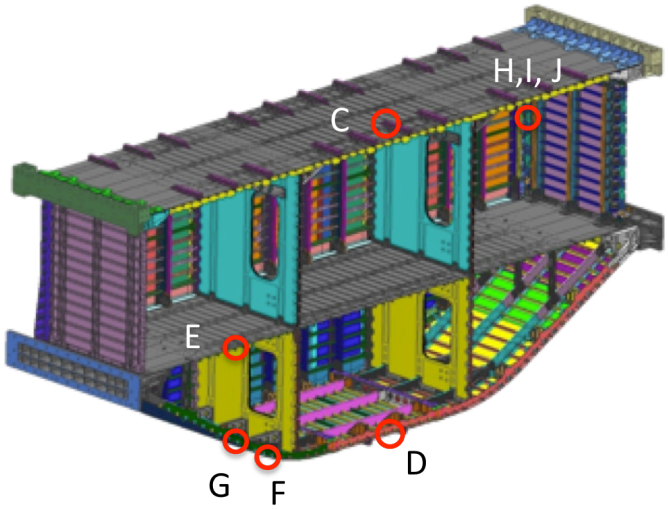

b) Interior

Figure 13. Strain gauge locations on fittings.

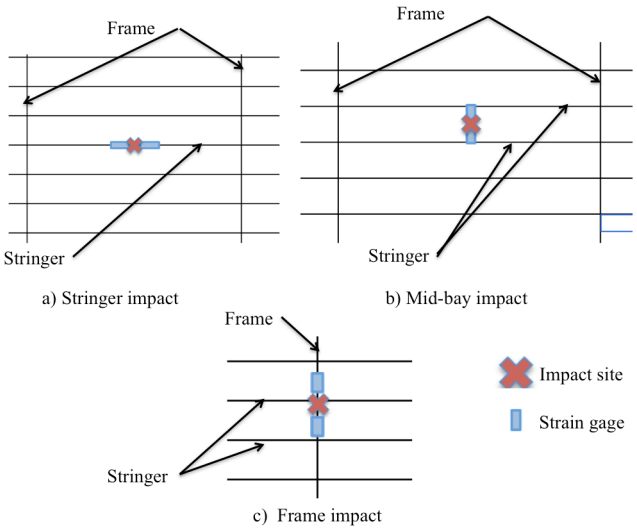

a-c) Interior on upper bulkhead

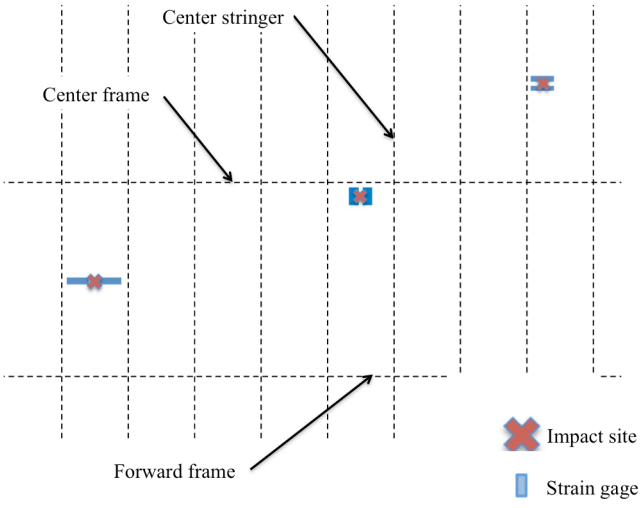

d) Exterior on center keel

Figure 14. Strain gauges associated with impact sites.

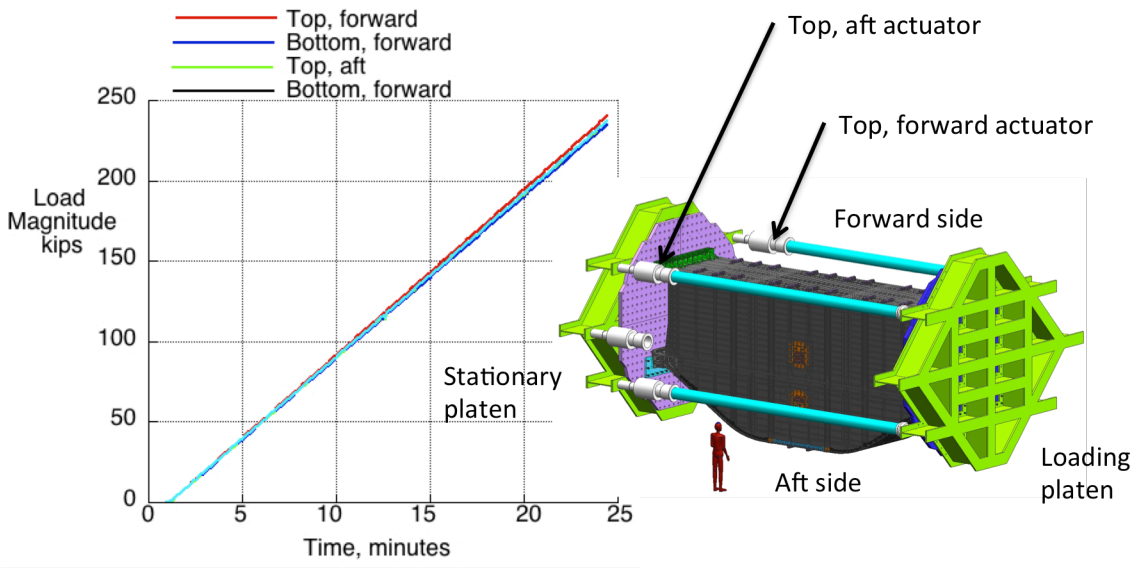

Figure 15. Actuator applied loads for the up-bending to DUL case.

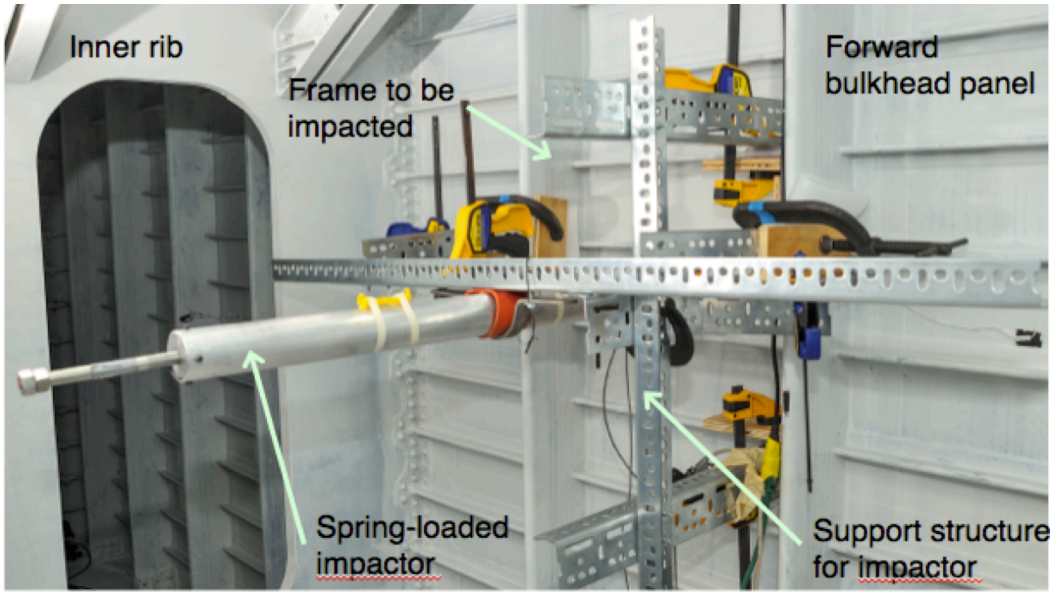

a) Interior bulkhead with spring-loader impactor

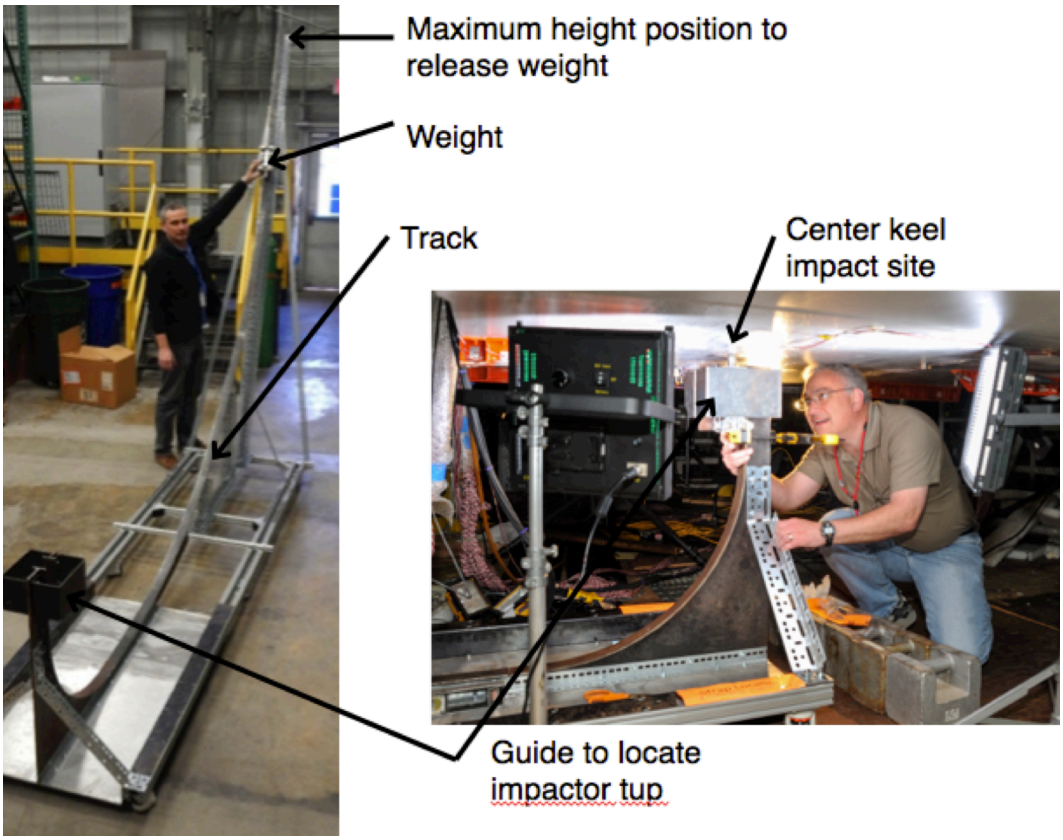

b) Exterior keel with the gravity-fed impactor

Figure 16. Impact approach.

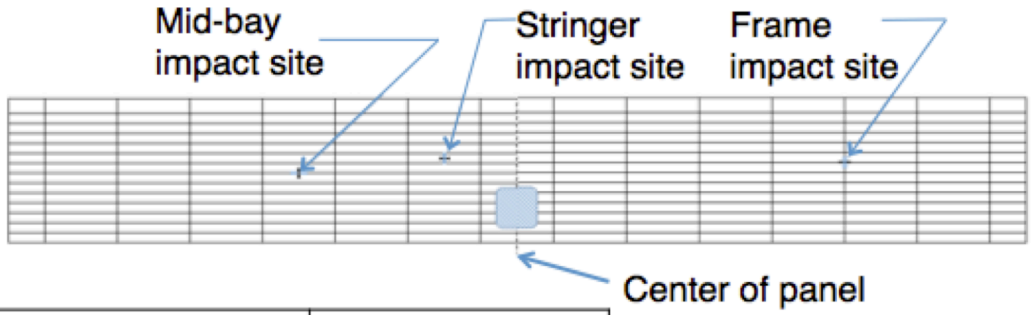

Location	Impact energy (ft-lb)
Mid-bay	15
Frame top	20
Stringer top	20

a) Interior impacts

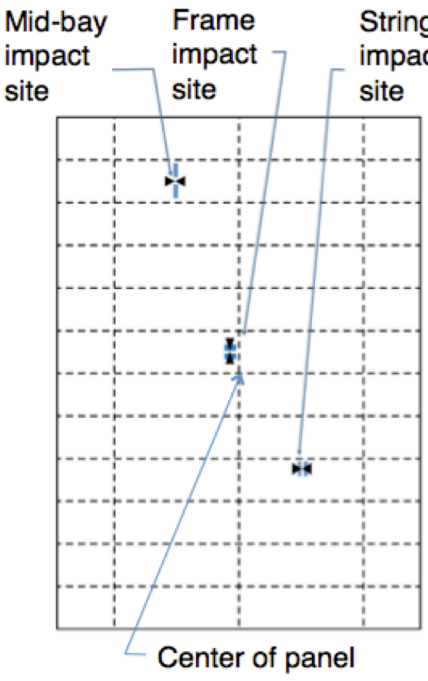

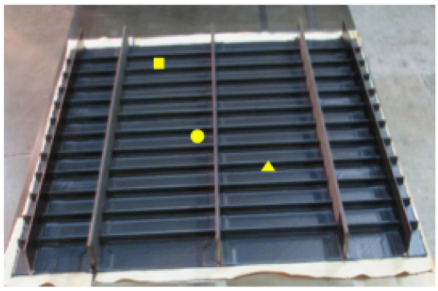

Location	Impact energy (ft-lb)
Mid-bay	15
Frame flange edge	60
Stringer flange edge	50

b) Exterior impacts

Figure 17. Impact sites.

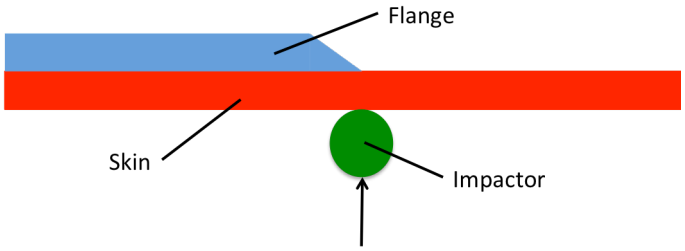

Figure 18. Exterior impact site.

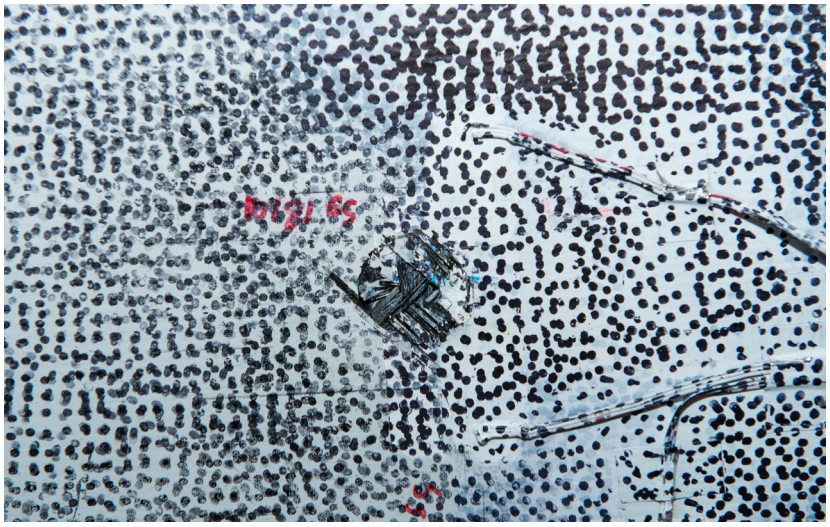

Figure 19. Impact causing a through-hole.

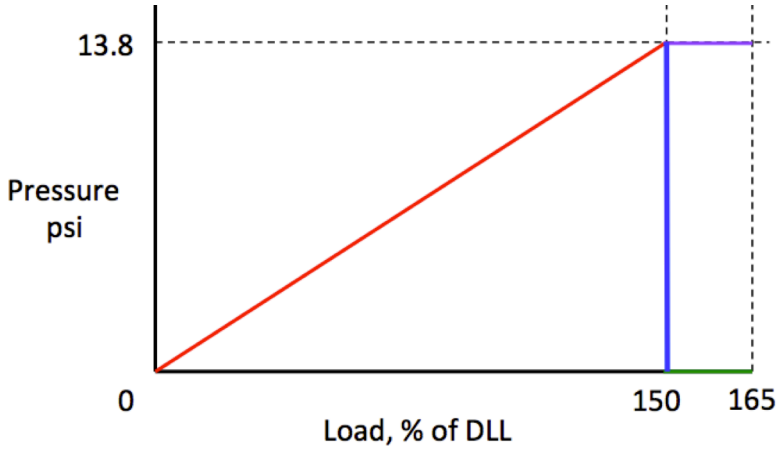

Figure 20. Loading to 110% DUL.

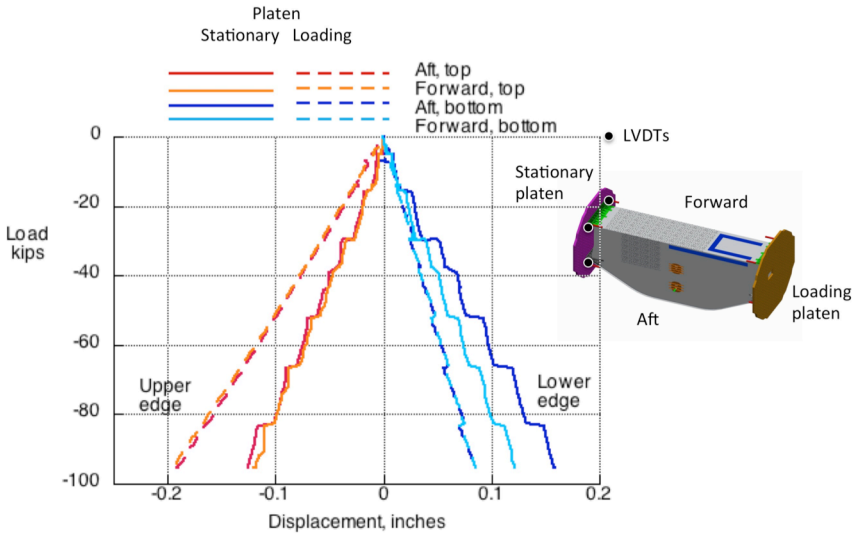

Figure 21. Platen displacements in the down-bending load case.

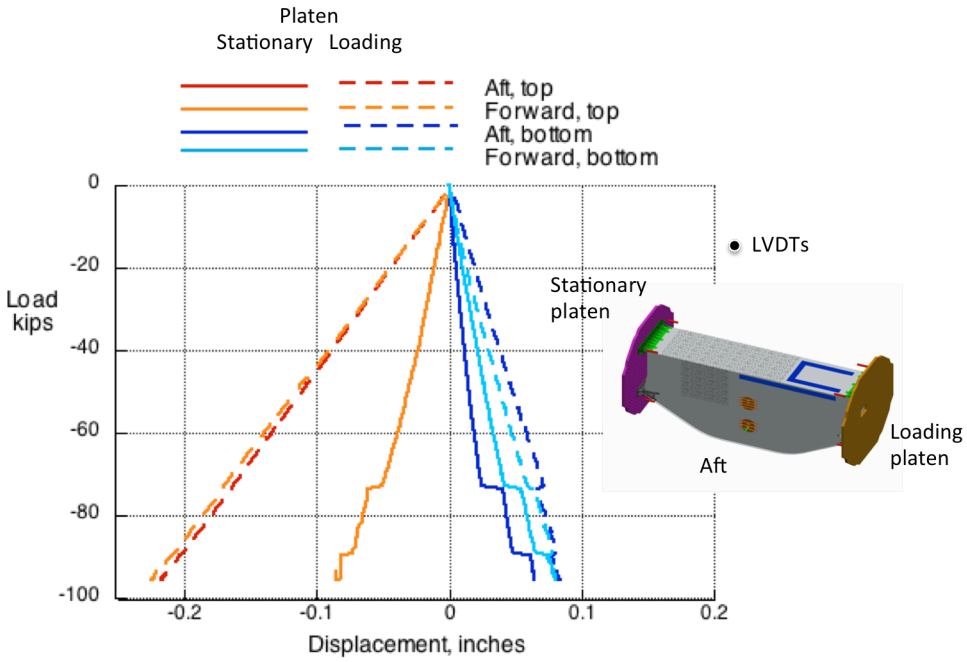

Figure 22. Platen displacements in the down-bending plus pressure load case.

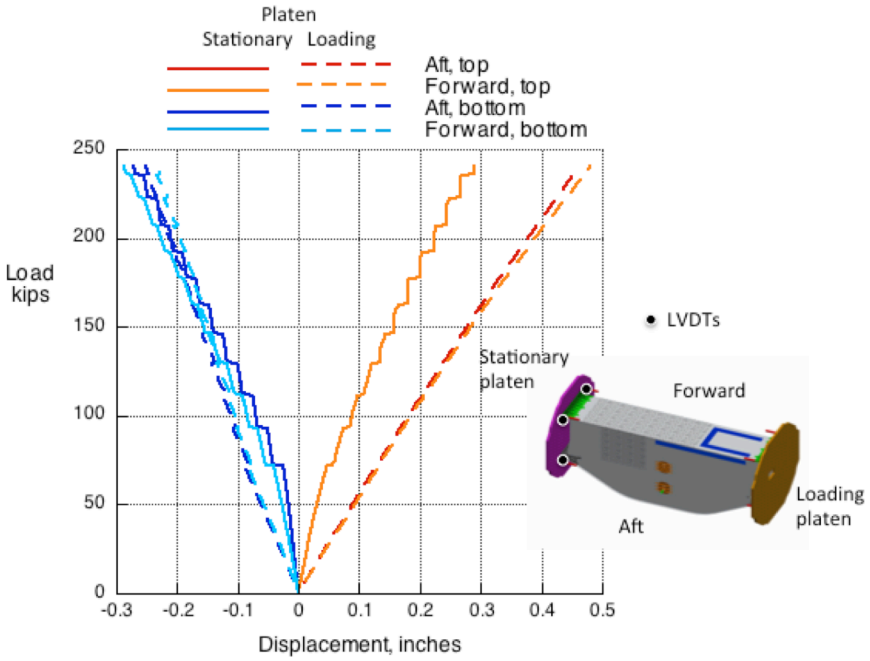

Figure 23. Platen displacements in the up-bending load case.

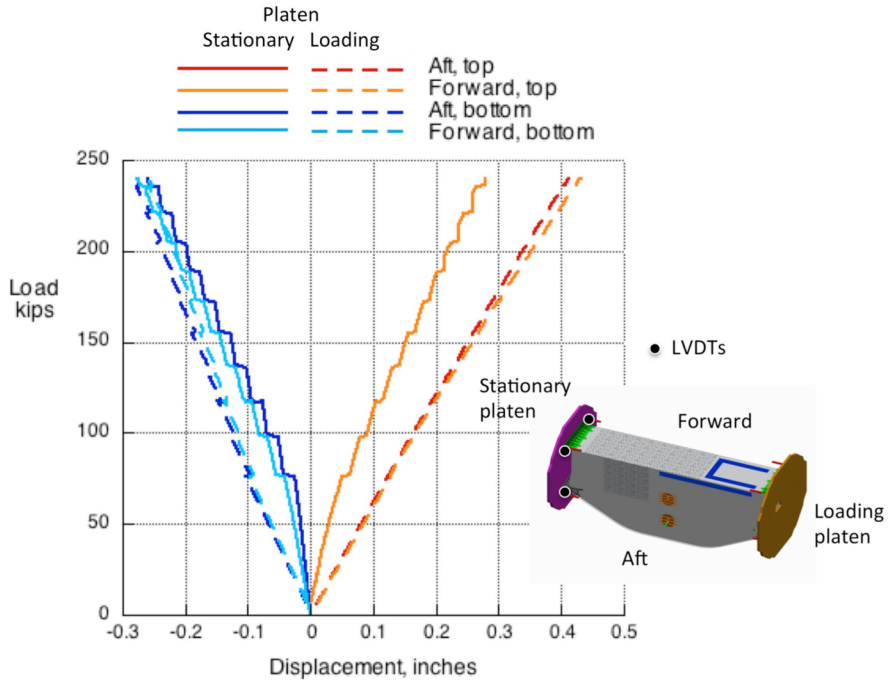

Figure 24. Platen displacements at DUL in the up-bending plus pressure load case.

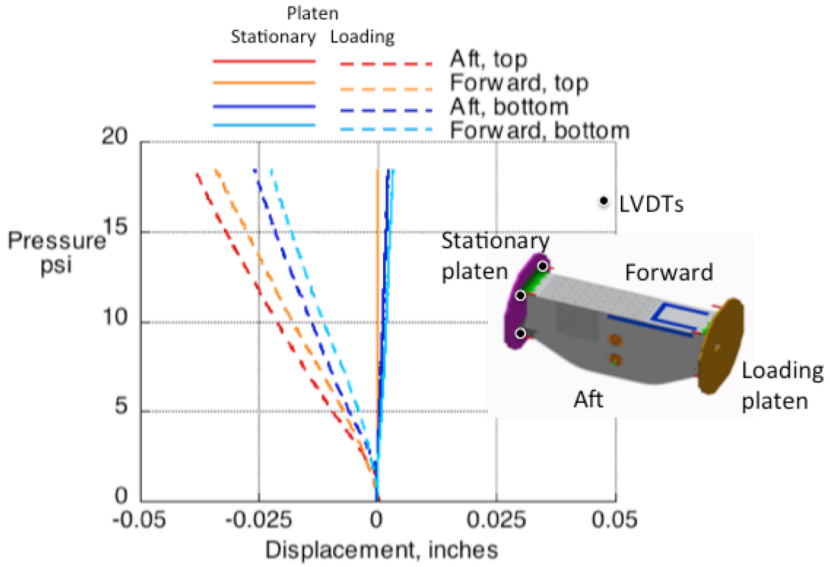

Figure 25. Platen displacements at 18.4 psi.

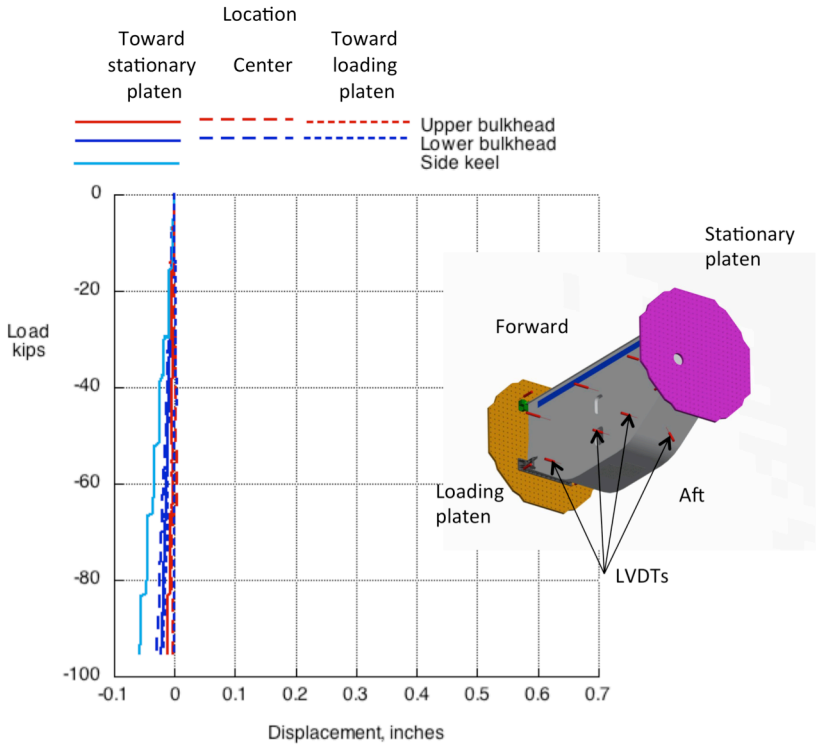

Figure 26. Bulkhead and keel displacements in the down-bending load case.

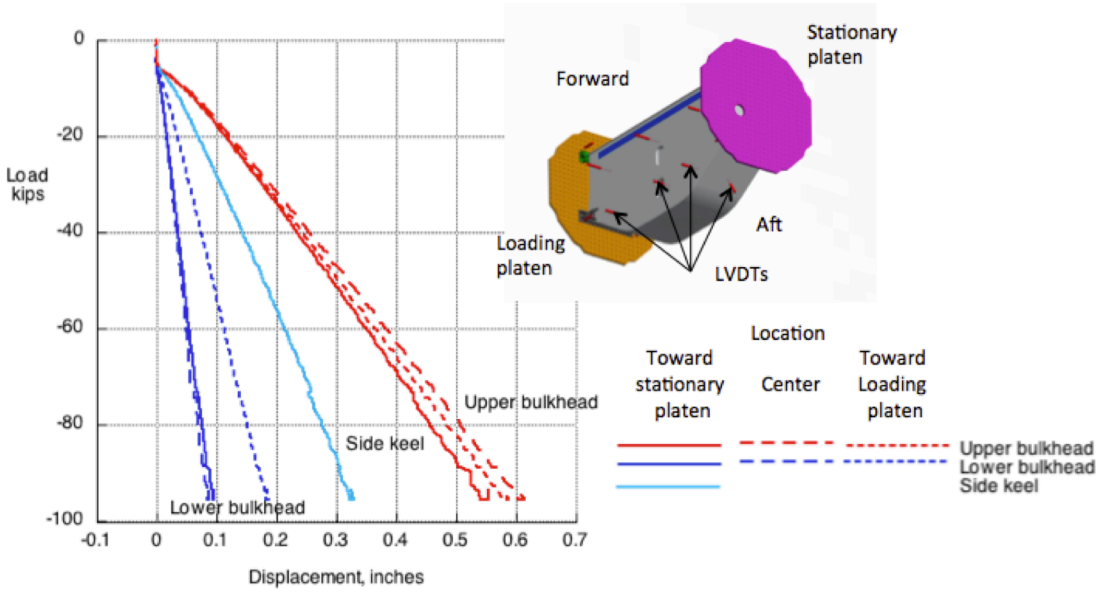

Figure 27. Bulkhead and keel displacements in the down-bending plus pressure load case.

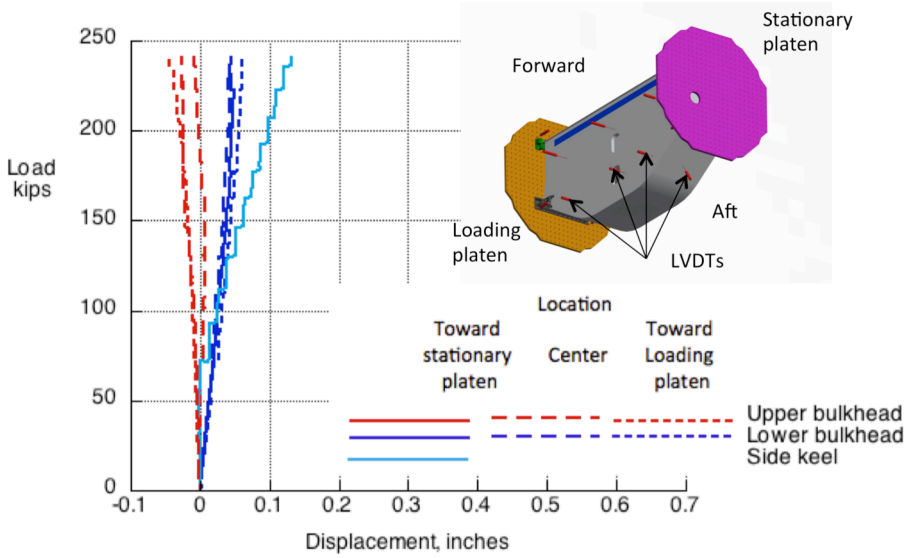

Figure 28. Bulkhead and keel displacements in the up-bending plus pressure load case.

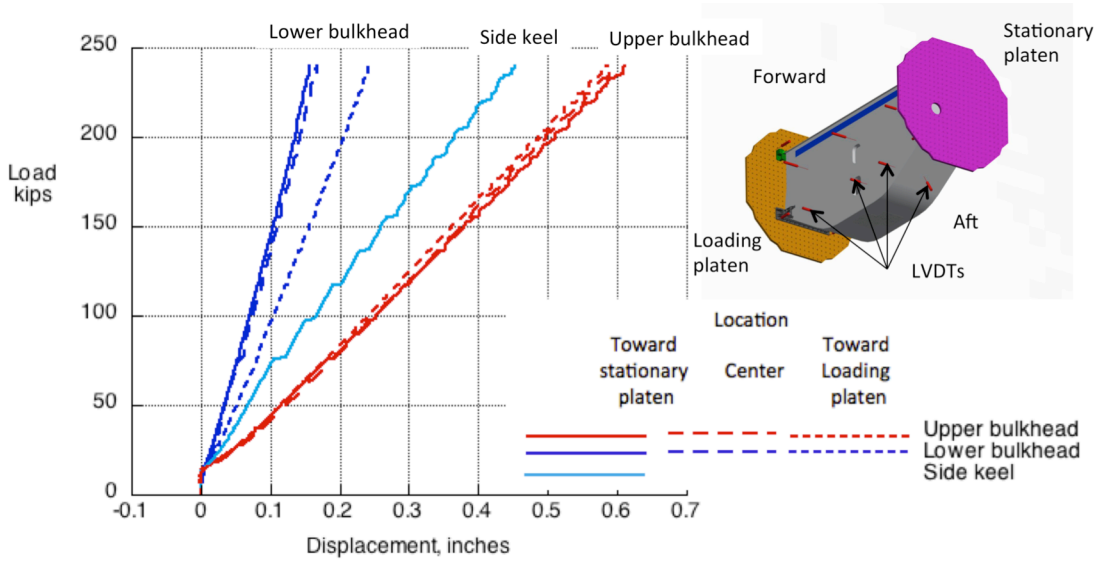

Figure 29. Bulkhead and keel displacements in the up-bending plus pressure load case.

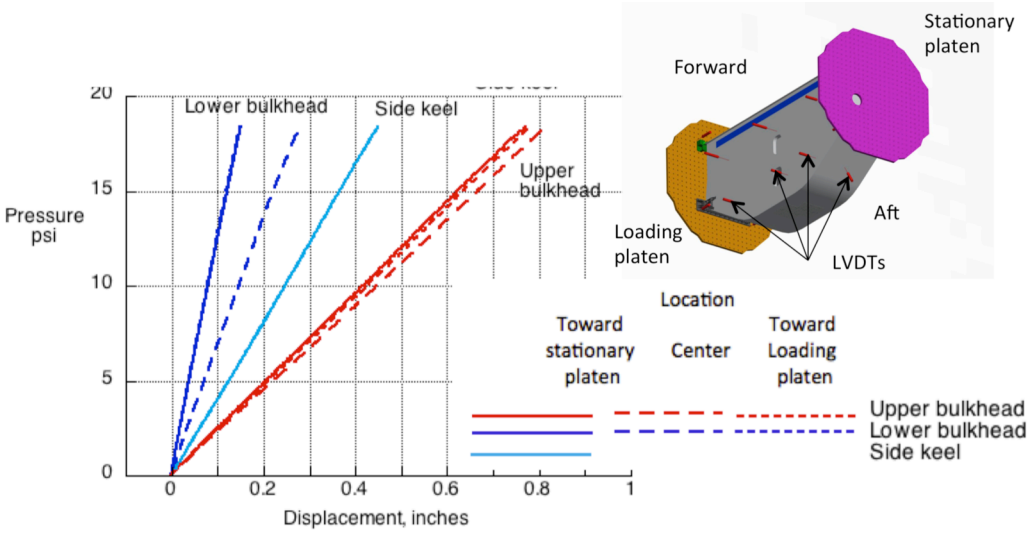

Figure 30. Bulkhead and keel displacements in the pressure-only load case.

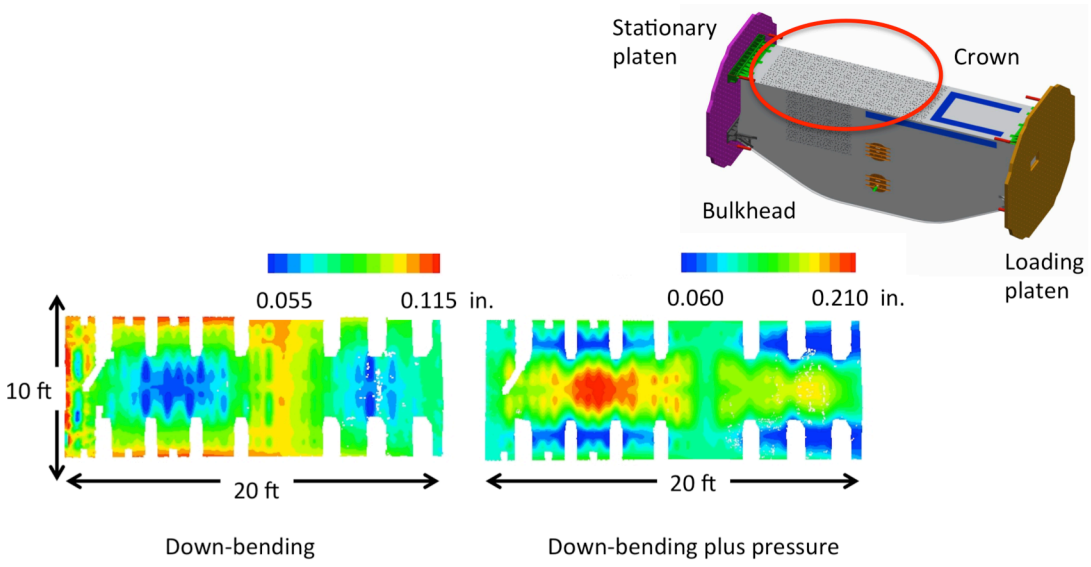

Figure 31. Crown full-field out-of-plane displacements for the down-bending and down-bending plus pressure load cases.

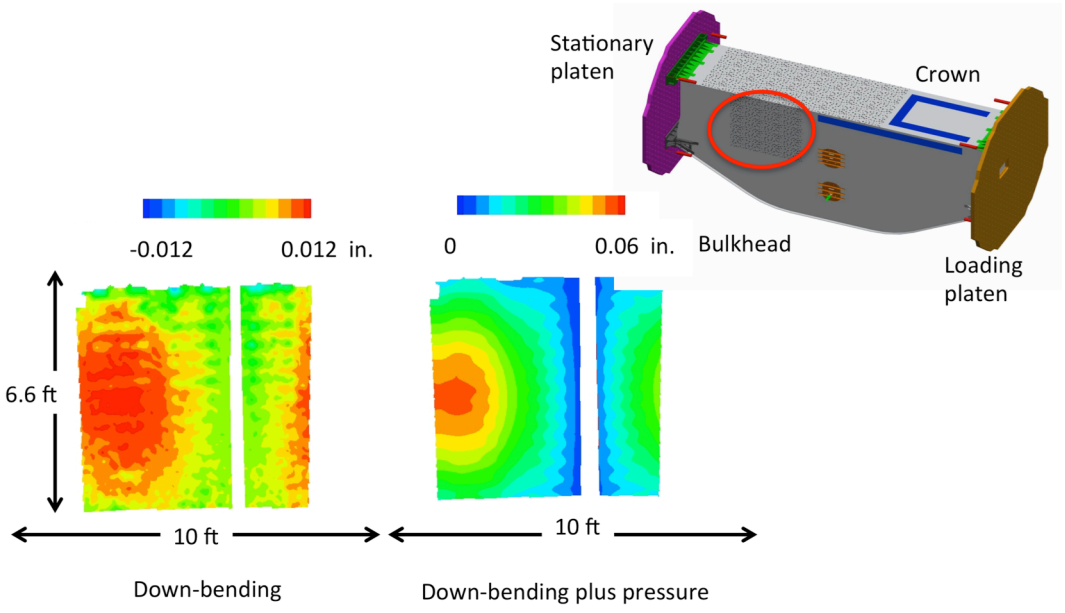

Figure 32. Bulkhead full-field out-of-plane displacements for the down-bending and down-bending plus pressure load cases.

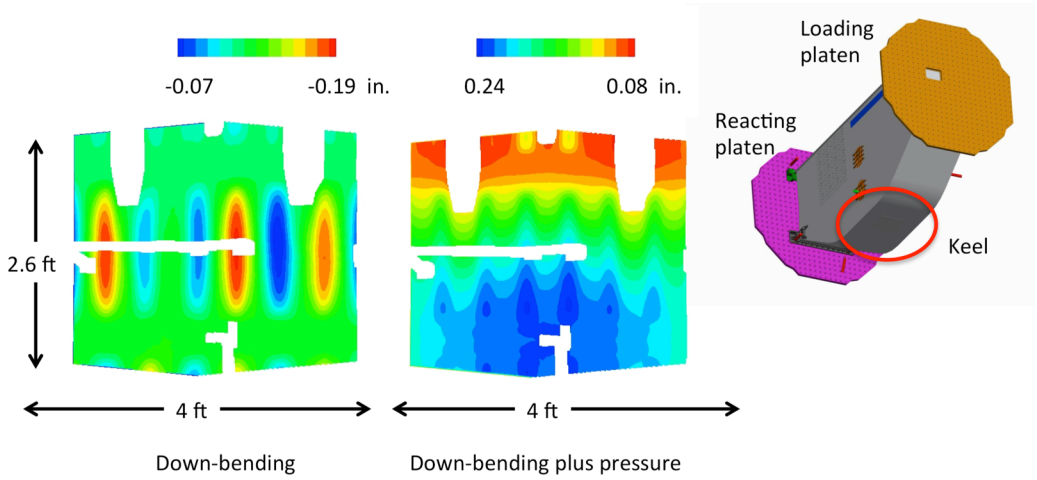

Figure 33. Center keel full-field out-of-plane displacements for the down-bending and down-bending plus pressure load cases.

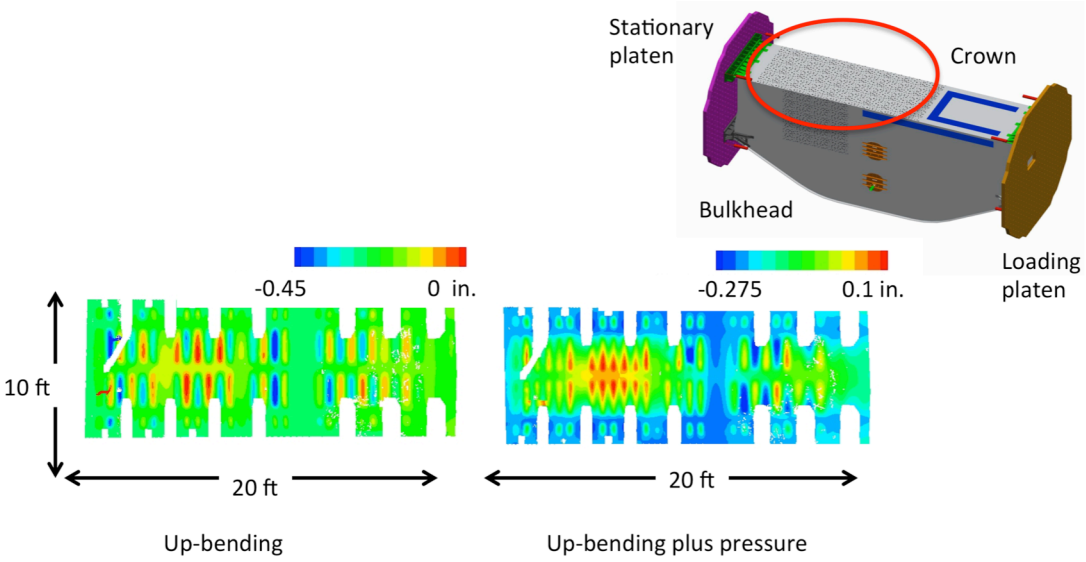

Figure 34. Crown full-field out-of-plane displacements for the up-bending and up-bending plus pressure load cases.

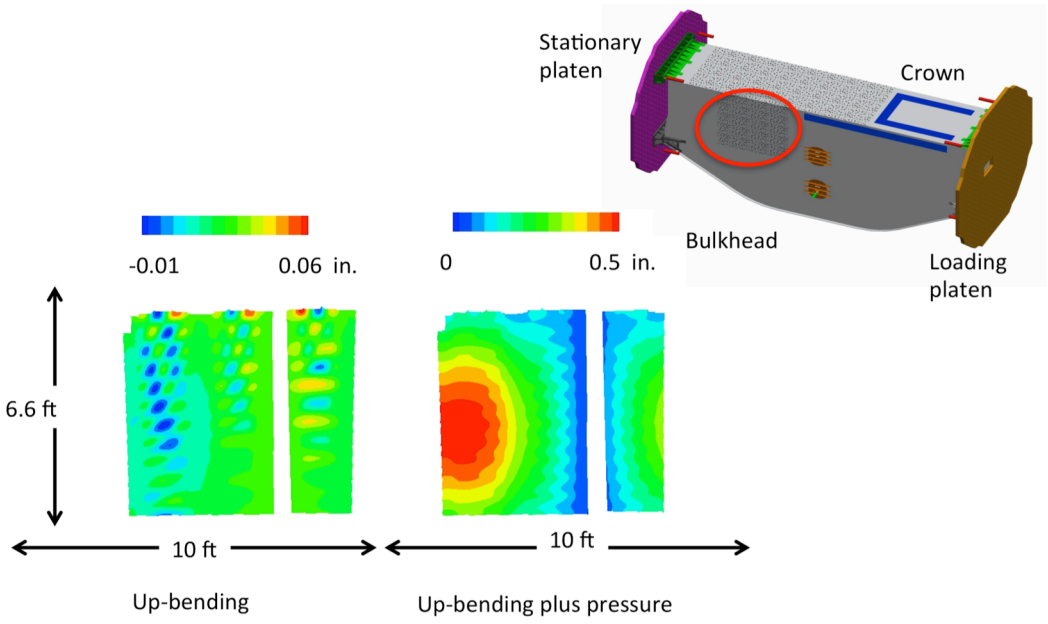

Figure 35. Bulkhead full-field out-of-plane displacements for the up-bending and up-bending plus pressure load cases.

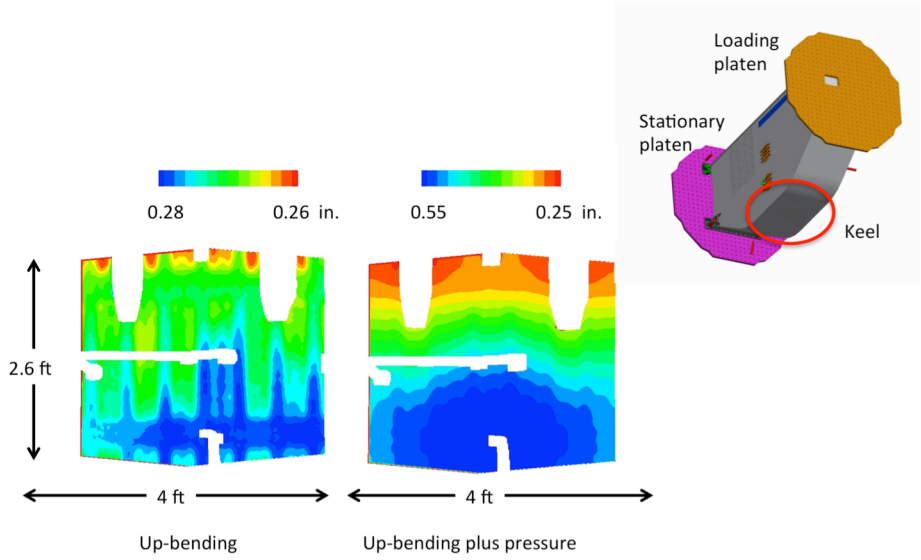

Figure 36. Center keel full-field out-of-plane displacements for the up-bending and up-bending plus pressure load cases.

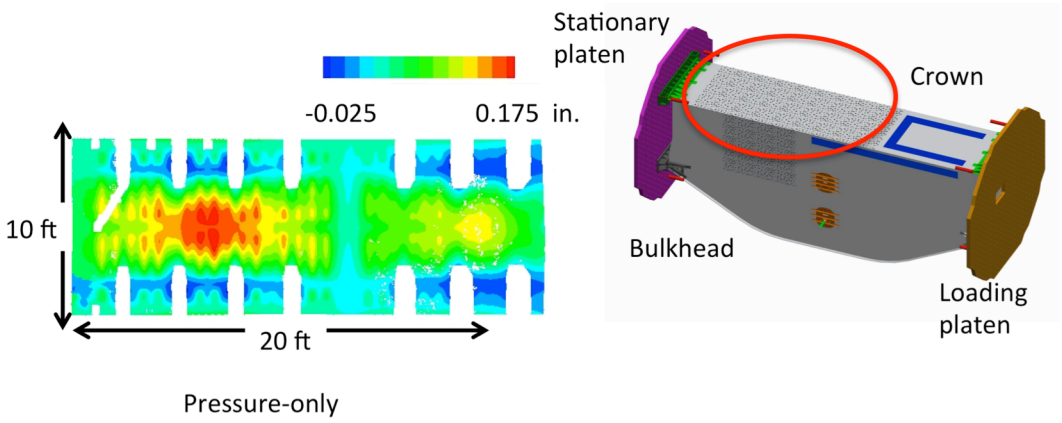

Figure 37. Crown full-field out-of-plane displacements for the pressure-only load case.

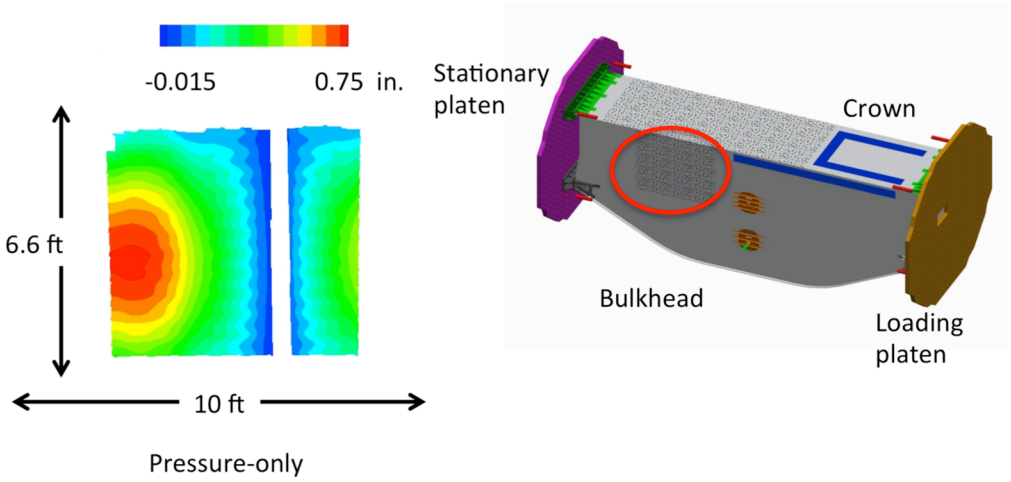

Figure 38. Bulkhead full-field out-of-plane displacements for the pressure-only load case.

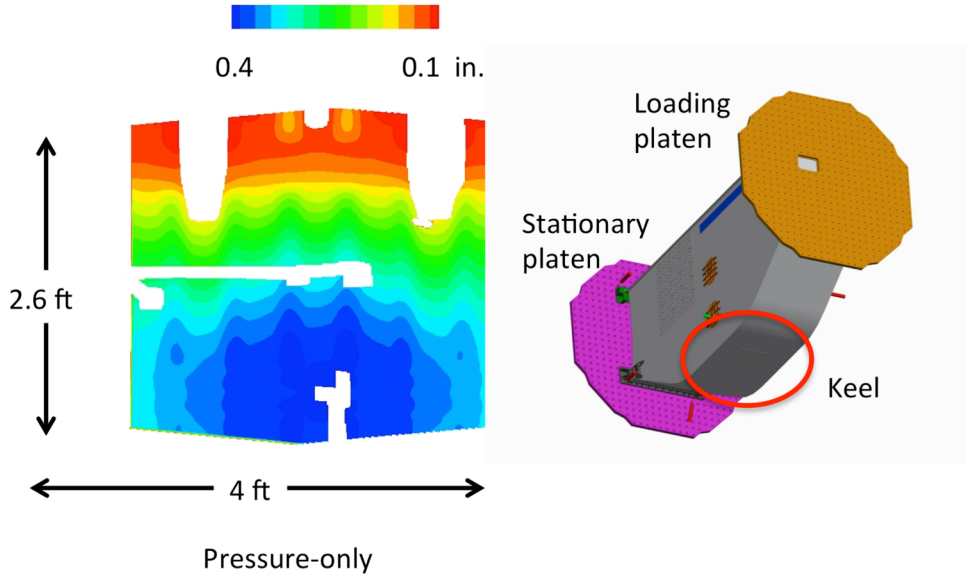

Figure 39. Center keel full-field out-of-plane displacements for the pressure-only load case.

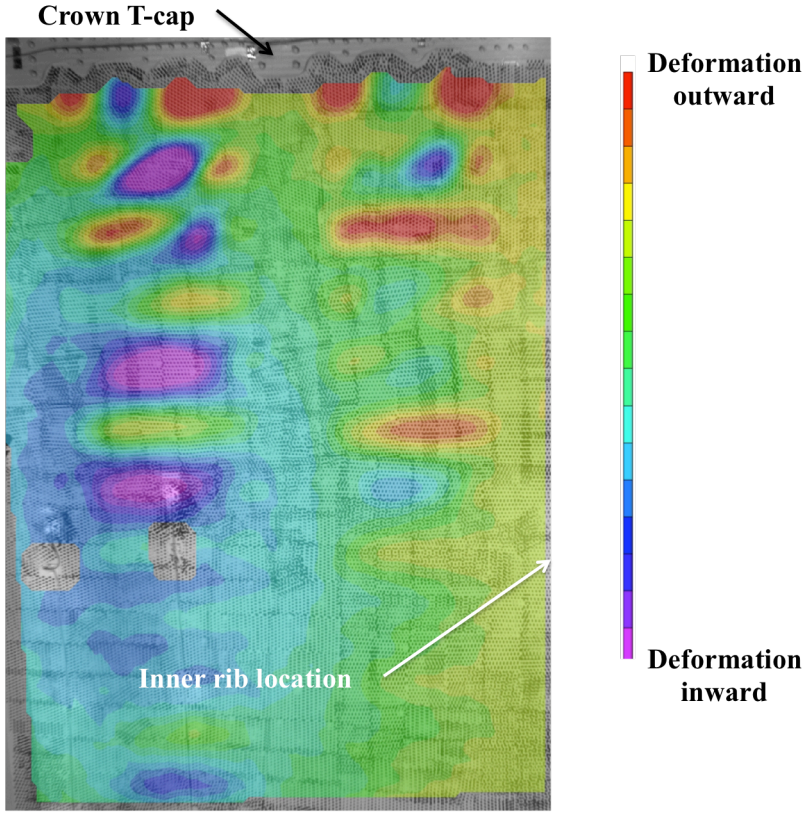

a) Approximately 60 percent DUL

Figure 40. Bulkhead out-of-plane deformation pattern changes as mechanical loading increases in the up-bending load case.

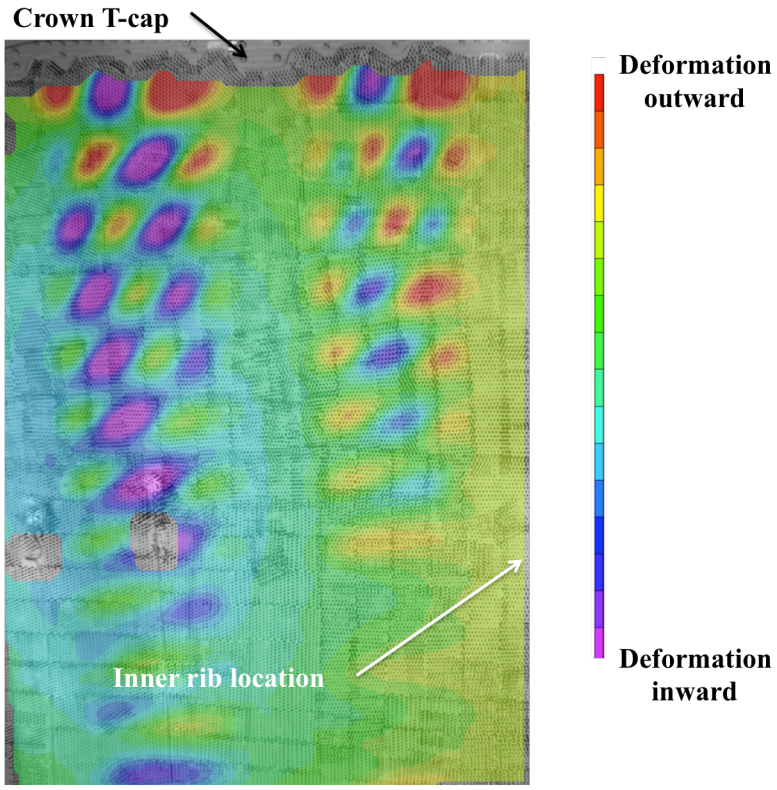

b) Approximately 90% DUL

Figure 40. Bulkhead out-of-plane deformation pattern changes as mechanical loading increases in the up-bending load case (concluded).

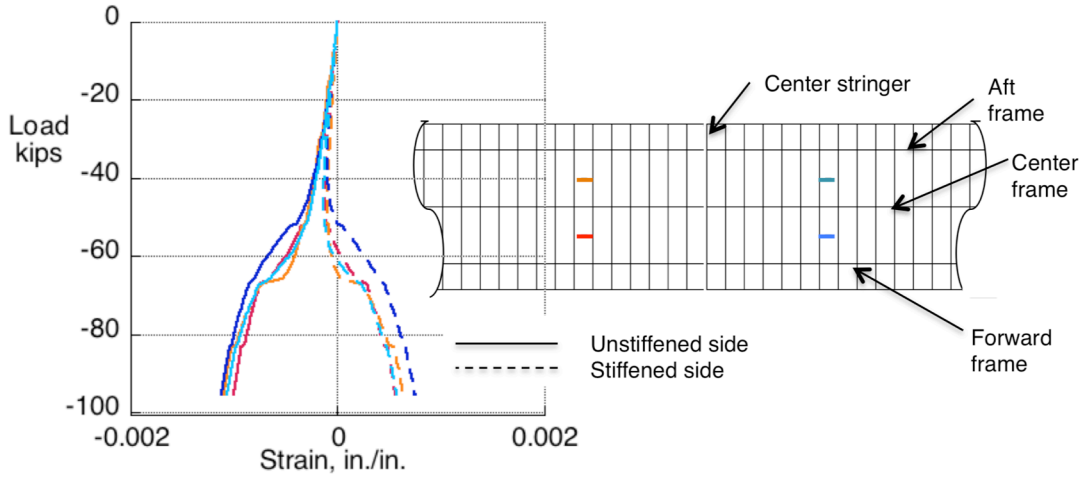

Figure 41. Strain in the floor skin.

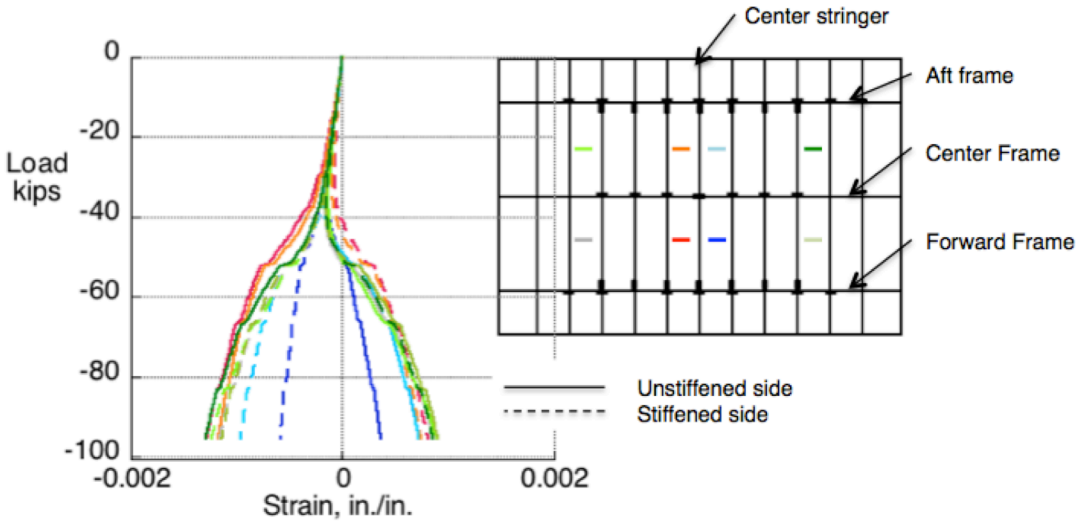

Figure 42. Strain in the center keel.

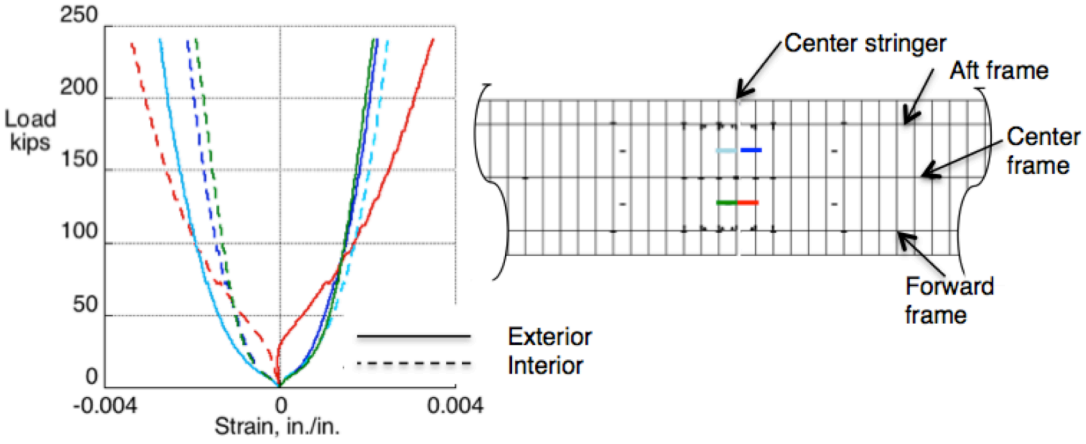

Figure 43. Strain in the crown skin at the back-to-back mid-bay gauges near the center stringer.

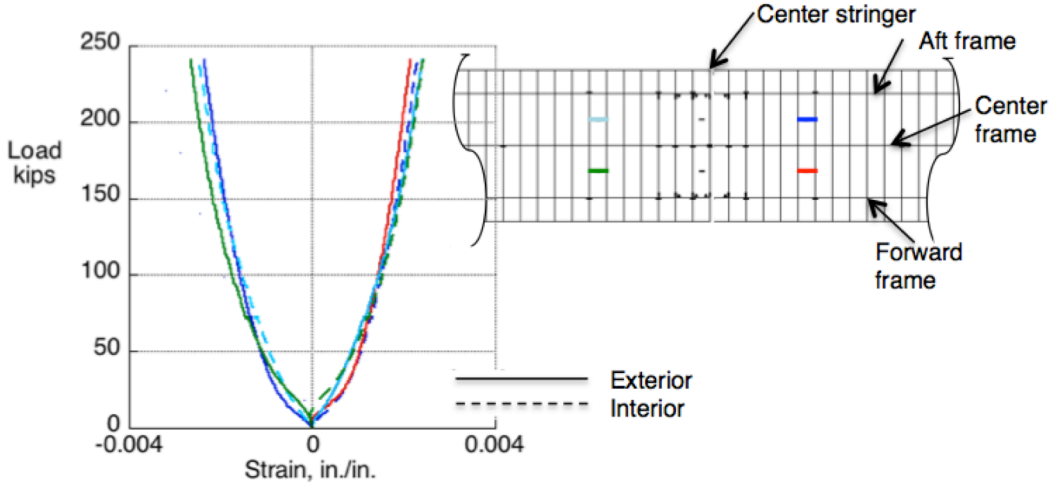

Figure 44. Strain in the crown skin at the back-to-back mid-bay gauges away from the center stringer.

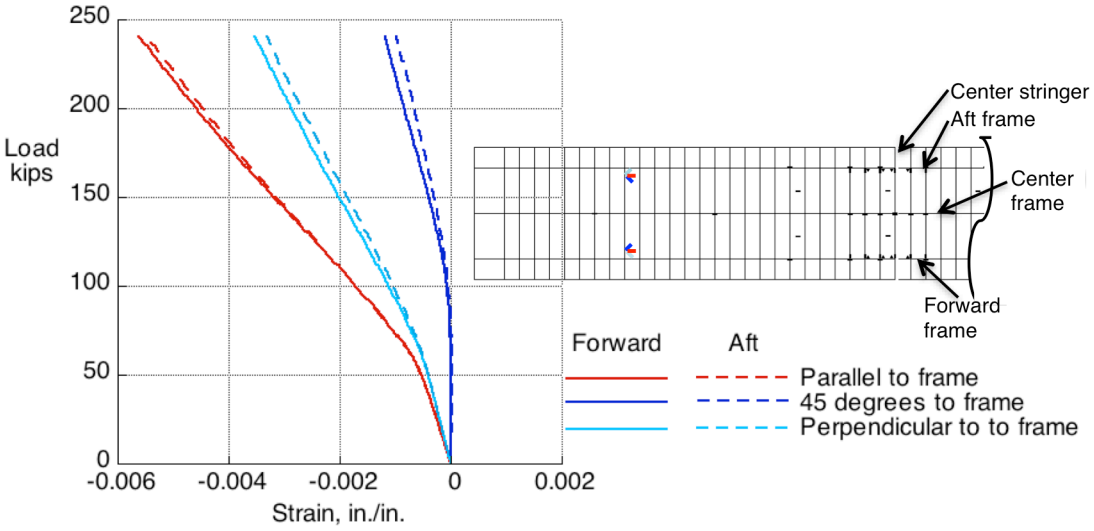

Figure 45. Strain in the crown skin from the interior rosette gauges.

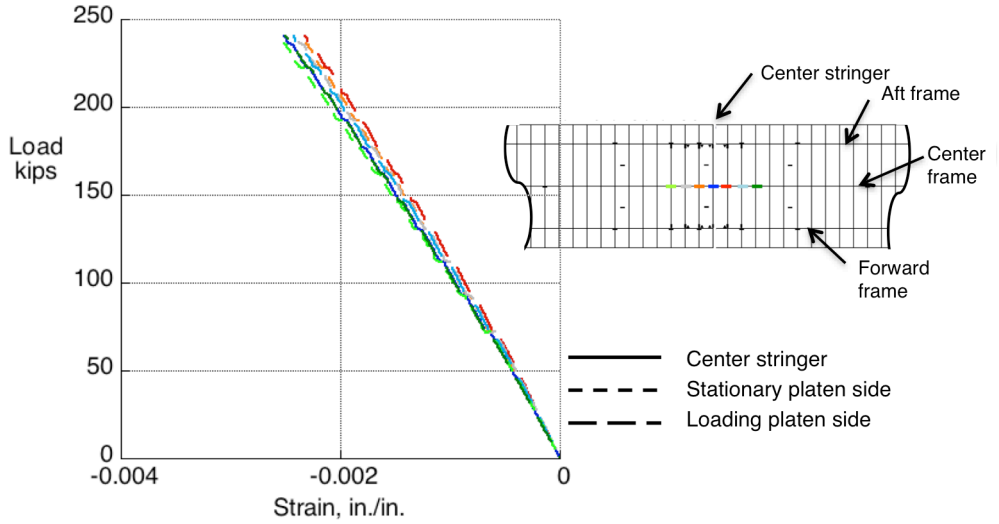

Figure 46. Strain in the crown center frame in the web above the keyholes.

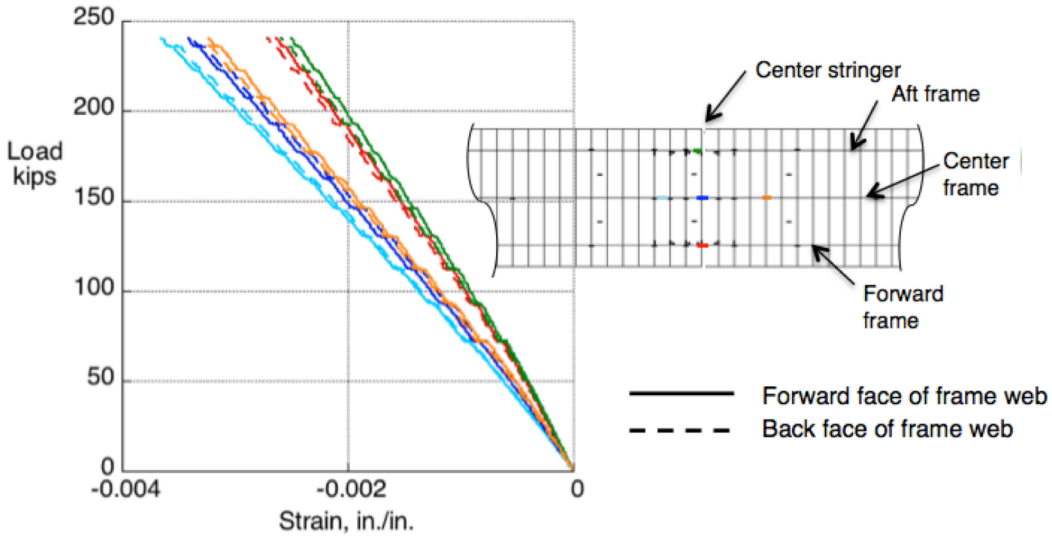

Figure 47. Strain in the crown frame web one inch away from the top of the frame.

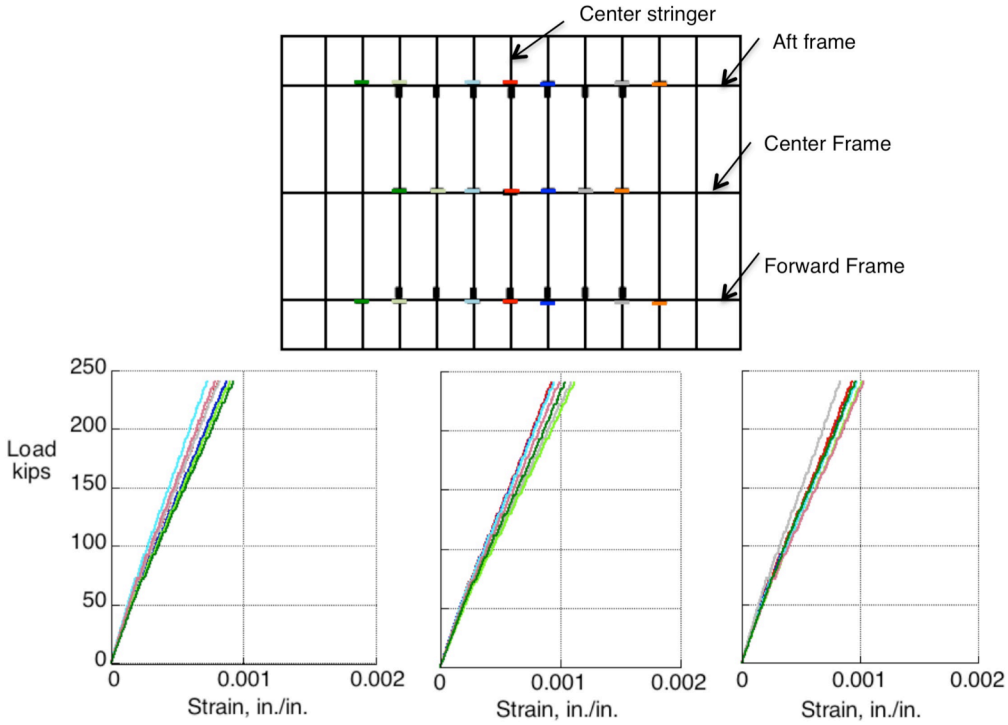

a) Center **b) Forward** **c) Aft**

Figure 48. Strain in the center keel frame webs.

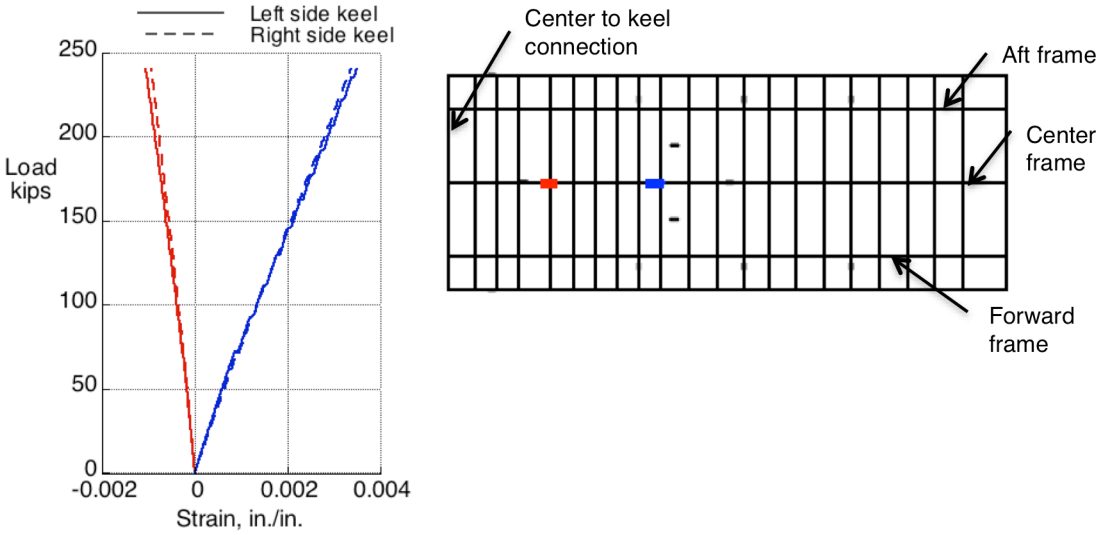

Figure 49. Strain on the top of the center frame in the side keels.

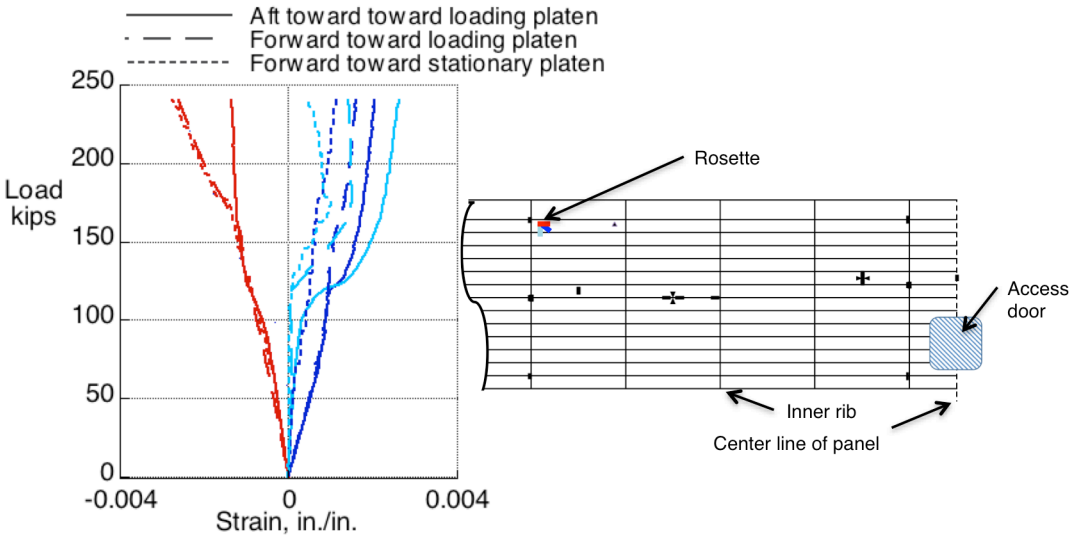

Figure 50. Strain on the exterior upper bulkhead skin from the outboard strain rosettes.

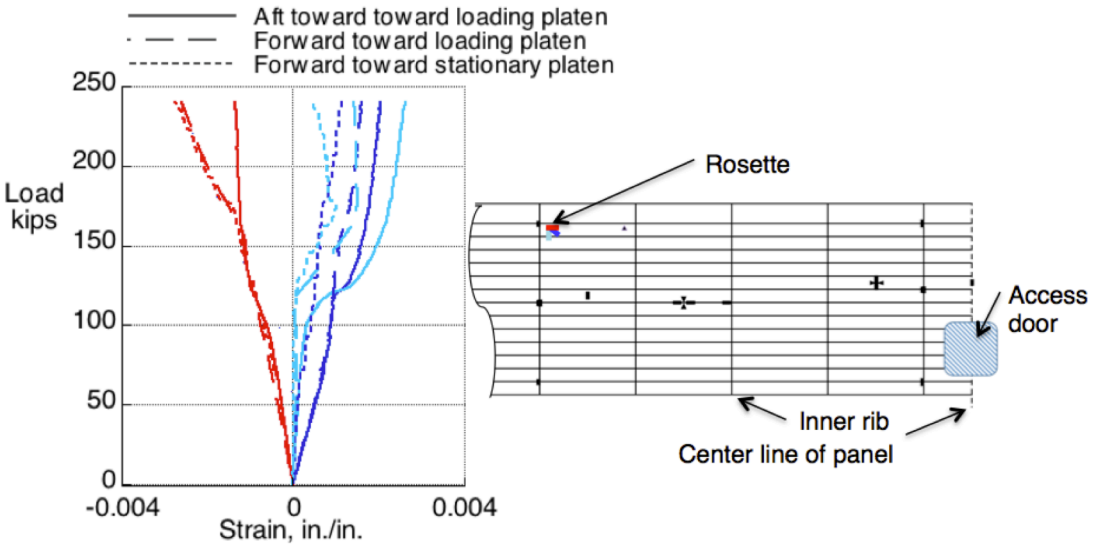

Figure 51. Strain on the exterior upper bulkhead skin from the inboard strain rosettes.

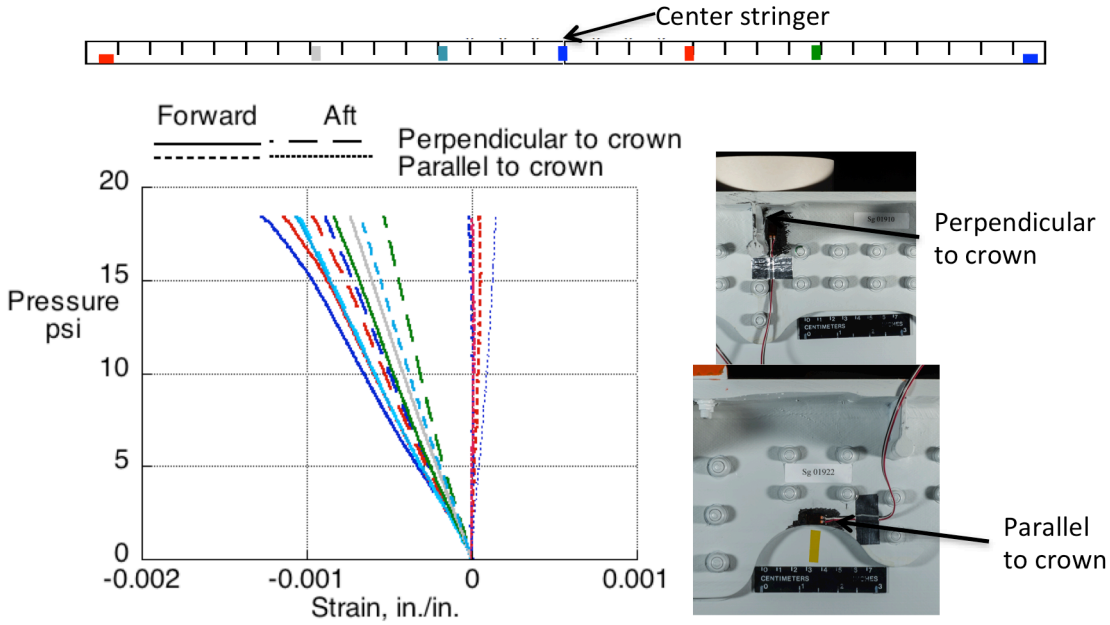

Figure 52. Strain on the exterior side of the crown T-caps.

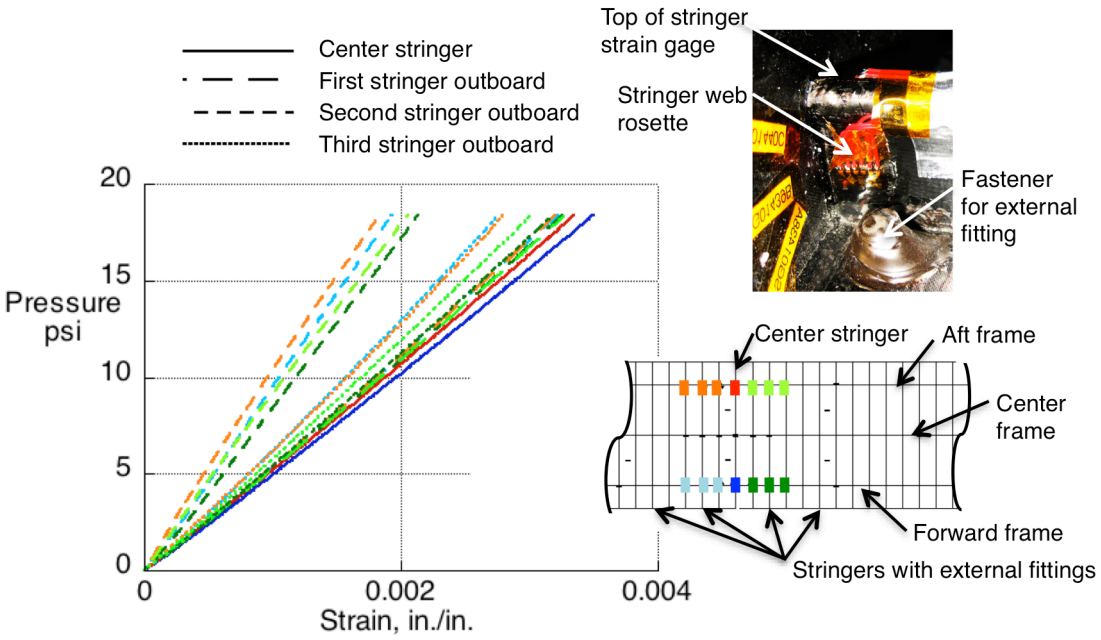

Figure 53. Strain on the top of stringers in the upper bulkheads.

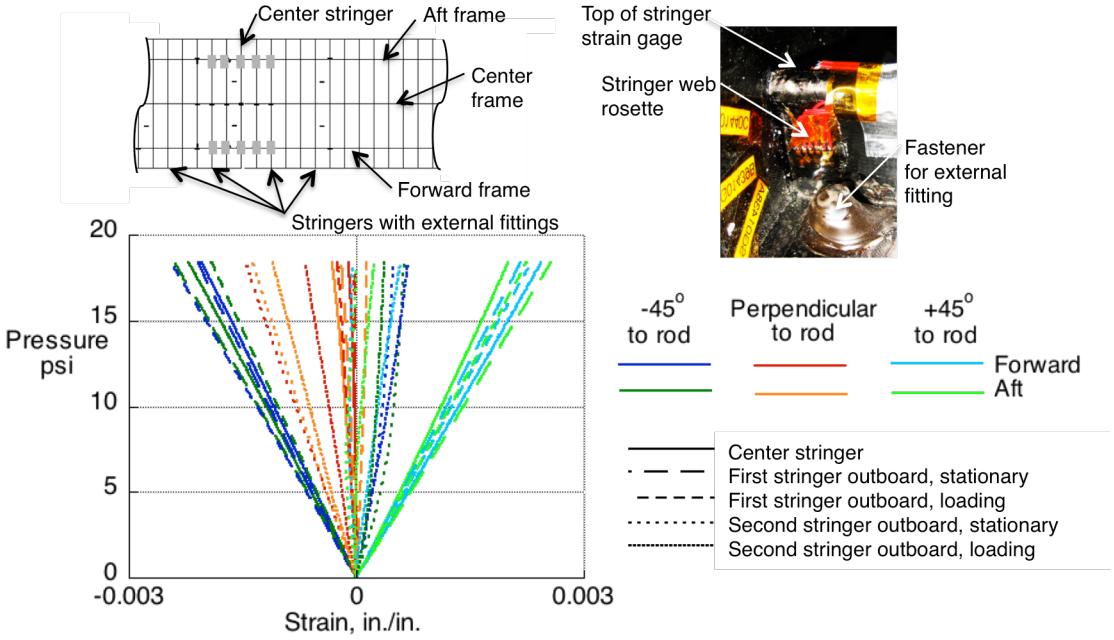

Figure 54. Strain in the upper bulkhead stringer webs.

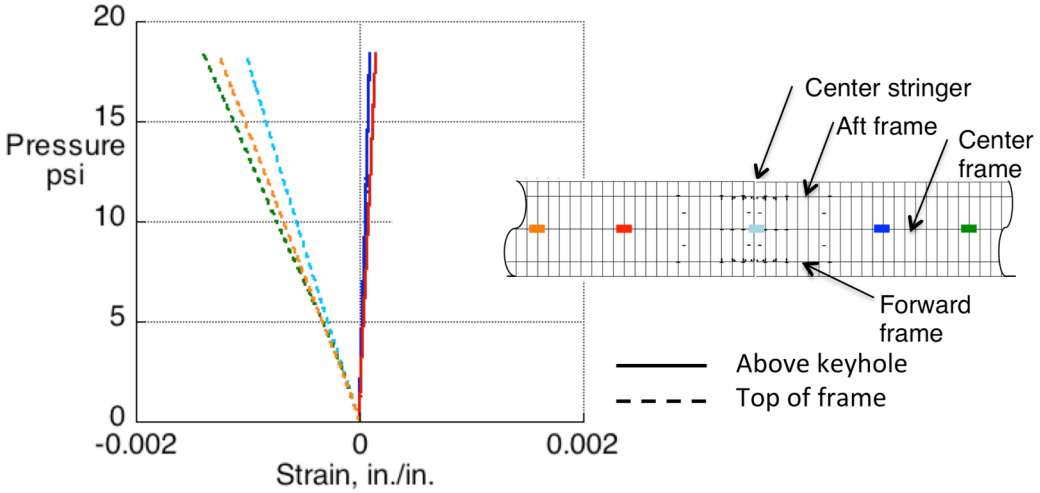

Figure 55. Strain in the upper bulkheads center frame webs.

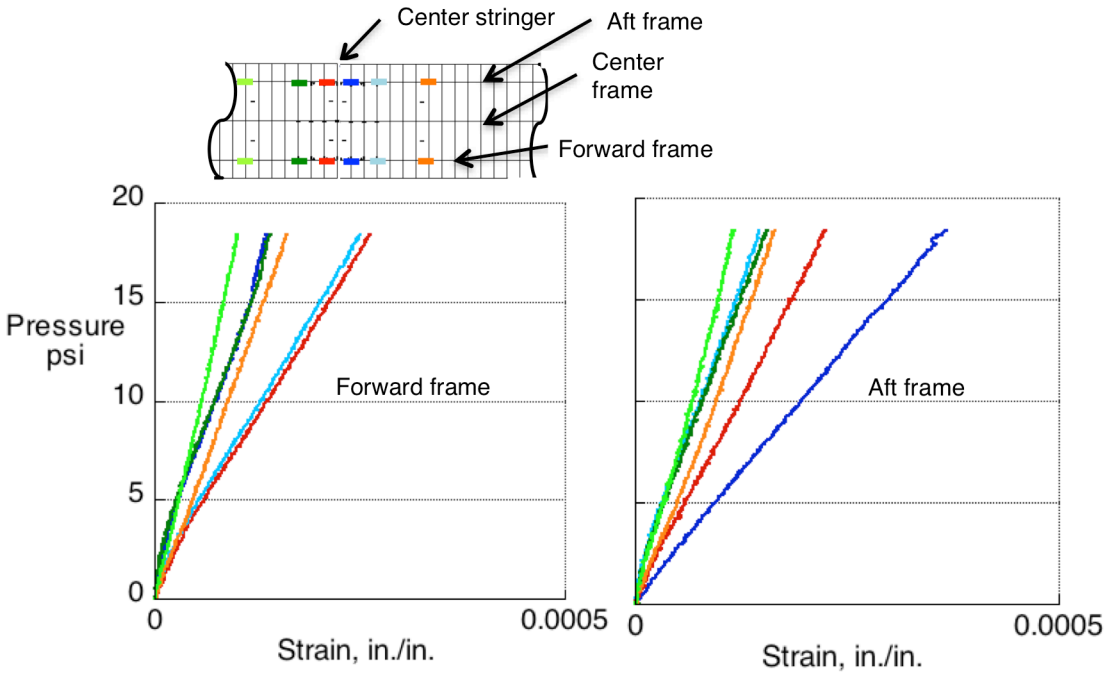

Figure 56. Strain in the upper bulkheads side frame webs.

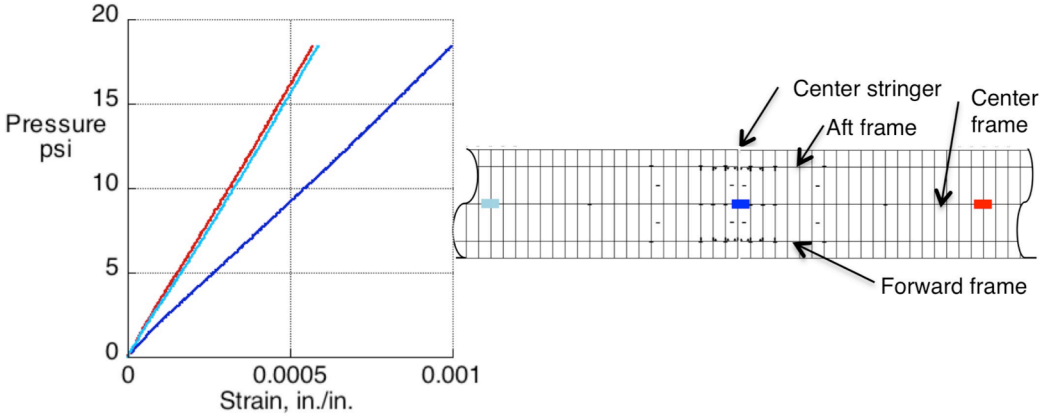

Figure 57. Strain on the upper bulkhead center frame on the exterior side.

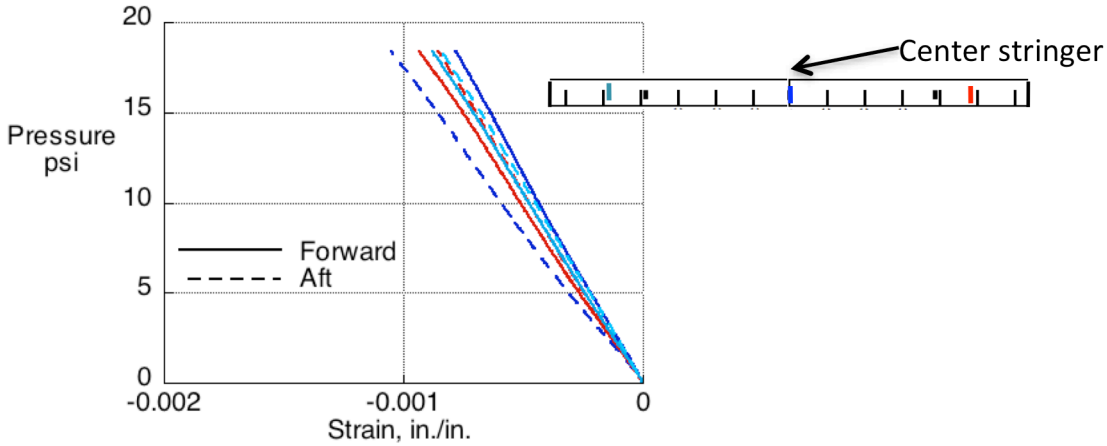

Figure 58. Strain on the exterior side of the center keel T-cap.

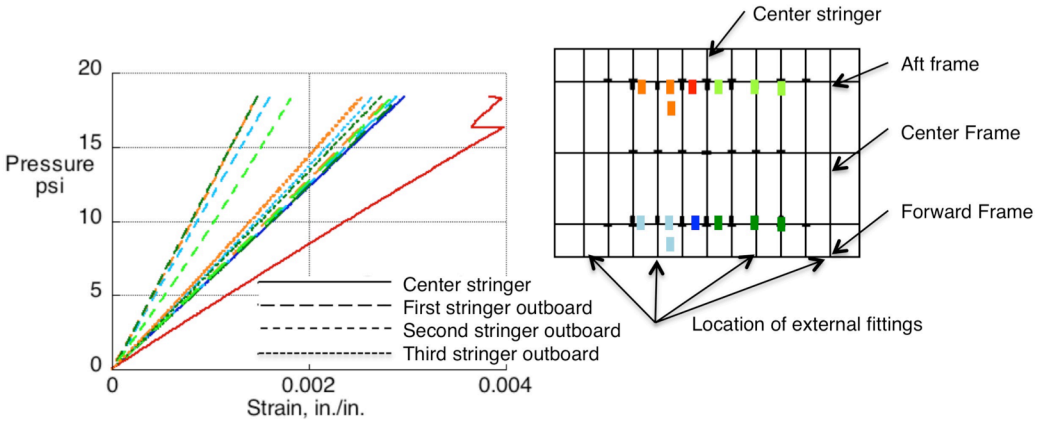

Figure 59. Strain on the top of stringers in the center keel.

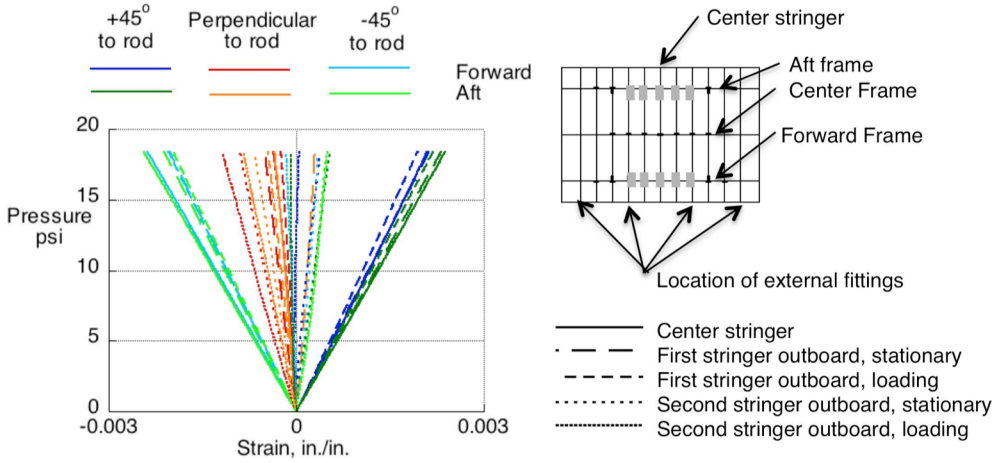

Figure 60. Strain in the center keel stringer webs from the rosette strain gauges.

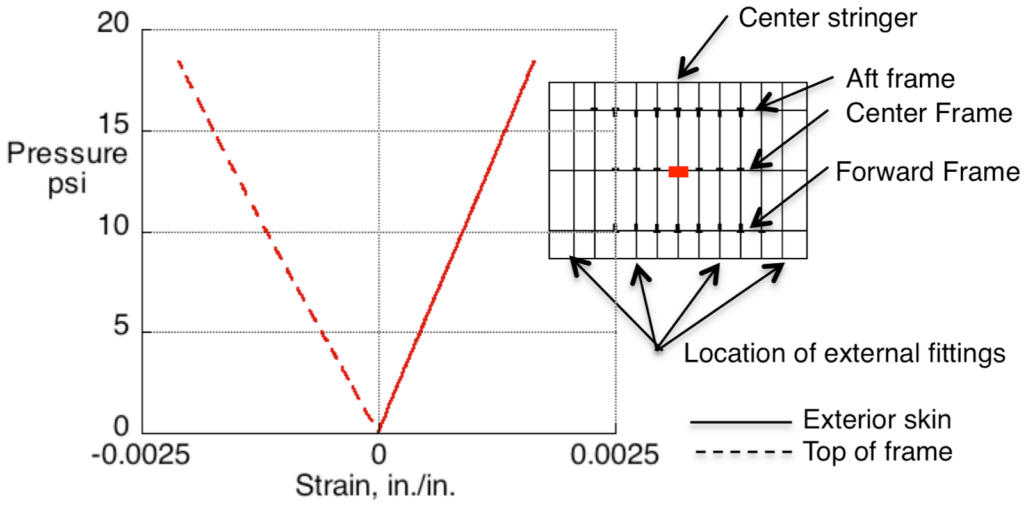

Figure 61. Strain at the center of the center keel.

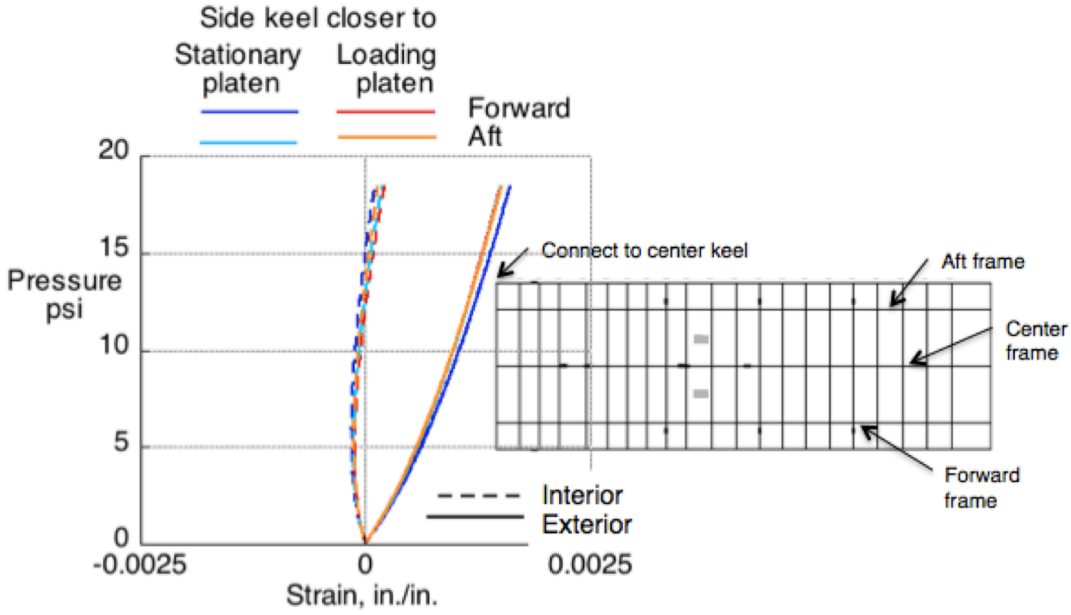

Figure 62. Strain in the skin of the side keels.

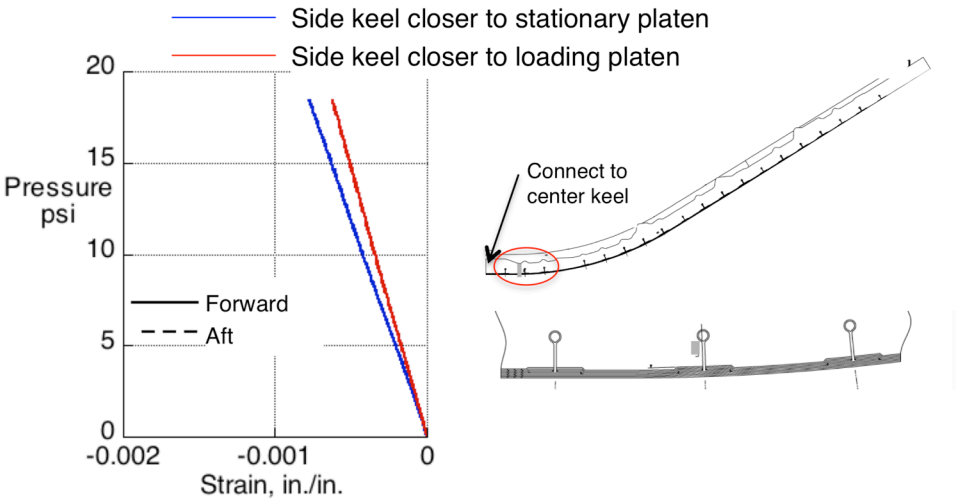

Figure 63. Strain in the side keel T-caps.

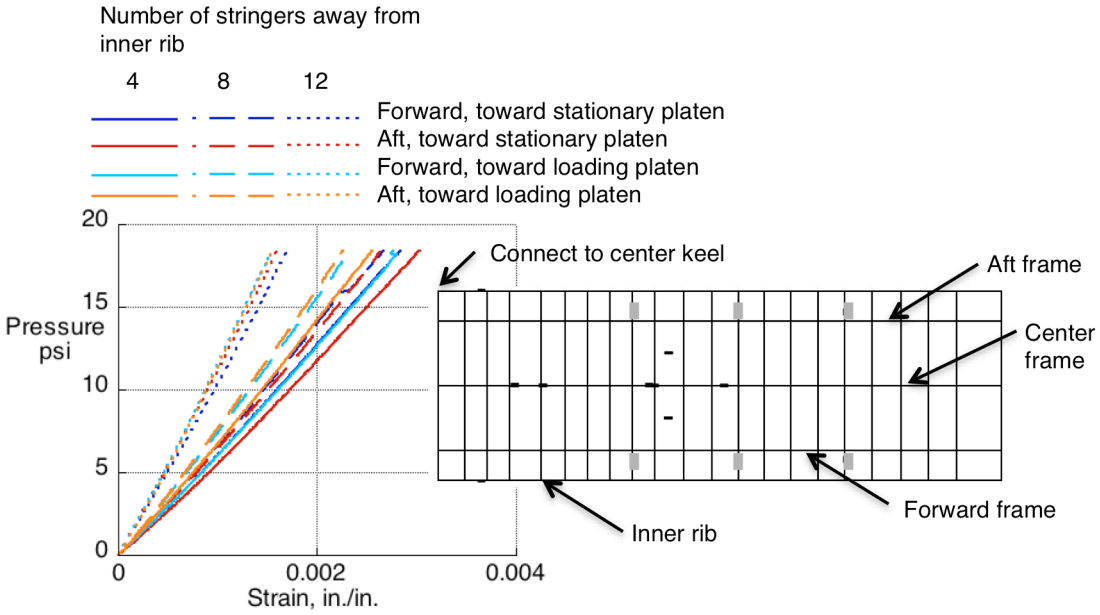

Figure 64. Strain on the top of the side keel stringers.

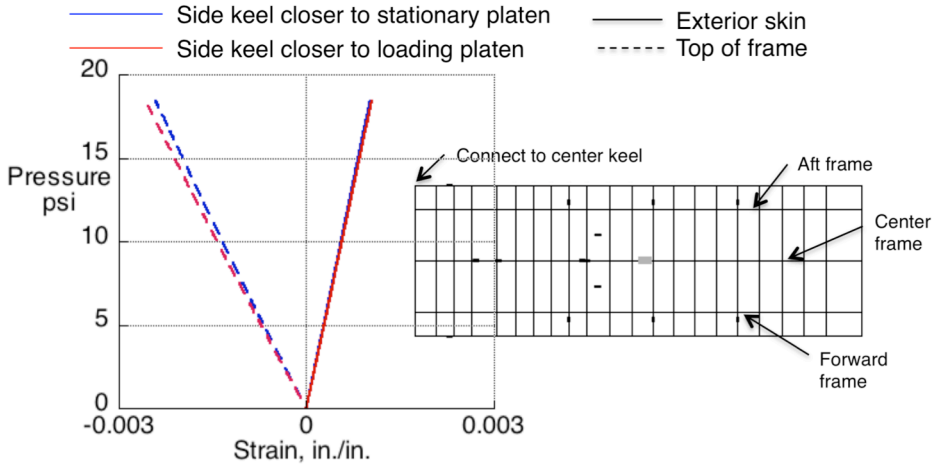

Figure 65. Strain on the top of the frame and at the frame on the external skin of the side keels.

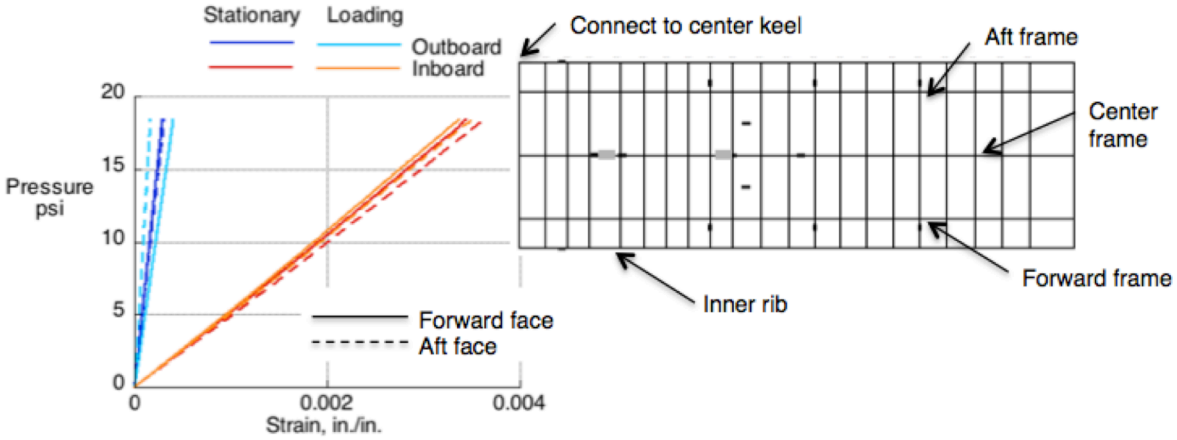

Figure 66. Strain on the side keel frame webs.

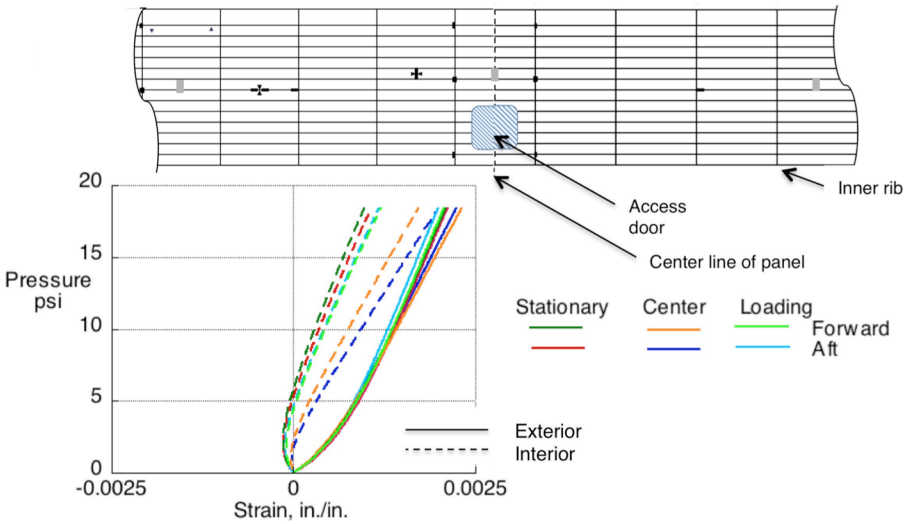

Figure 67. Strain on the exterior upper bulkhead skin.

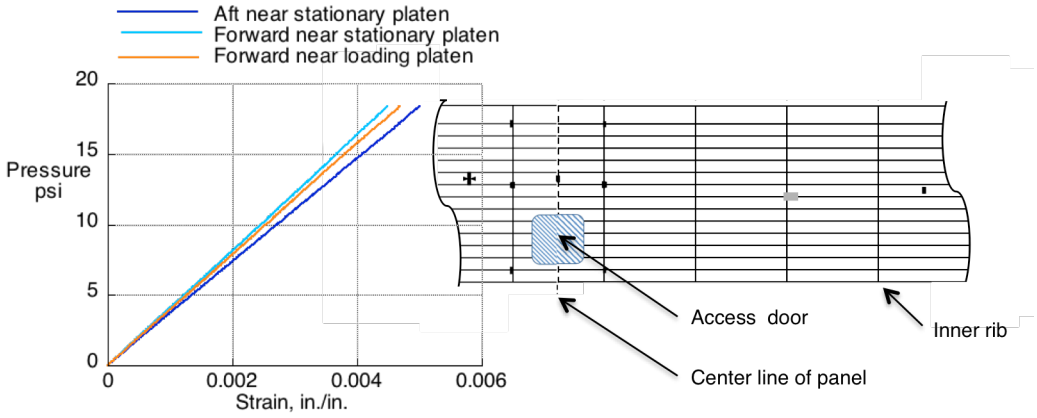

Figure 68. Strain in the top of the stringers in the upper bulkheads.

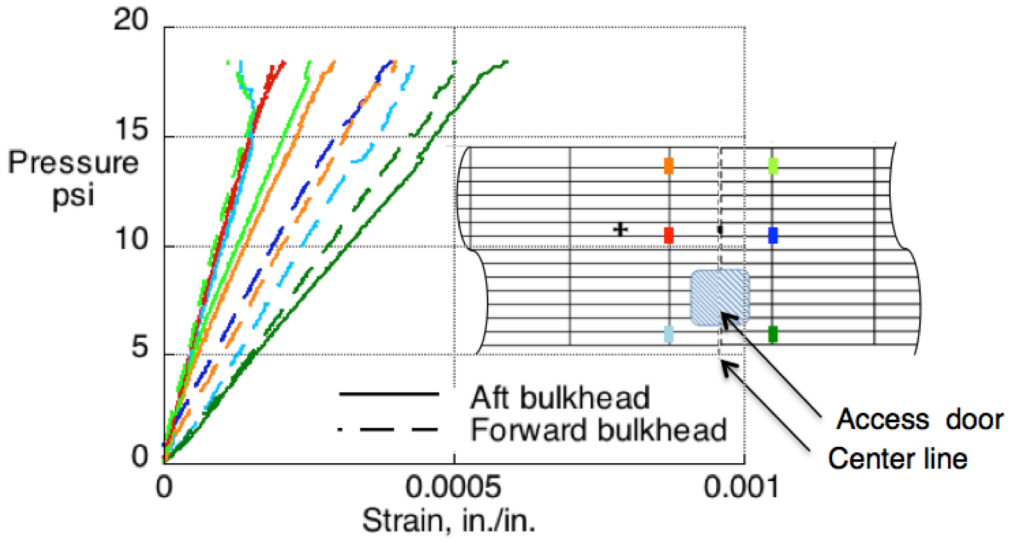

Figure 69. Strain on top of frames in the upper bulkheads near the access doors.

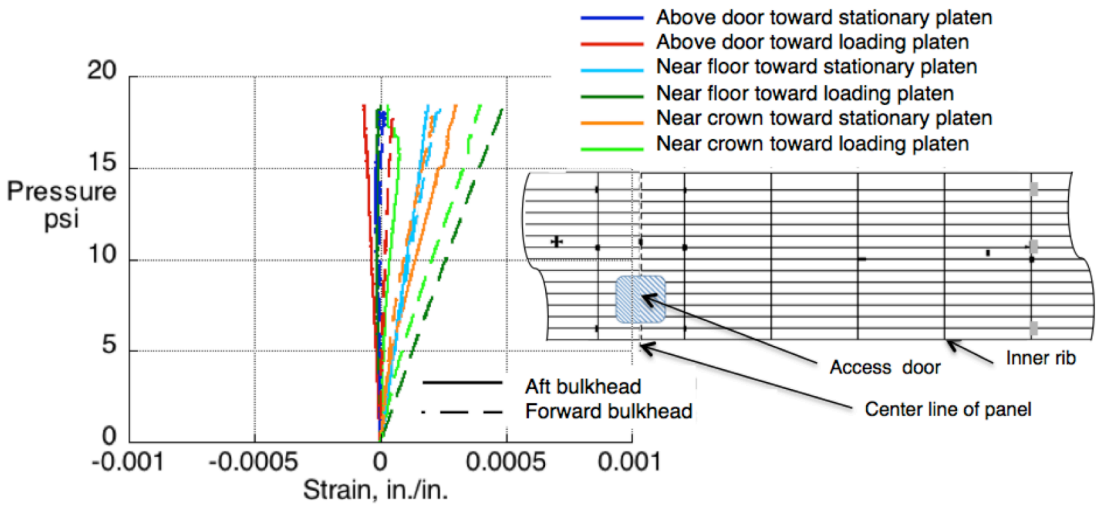

Figure 70. Strain at the keyholes in the upper bulkheads near the inner ribs.

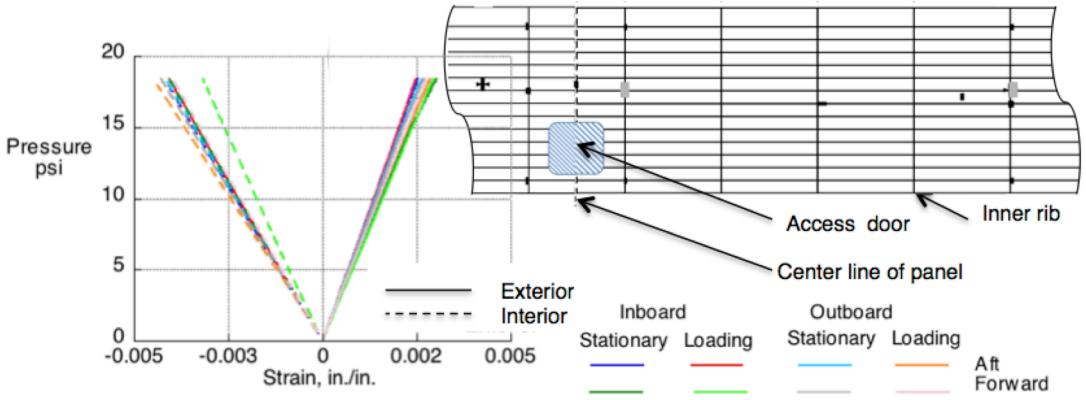

Figure 71. Strain on the top of the frame and at the frame on the external skin of the upper bulkheads.

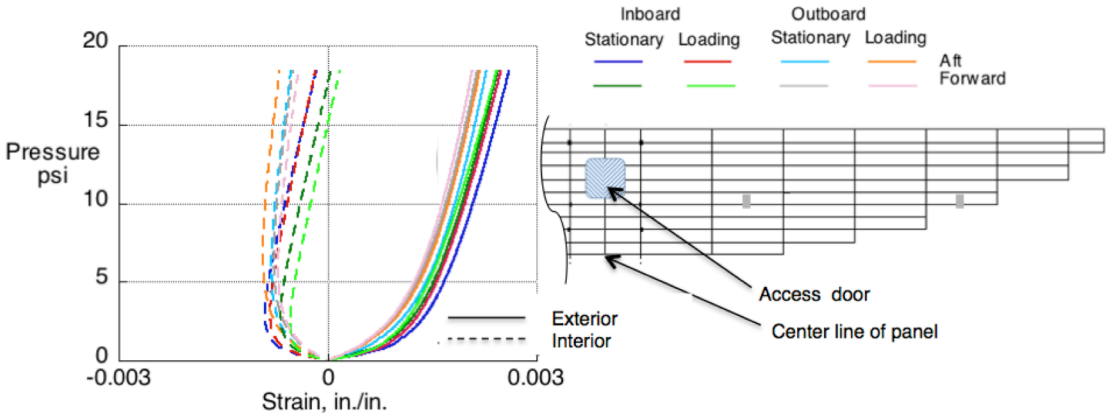

Figure 72. Strain in the lower bulkheads skin.

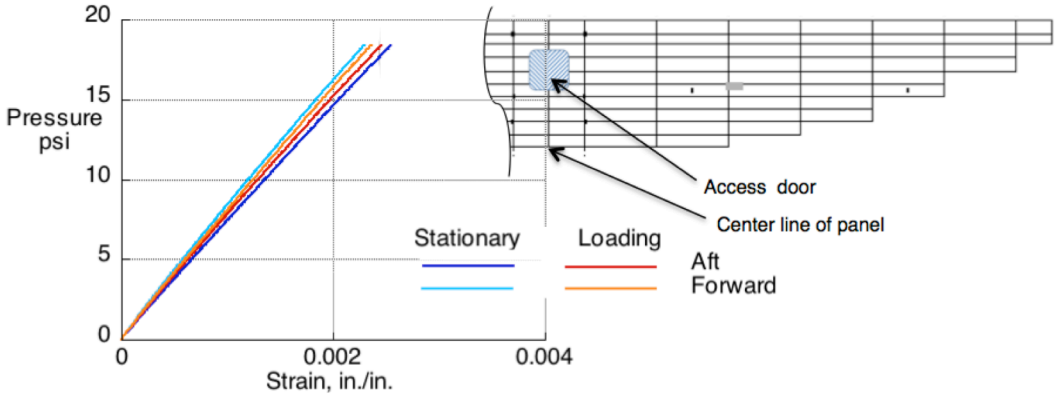

Figure 73. Strain on top of the stringers on the lower bulkheads.

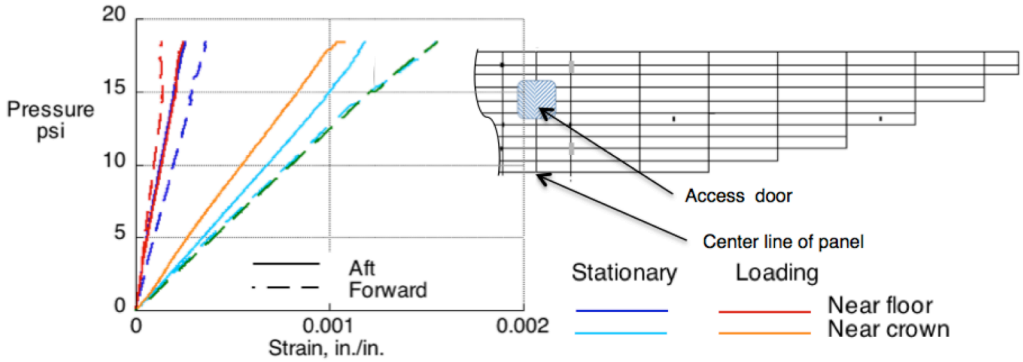

Figure 74. Strain at the lower bulkhead keyholes.

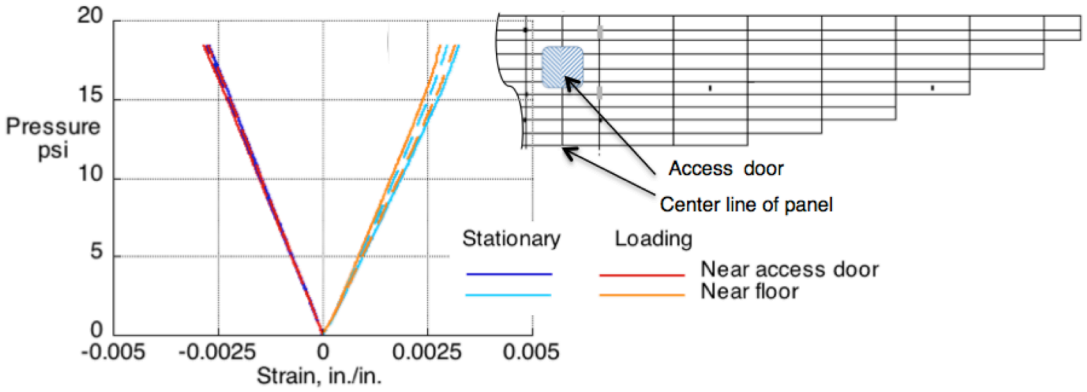

Figure 75. Strain on the top of stringers in the lower bulkhead.

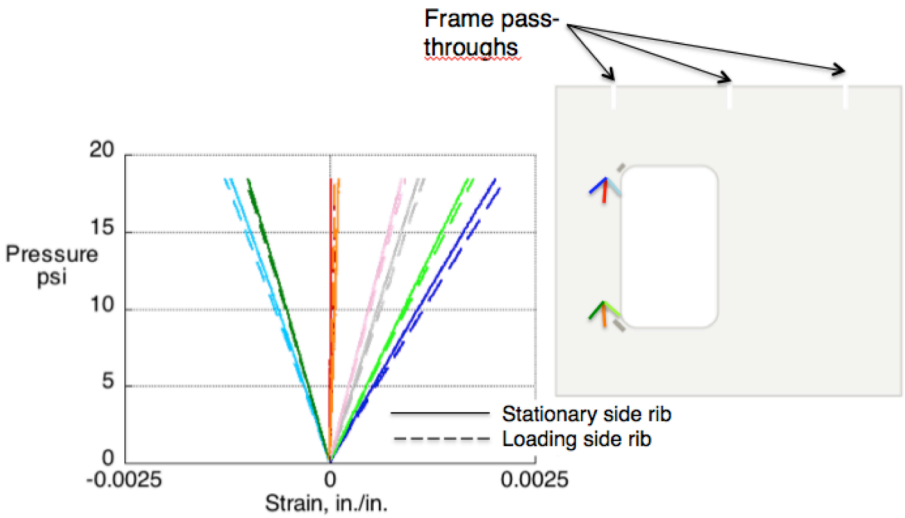

Figure 76. Strain in the upper inner ribs from rosettes strain gauges (Color indicates the arm of the gauge).

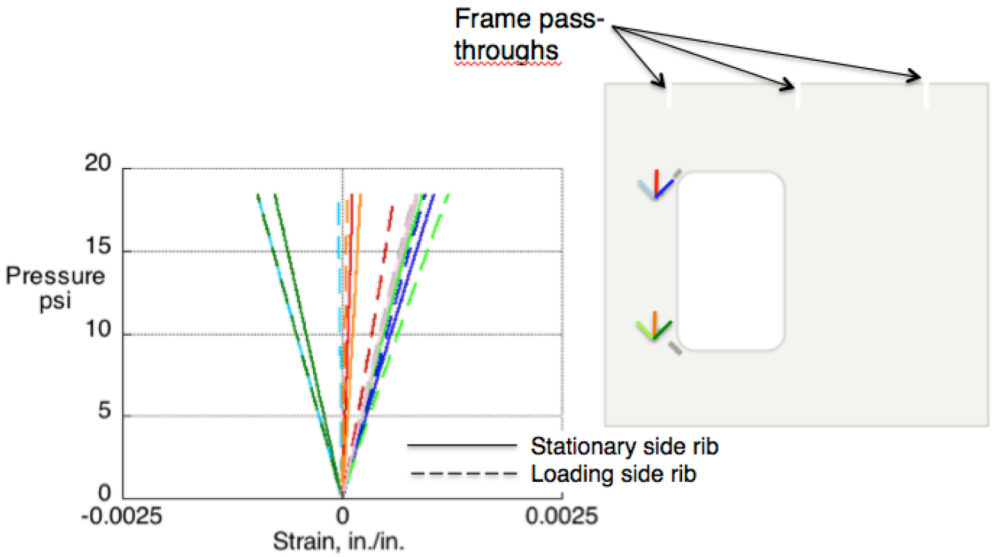

Figure 77. Strain in the lower inner ribs from rosettes strain gauges (Color indicates the arm of the gauge).

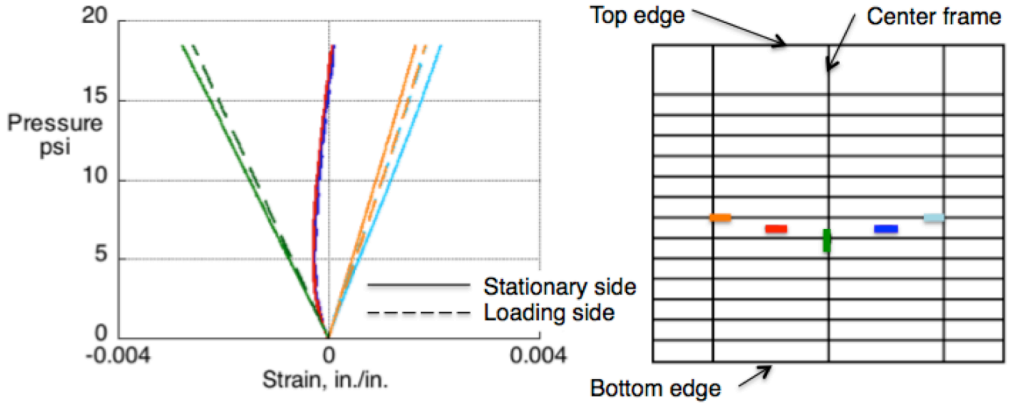

Figure 78. Strains in the outer ribs.

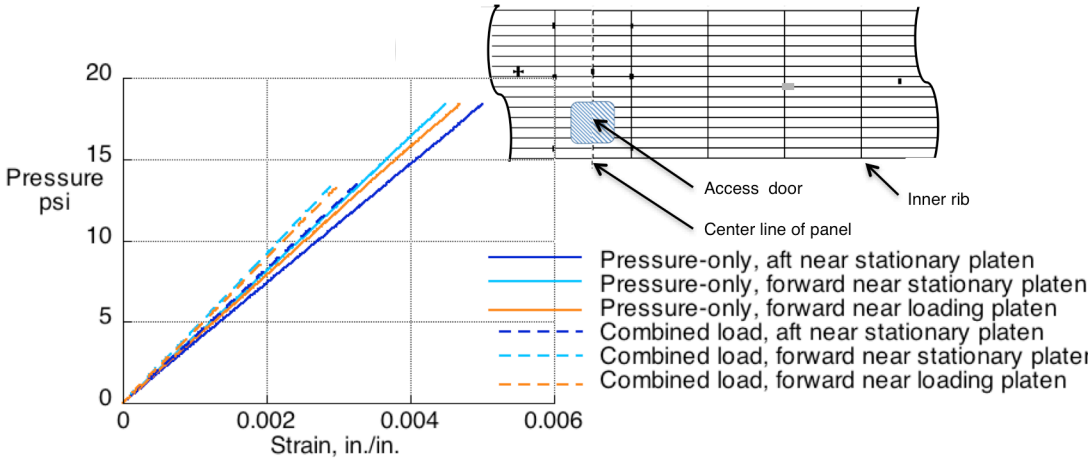

Figure 79. Strain in the top of the stringers of the upper bulkheads for the up-bending plus pressure and pressure-only load cases.

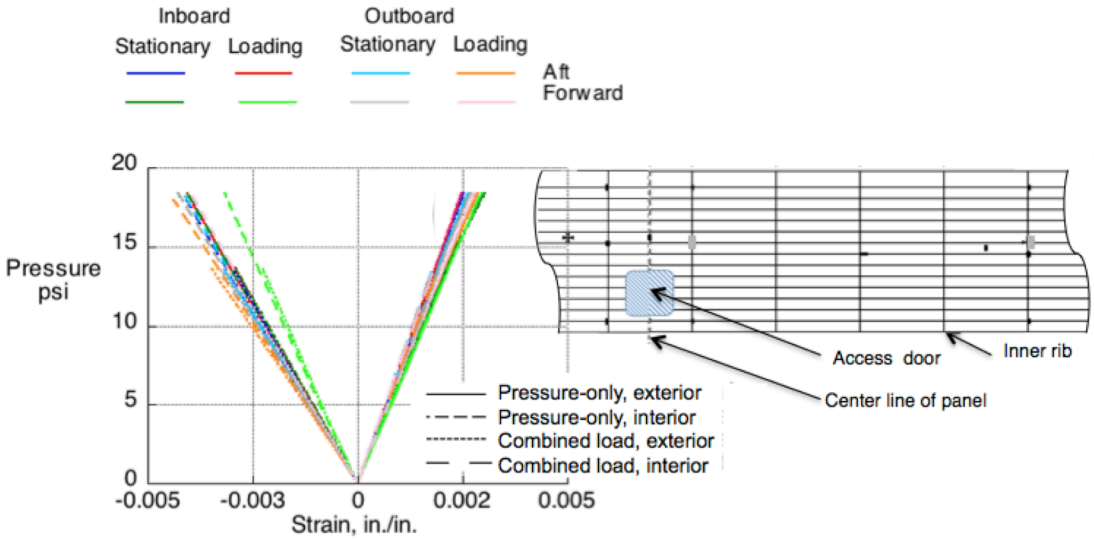

Figure 80. Strain in the top of the frames of the upper bulkhead for the up-bending plus pressure and pressure-only load cases.

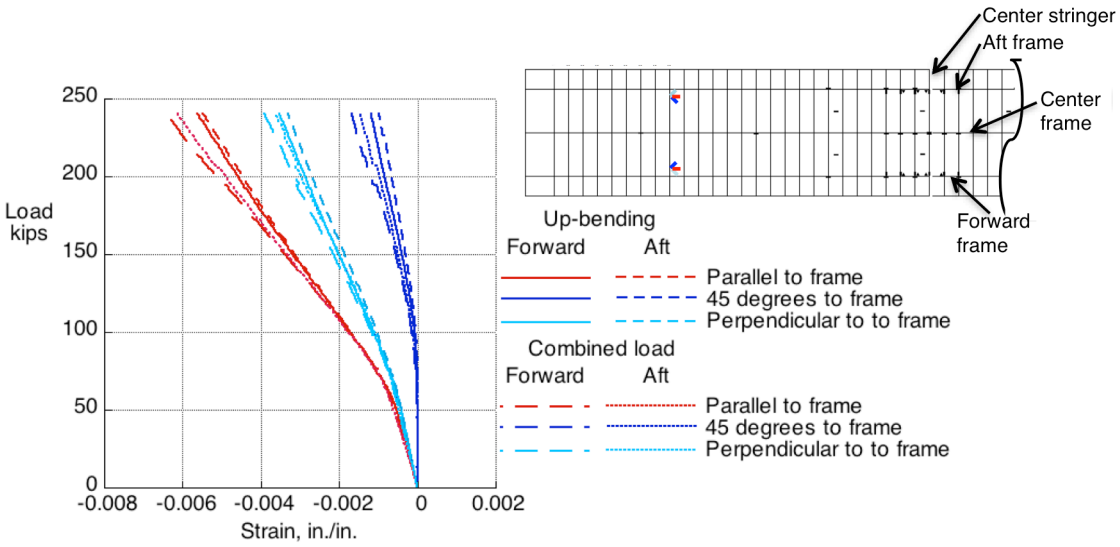

Figure 81. Strain in the strain rosettes on the interior of the crown in the up-bending plus pressure and pressure-only load cases.

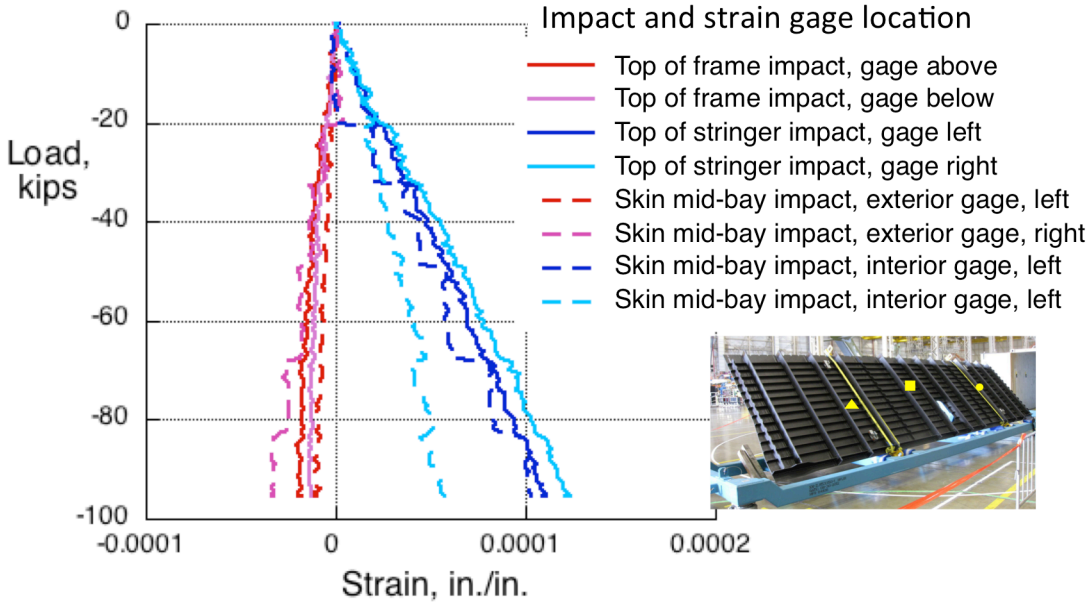

Figure 82. Strain at the interior impact sites for the down-bending load case.

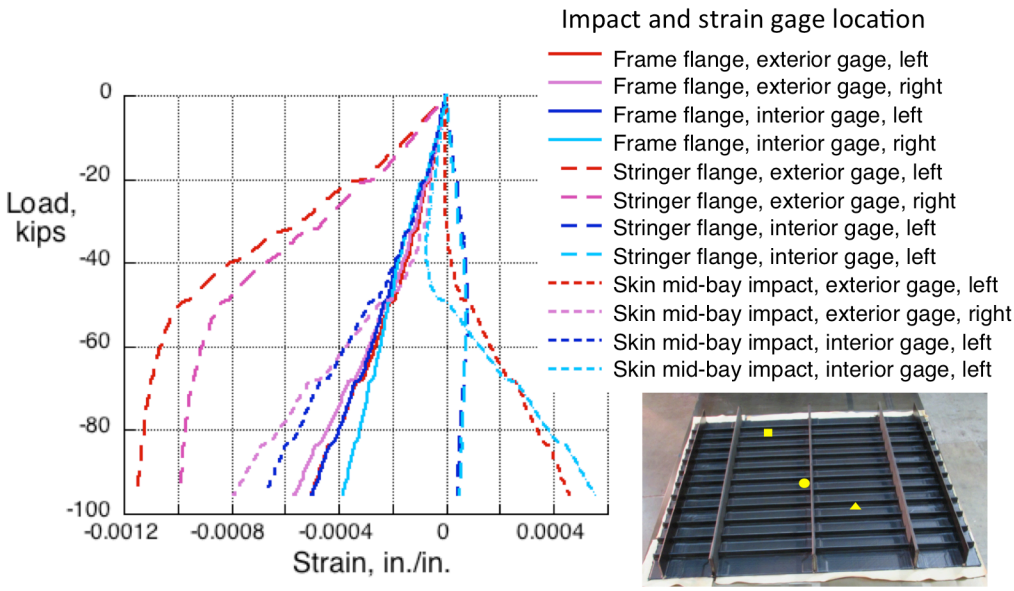

Figure 83. Strain at the exterior impact sites for the down-bending load case.

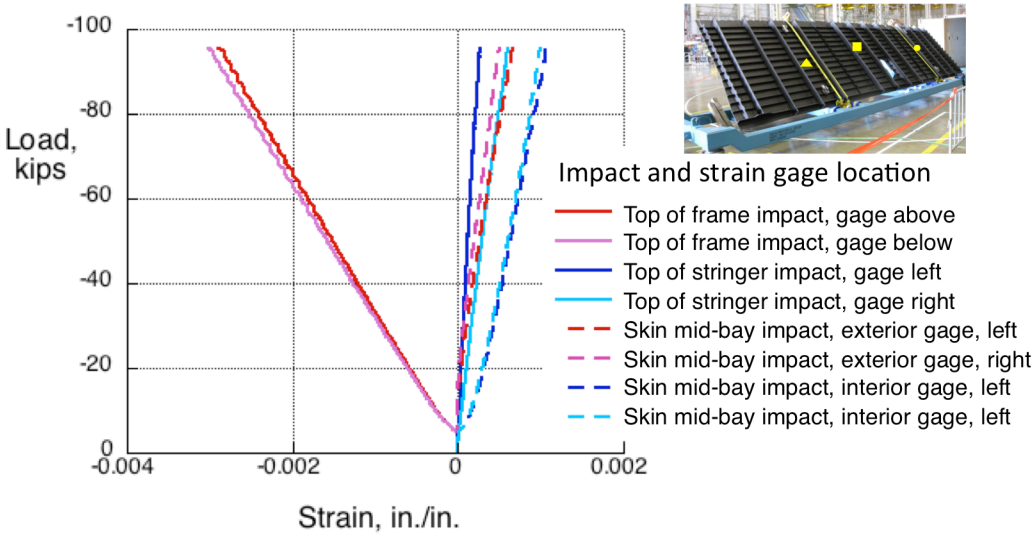

Figure 84. Strain at the interior impact sites for the down-bending plus pressure load case.

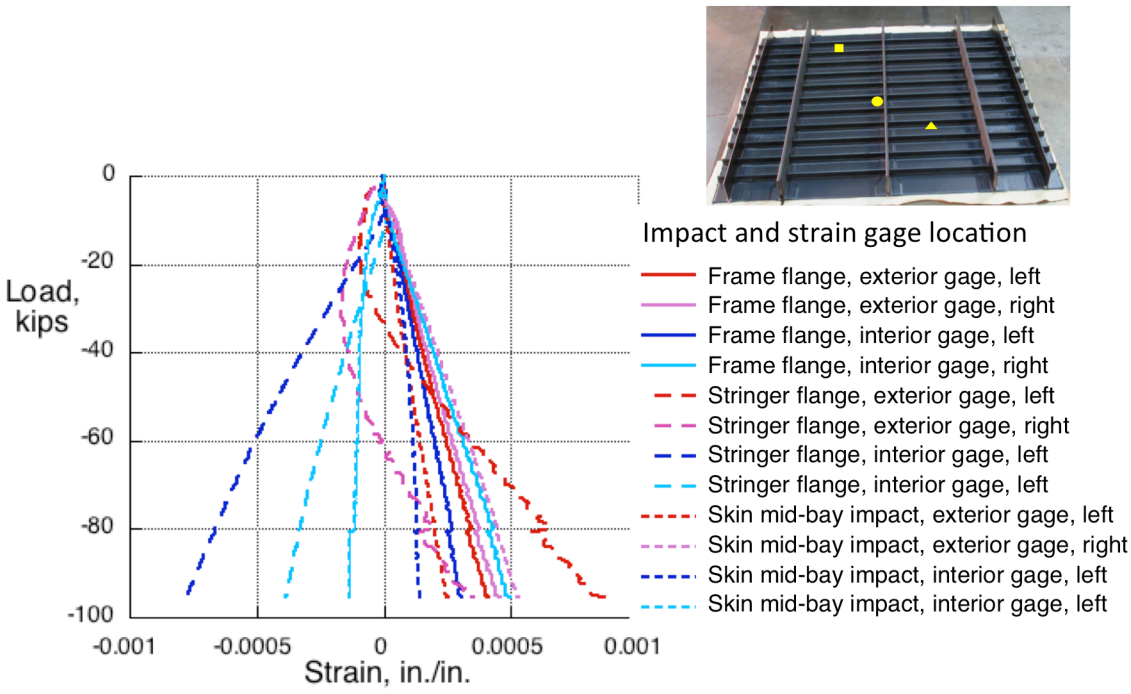

Figure 85. Strain at the exterior impact sites for the down-bending plus pressure load case.

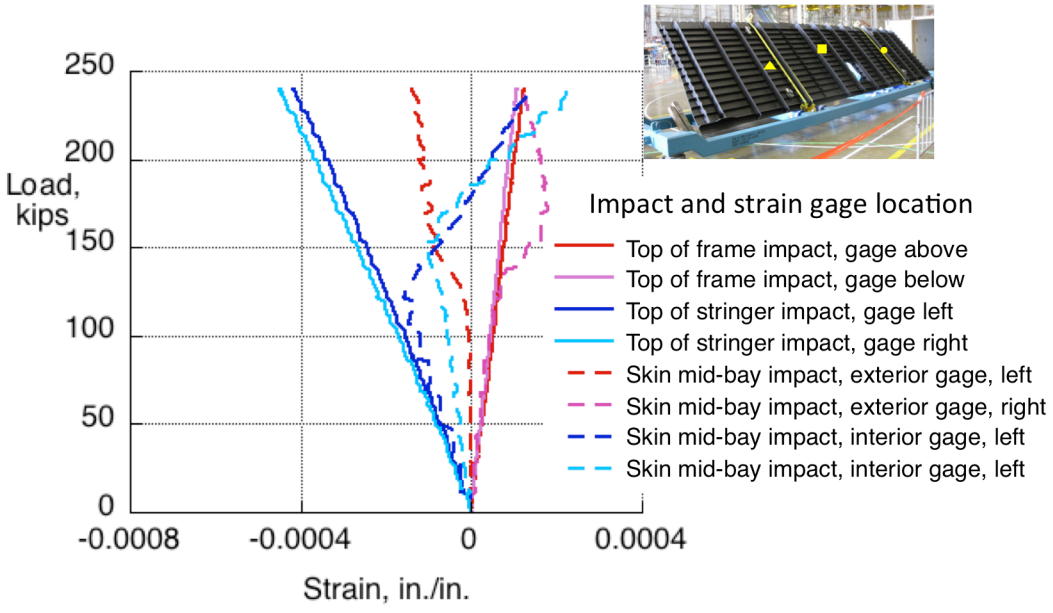

Figure 86. Strain at the interior impact sites for the up-bending load case.

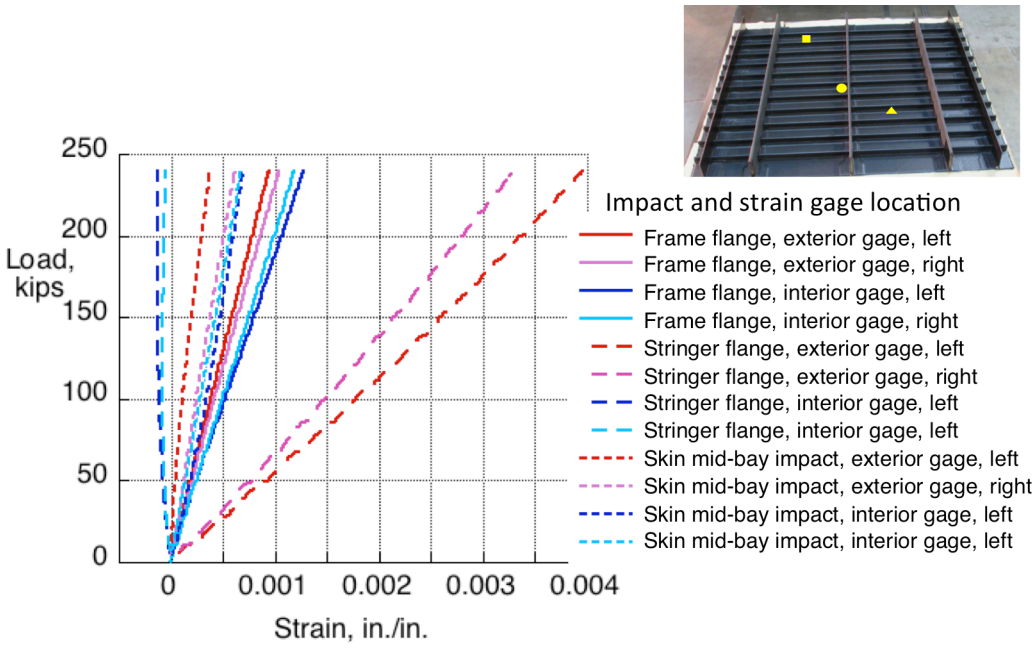

Figure 87. Strain at the exterior impact sites for the up-bending load case.

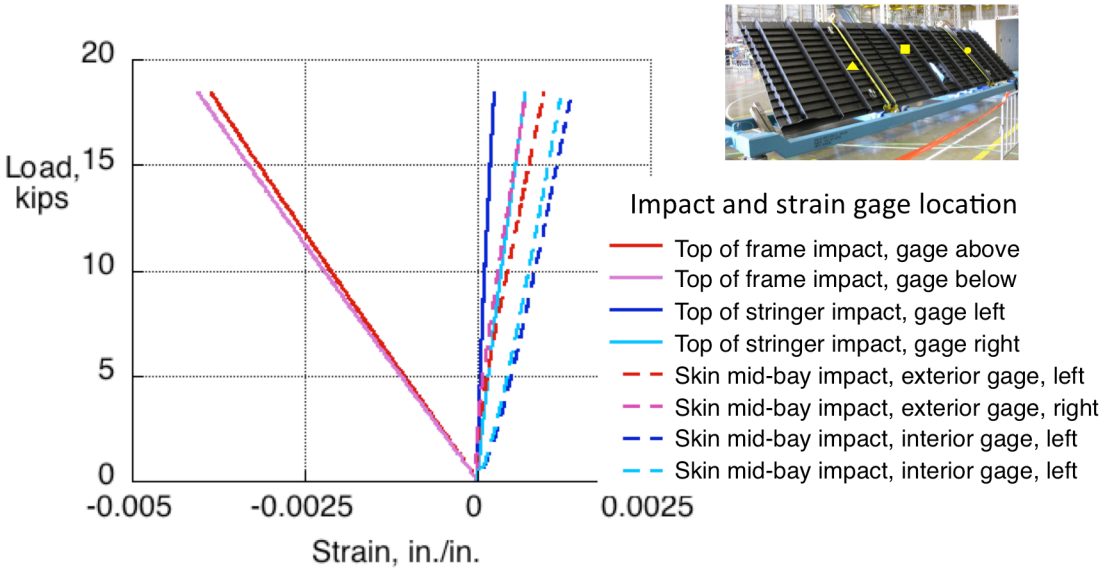

Figure 88. Strain at the interior impact sites for the pressure-only load case.

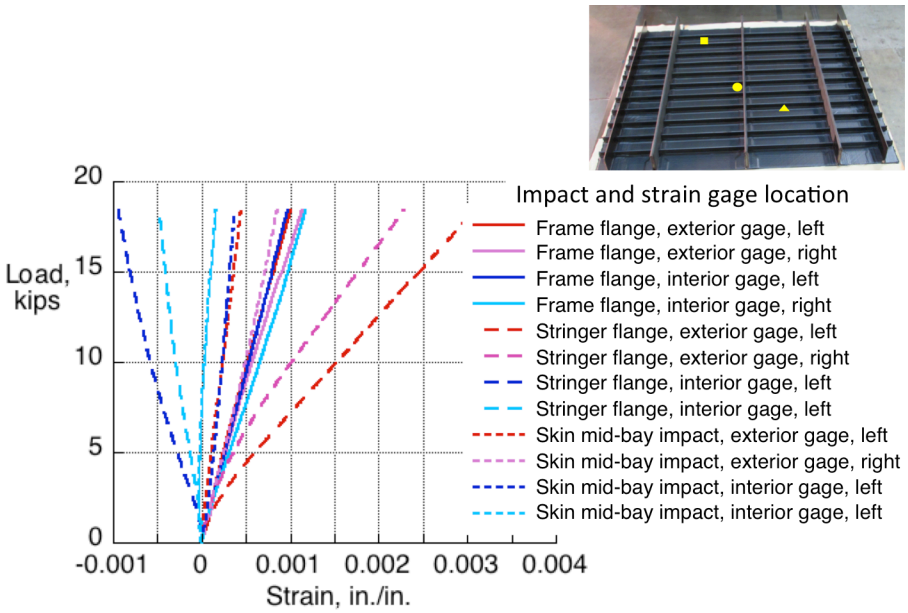

Figure 89. Strain at the exterior impact sites for the pressure-only load case.

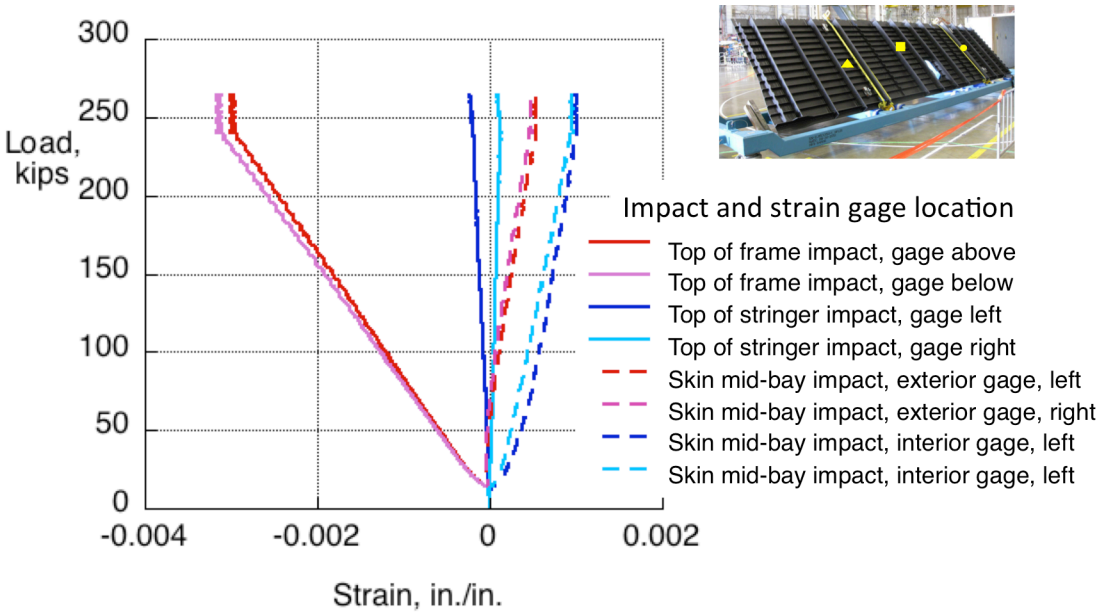

Figure 90. Strain at the interior impact sites for the up-bending with pressure load case.

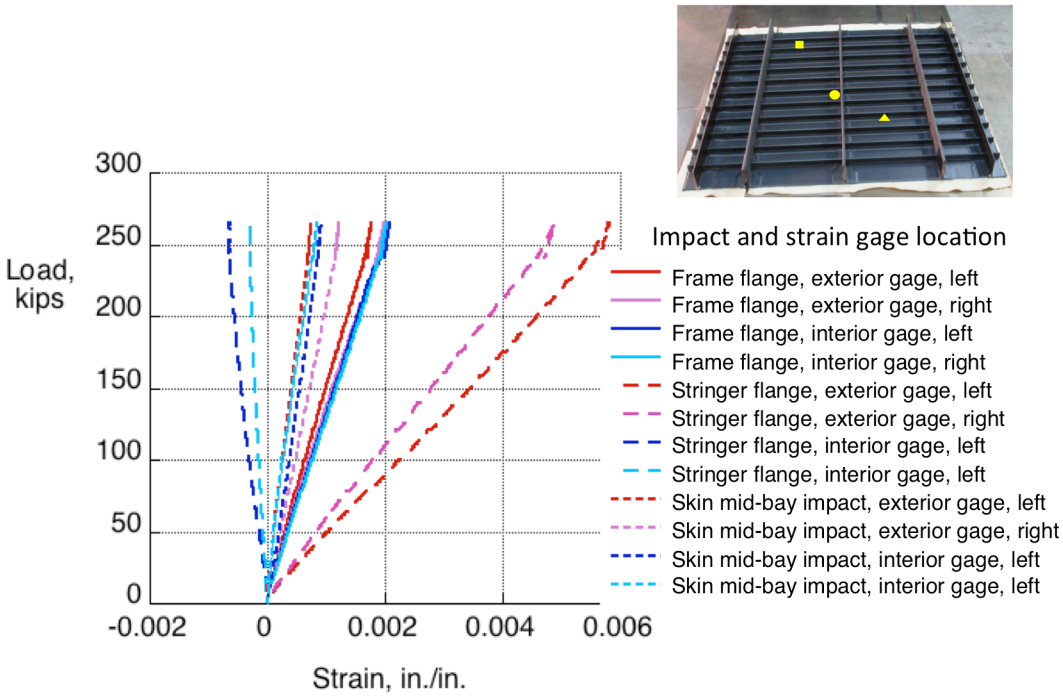

Figure 91. Strain at the exterior impact sites for the up-bending with pressure load case.

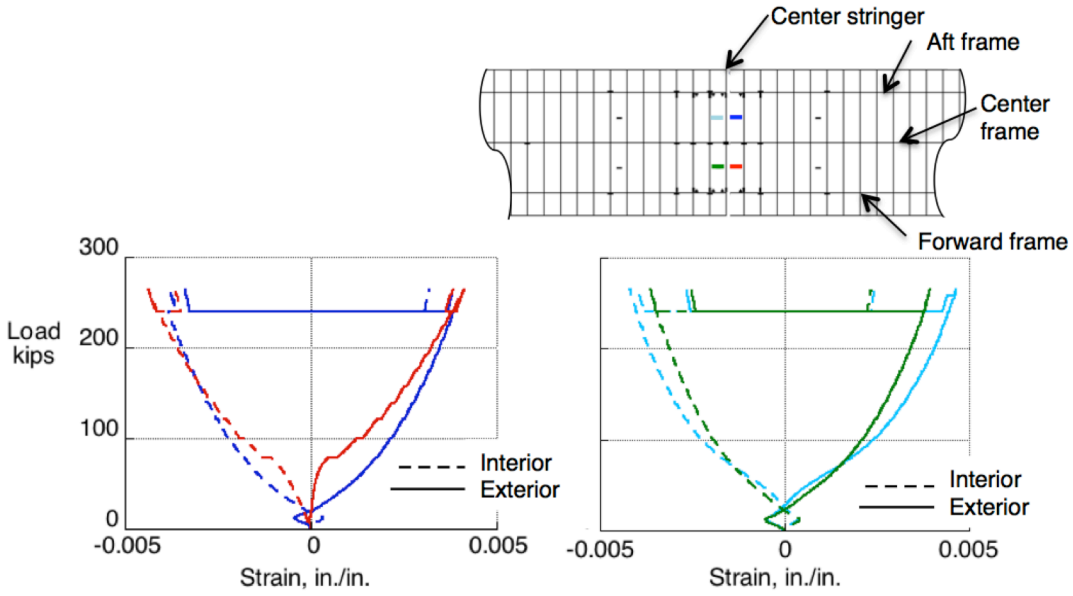

Figure 92. Strain in the crown skin in the load case to a load greater than DUL.

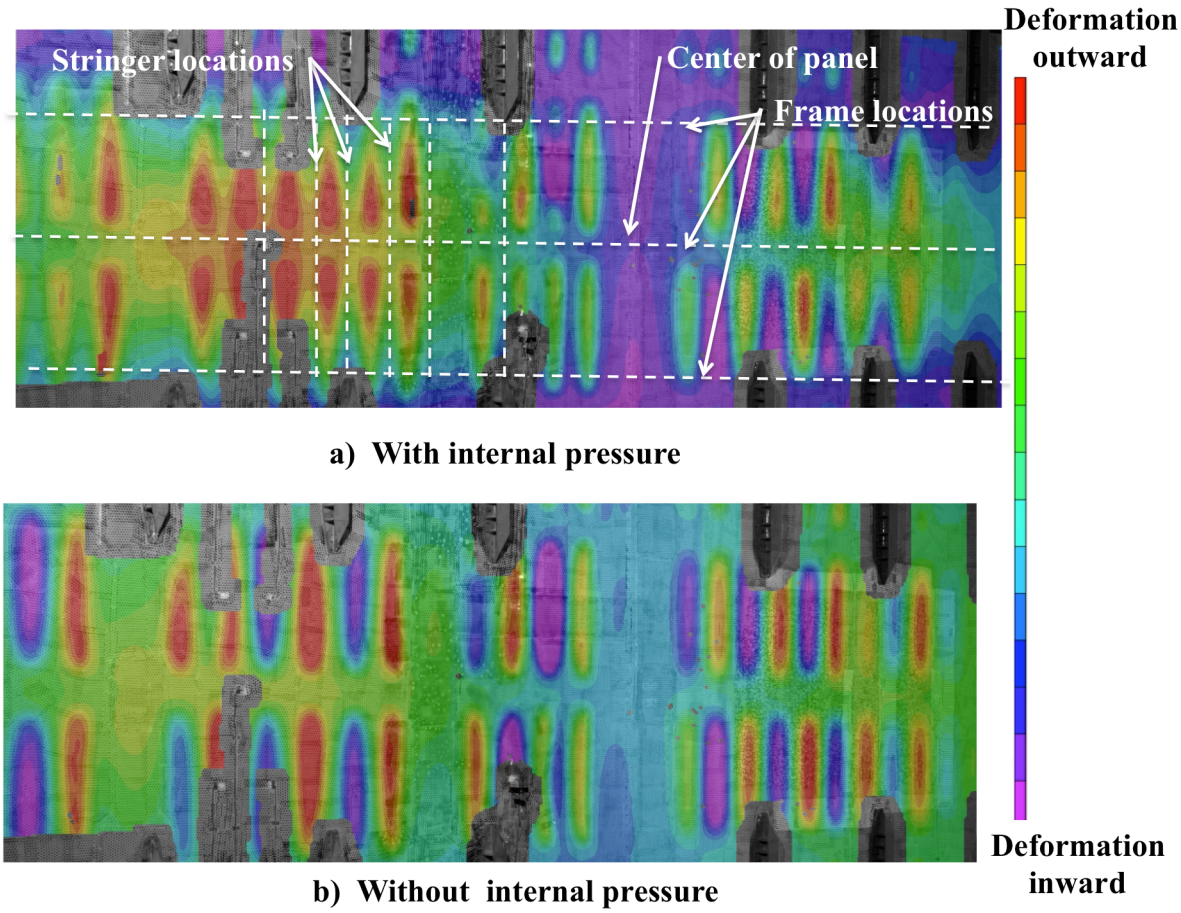

Figure 93. Crown deformation with a mechanical load of 110% DUL.

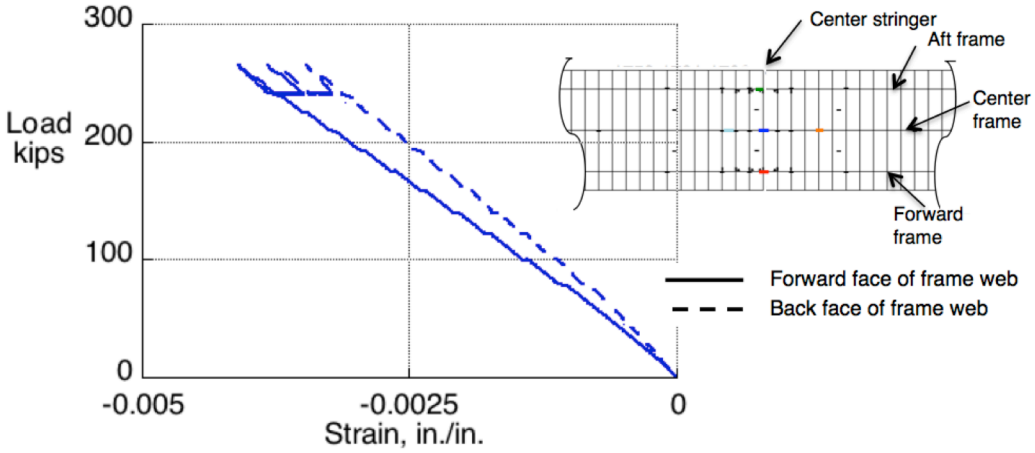

Figure 94. Strain in the crown frame web for the load case to load greater than DUL.

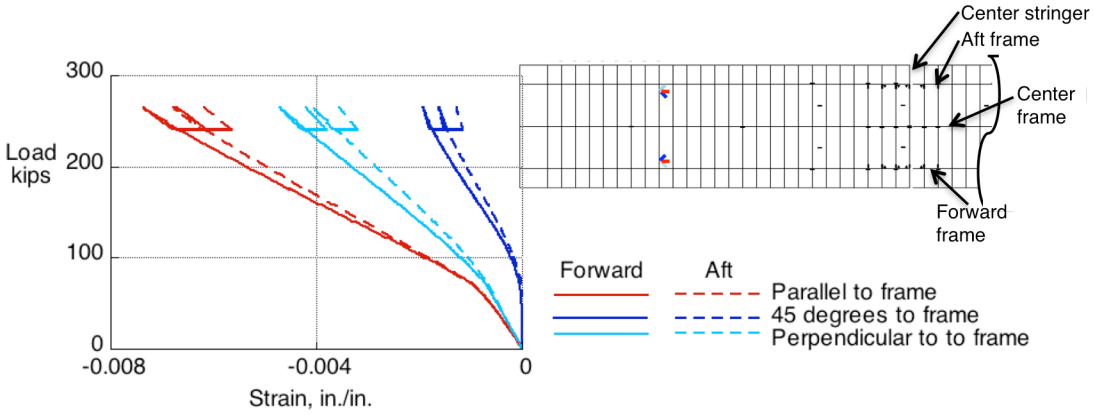

Figure 95. Strain in the crown skin from rosettes strain gauges for the load case to load greater than DUL.

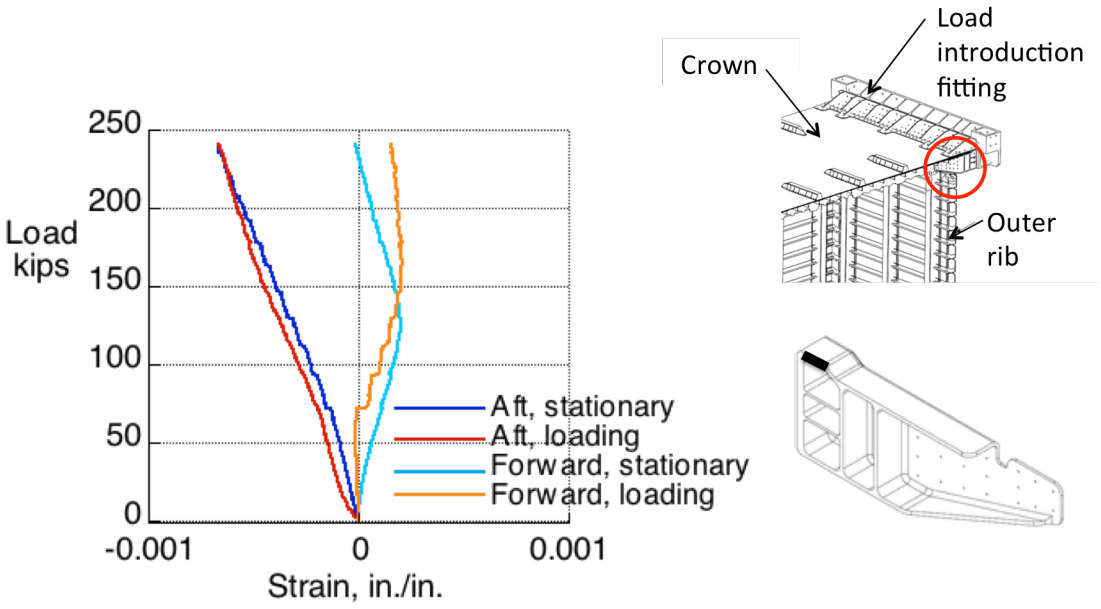

Figure 96. Strain in the external fitting at the upper load introduction structure (point A in Figure 13).

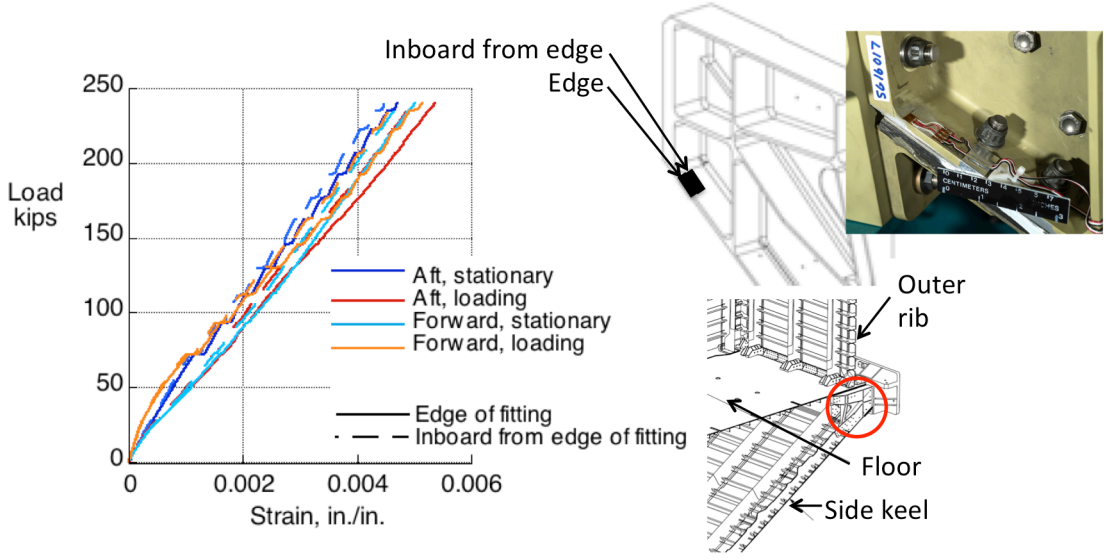

Figure 97. Strain in the external fitting at the lower load introduction structure (point B in Figure 13).

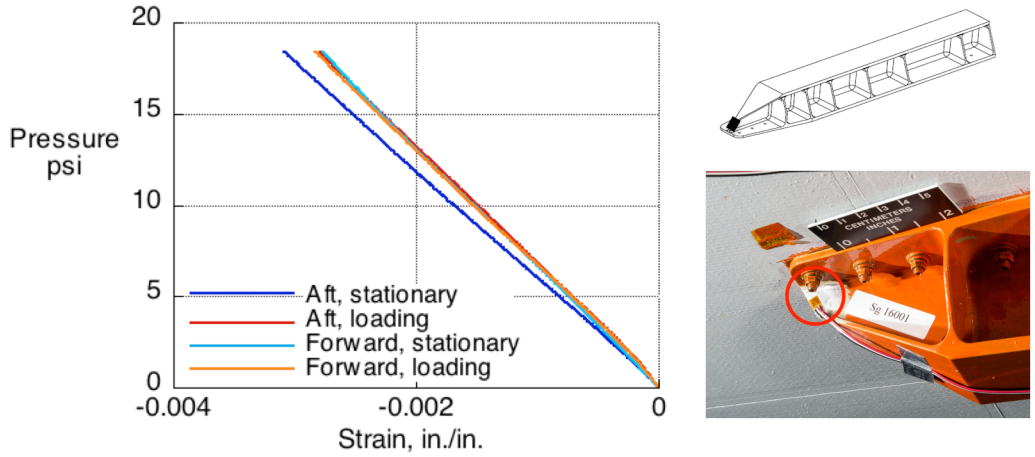

Figure 98. Strain in the external fitting at the edge of the third stringer from the center of keel (point C in Figure 13).

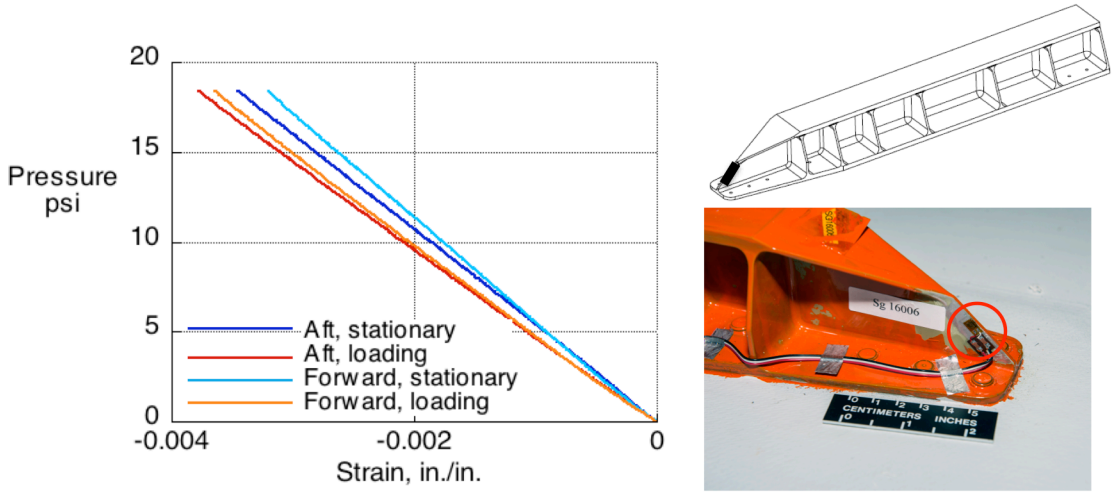

Figure 99. Strain in the external fitting at the edge of the third stringer from the center of crown (point D in Figure 13).

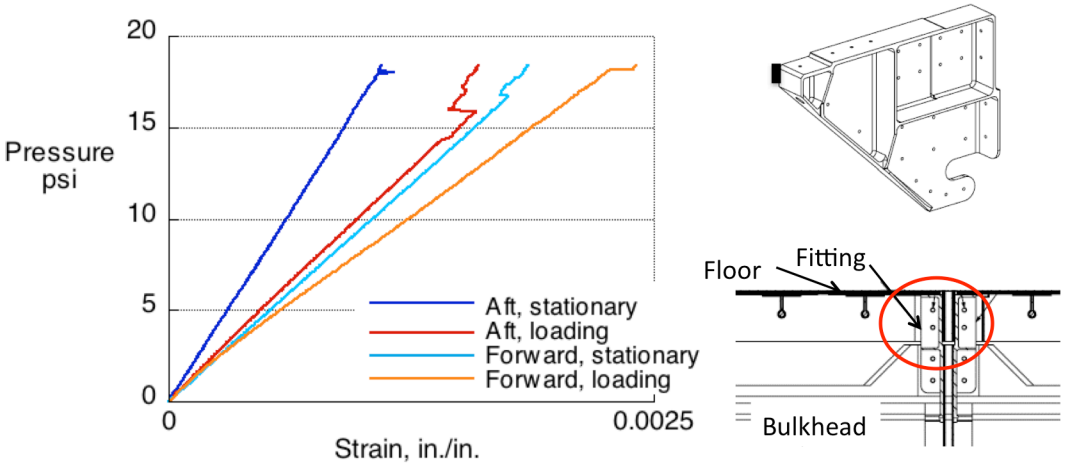

Figure 100. Strain in internal the fitting at the connection between the floor and lower bulkhead (point E in Figure 13).

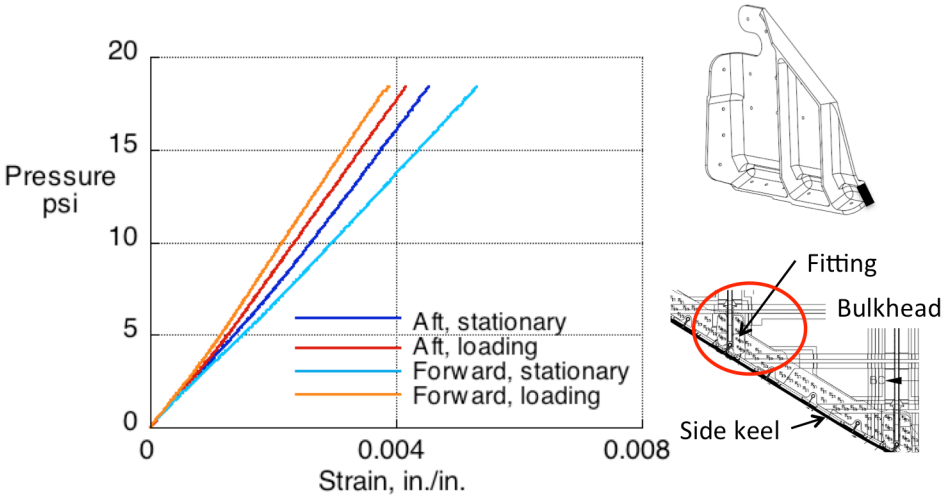

Figure 101. Strain in the internal fitting at the connection between the side keel and lower bulkhead (point F in Figure 13).

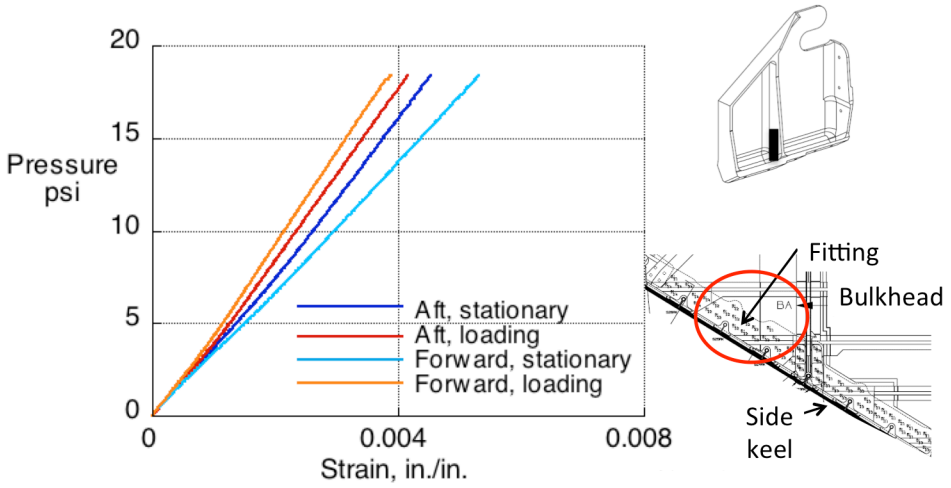

Figure 102. Strain in the internal fitting at the connection between the side keel and lower bulkhead (point G in Figure 13).

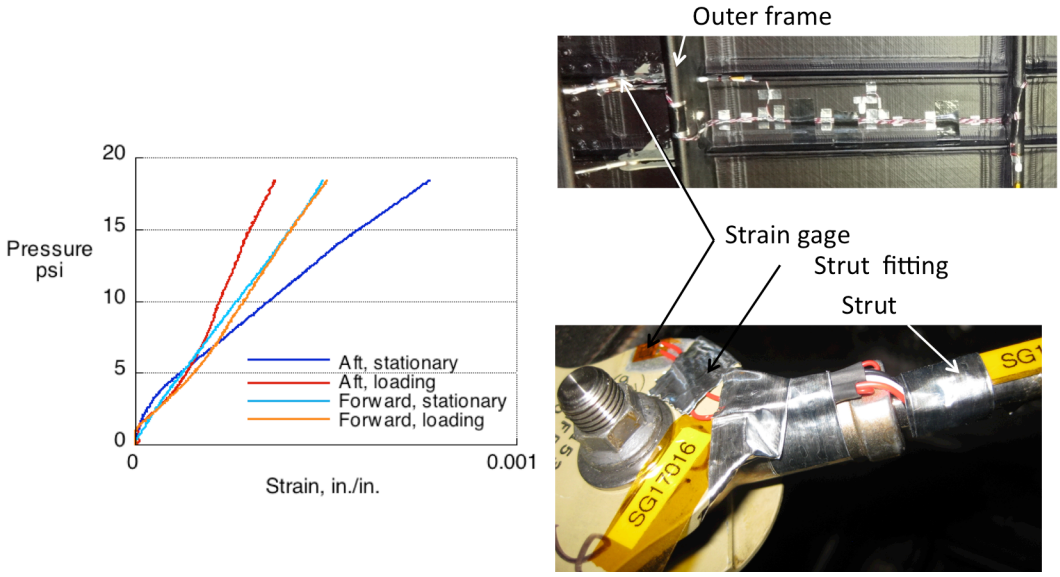

Figure 103. Strain in the internal strut fitting at the connection between the outer rib upper bulkhead (point H in Figure 13).

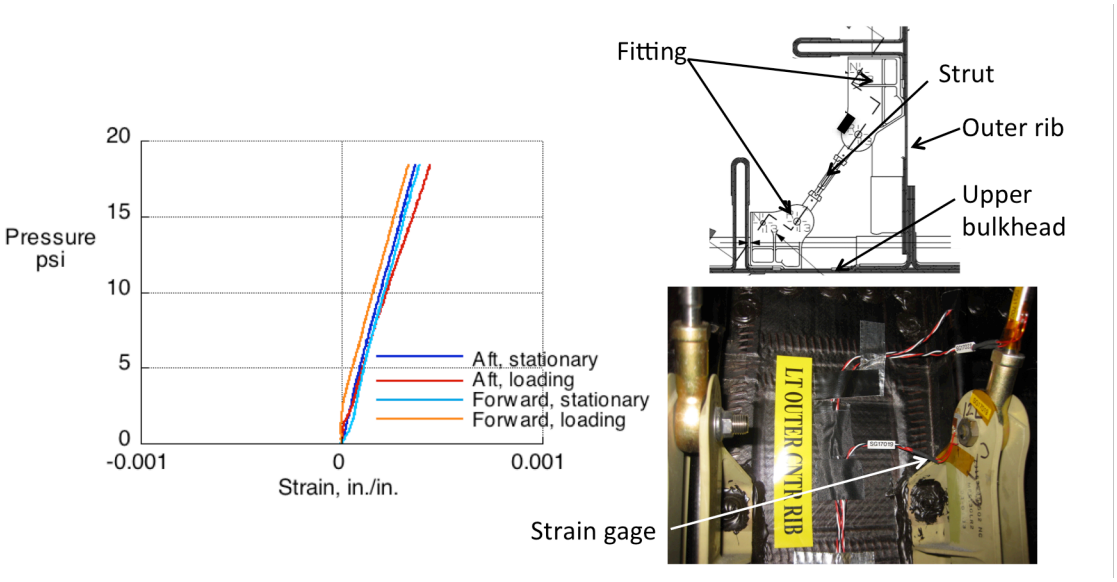

Figure 104. Strain in the internal fitting at the connection between the outer rib and upper bulkhead (point I in Figure 13).

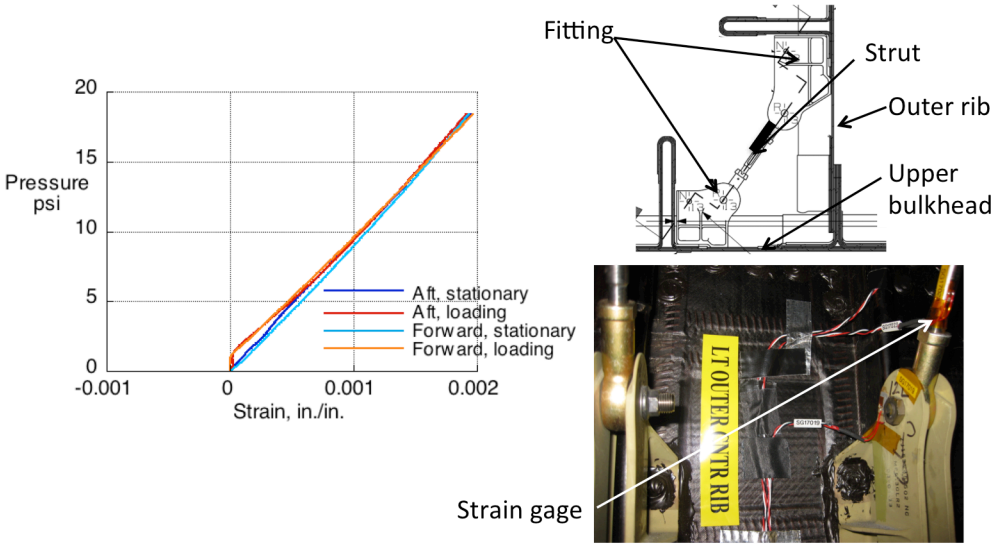

Figure 105. Strain in the internal strut connection between the outer rib and upper bulkhead (point J in Figure 13).

REPORT DOCUMENTATION PAGE

Form Approved
OMB No. 0704-0188

1. REPORT DATE *(DD-MM-YYYY)*	2. REPORT TYPE	3. DATES COVERED *(From - To)*
01- 04 - 2016	Technical Memorandum	

4. TITLE AND SUBTITLE

The Behavior of a Stitched Composite Large-Scale Multi-Bay Pressure Box

5a. CONTRACT NUMBER

5b. GRANT NUMBER

5c. PROGRAM ELEMENT NUMBER

6. AUTHOR(S)

Jegley, Dawn C.; Rouse, Marshall; Przekop, Adam; Lovejoy, Andrew E.

5d. PROJECT NUMBER

5e. TASK NUMBER

5f. WORK UNIT NUMBER

338881.02.22.07.01.01

7. PERFORMING ORGANIZATION NAME(S) AND ADDRESS(ES)

NASA Langley Research Center
Hampton, VA 23681-2199

8. PERFORMING ORGANIZATION REPORT NUMBER

L-20630

9. SPONSORING/MONITORING AGENCY NAME(S) AND ADDRESS(ES)

National Aeronautics and Space Administration
Washington, DC 20546-0001

10. SPONSOR/MONITOR'S ACRONYM(S)

NASA

11. SPONSOR/MONITOR'S REPORT NUMBER(S)

NASA-TM-2016-218972

12. DISTRIBUTION/AVAILABILITY STATEMENT

Unclassified - Unlimited
Subject Category 39
Availability: NASA STI Program (757) 864-9658

13. SUPPLEMENTARY NOTES

14. ABSTRACT

NASA and The Boeing Company have worked together to develop a structural concept that is lightweight and an advancement beyond state-of-the-art composite structures. The Pultruded Rod Stitched Efficient Unitized Structure (PRSEUS) is an integrally stiffened panel design where elements are stitched together and designed to maintain residual load carrying capabilities under a variety of damage scenarios. The final step in the building block series is an 80% scale pressure box representing a portion of the center section of a Hybrid Wing Body (HWB) transport aircraft. The testing of this article under maneuver load and internal pressure load conditions is the subject of this paper. The experimental evaluation of this article, along with the other building blocks and the accompanying analyses, has demonstrated the viability of a PRSEUS center body for the HWB vehicle.

15. SUBJECT TERMS

Blended wing body; Composite; Graphite-epoxy; Hybrid wing body; PRSEUS; Stitching

16. SECURITY CLASSIFICATION OF:			17. LIMITATION OF ABSTRACT	18. NUMBER OF PAGES	19a. NAME OF RESPONSIBLE PERSON
a. REPORT	b. ABSTRACT	c. THIS PAGE			STI Help Desk (email: help@sti.nasa.gov)
					19b. TELEPHONE NUMBER *(Include area code)*
U	U	U	UU	93	(757) 864-9658